System-Wide Evaluation of Inertia Support Potentials from Wind Farms

Project Report

Paul Jung

Department of Department of Energy & Environment
Chalmers University of Technology
Gothenburg, Sweden 2017

System-Wide Evaluation of Inertia Support Potentials from Wind Farms

Project Report

PAUL JUNG

Department of Energy & Environment
Division of Electric Power Engineering
CHALMERS UNIVERSITY OF TECHNOLOGY
Gothenburg 2017

System-Wide Evaluation of Inertia Support Potentials from Wind Farms
Project Report
PAUL JUNG

Department of Energy & Environment
Division of Electric Power Engineering
Chalmers University of Technology
SE–412 96 Gothenburg
Sweden
Telephone +46 (0)31–772 1000

Cover:
Wind energy converter and measurements from a frequency disturbance.
Photo of wind energy converter by wikipedia user Molgreen, licensed under Creative Commons Attribution-Share Alike 3.0 Unported:
`https://commons.wikimedia.org/wiki/File:20090808_l_xl_wiki_1938.jpg`
Frequency disturbance data from M. Persson, "Frequency response by wind farms in islanded power systems with high wind power penetration", Department of Energy and Environment, Electric Power Engineering, Chalmers University of Technology, 2015.

Teknologtryck
Gothenburg 2017

System-Wide Evaluation of Inertia Support Potentials from Wind Farms
Project Report
PAUL JUNG
Department of Energy & Environment
Division of Electric Power Engineering
Chalmers University of Technology

Abstract

In order to limit anthropogenic climate change as well as the dependency on fossil fuels, the wind power generation is rising world wide. Since modern wind turbines are usually variable speed wind turbines, which are connected to the grid via a converter, this causes a decrease in grid coupled inertia. Because decreased inertia causes faster and greater frequency changes for the same disturbances, it is discussed widely how variable speed wind turbines can contribute inertia to the power system.

In this project report, inertial response from wind turbines at the system level is investigated with a focus on the swedish power system. An existing database of wind turbines and a metereological model containing wind speeds on defined grid points are used to determine the operating points of all wind turbines included in the database for each hour in the investigated time span 2010 to 2015. Furthermore, the performance of these turbines in three different fixed trajectory inertial response approaches is simulated, aggregated to the system level and analysed accordingly.

In this work it is shown that a reliable amount of inertial support in relation to their production can be expected from wind turbines. Although the number of online wind turbines and the total energy production from wind turbines are not strongly correlate, it could been proven that for the fixed power and time inertial response approach a linear relation between the aggregated inertial response capability and total energy production exists. The support power from wind turbines amounts under this conditions to 1.13 times their steady state power. It could further been shown that the assumed inertial response strategies would allow for the compensation of a dimensioning fault.

Keywords:
Frequency stability, inertial response, synthetic inertia, inertia emulation, frequency control, variable speed wind turbine, rate of change of frequency.

Acknowledgements

This work was carried out at the Department of Energy and Environment, Division of Electric Power Engineering at Chalmers University of Technology during a semester abroad in the European Union ERASMUS+ programme. I am thankful for this unique possibility and experience and would like to acknowledge the provided facilities as well as to thank the people that made this exchange possible.
My profound thanks and gratitude go to my supervisor and examiner Assoc. Professor Peiyuan Chen for giving me the possibility of working on and learning through this project. I am very grateful for his excellent guidance, support and patience. Thank you for your dedication and trust.
I would also like to thank Mattias Persson for his help, the interesting discussions and the fruitful ideas.
I am thankful for the help of Kalid Yunus, which spared me a lot of tedious datamining.
I appreciate the assistance provided by Professor Torbjörn Thiringer and Jon Olauson.
Furthermore I would like to thank Professor Lutz Hofmann and Hauke Huisinga for their interest and their support with the administrational part of this project.
For a project like this, a productive and positive working atmosphere is crucial. In this context I would like to thank the staff and my fellow students in Gothenburg and at the Institute of Electric Power Systems at Leibniz Universität Hannover, where this project report has been finished. My special thanks go out to my flatmates and friends in Gothenburg and Hannover and to my family, who all have supported and motivated me.

Paul Jung
Hannover, Germany
January 2017

Symbols

Symbol	Units	Description
A	m^2	Rotor area
A_r	m^2/W	Rotor area by rated power
C_P	–	Power coefficient
$C_{P,Betz}$	–	Betz-factor - maximum power coefficient
$C_{P,max}$	–	Wind turbines maximum power coefficient
d	m	Displacement height
E_{bal}	J	Energy balance of inertial response
E_{el}	J	Electrical energy
E_{mech}	J	Mechanical energy
E_{pfc}	J	Energy supplied by primary frequency control
E_{rot}	J	Rotational kinetic energy
E_{rec}	J	Additional energy fed into the grid during the inertial response recovery phase
E_{sup}	J	Additional energy fed into the grid during the inertial response support phase
$E_{sys,bal}$	J	System-wide energy balance of inertial response
$E_{sys,rec}$	J	System-wide sum of additional energy during inertial response recovery phase
$E_{sys,rot}$	J	System-wide sum of rotational kinetic energy in WEC's
$E_{sys,rot,syn}$	J	System-wide sum of rotational kinetic energy in synchronously connected generation and load

$E_{\mathrm{sys,sup}}$	J	System-wide sum of additional energy during inertial response support phase
f	Hz	Electrical frequency
f_0	Hz	Electrical frequency directly before the disturbance
f_{hr}	Hz	High resolution electrical frequency measurement
f_{lr}	Hz	Low resolution electrical frequency measurement
f_{nadir}	Hz	Minimum frequency during the disturbance, nadir frequency
h	m	WEC hub height
H	s	Inertia constant
H_{WEC}	s	Wind turbine inertia constant
H_{sys}	s	Power system aggregated inertia constant
J	$\mathrm{kg\,m^2}$	Moment of inertia
k	–	Sample number
$k_{\mathrm{support,end}}$	–	Sample number of the end of the support phase
$k_{\mathrm{support,start}}$	–	Sample number of the start of the support phase
K_{b}	m rad/s	Tip-speed ratio constant
N_{WEC}	–	Total number of WEC's in the power system, excluding fixed speed turbines
p	–	WEC instantaneous generation penetration
P_{Betz}	W	Maximum power extractable from wind
P_{e}	W	Electrical power
P_{el}	W	Wind turbine electrical power output
$P_{\mathrm{el,inmax}}$	W	Wind turbine electrical power output short term maximum during inertial response
$P_{\mathrm{el,inmin}}$	W	Wind turbine electrical power output minimum during inertial response recovery phase
$P_{\mathrm{el,stat}}$	W	Stationary wind turbine electrical power output, only different from P_{el} during inertial response
P_{gen}	W	Aggregated power generation
P_{load}	W	Aggregated power load
P_{m}	W	Mechanical power

P_{mech}	W	Wind turbine mechanical power
$P_{\mathrm{mech,max}}$	W	Wind turbine mechanical power short term maximum during inertial response
$P_{\mathrm{mech,min}}$	W	Wind turbine mechanical power short term minimum during inertial response
P_{n}	W	Rated active power
P_{WEC}	W	WEC aerodynamical power
$P_{\mathrm{WEC,comp}}$	W	System-wide sum of hourly average of power for all WEC's in the system, taken from the reference for comparison
$P_{\mathrm{WEC},\omega_{\mathrm{max}}}$	W	Power when maximum rotor speed is reached
$P_{\mathrm{WEC,sys}}$	W	System-wide sum of hourly average of power for all WEC's in the system, excluding fixed speed turbines
$P_{\mathrm{WEC,sys,inmax}}$	W	System-wide sum of WEC maximum power during inertial response
$P_{\mathrm{WEC,sys,inmin}}$	W	System-wide sum of WEC minimum power during inertial response
P_{wind}	W	Power of wind stream
r	–	Pearson correlation coefficient
R	m	Rotor radius
S_{n}	VA	Rated apparent power
S_{sys}	VA	Rated apparent power of all synchronous connected generation and load
t	s	Time
t_{rec}	s	Length of inertial response recovery
t_{sup}	s	Length of inertia support
T_{e}	N m	Electrical torque
T_{m}	N m	Mechanical torque
v	m/s	Wind speed
$\bar{v}$	m/s	Average wind speed during complete considered timespan (i.e. years 2010 - 2015)
v_{in}	m/s	Cut-in wind speed
v_{out}	m/s	Cut-out wind speed

$v_{P_{\max}}$	m/s	Wind speed at which maximum power is reached, rated wind speed
v_{u}	m/s	Eastward wind speed
v_{v}	m/s	Northward wind speed
$v_{\omega_{\max}}$	m/s	Wind speed at which maximum rotor speed is reached
Δf	Hz	Frequency difference
Δf_{WEC}	Hz	Frequency difference considering WEC inertial response
ΔP	W	Power imbalance
ΔP_{mod}	W	Absolute difference in wind generation between improved model and reference
$\Delta P_{\mathrm{mod,rel}}$	–	Relative difference in wind generation between improved model and reference
ΔP_{sys}	W	Power system power imbalance
$\Delta P_{\mathrm{sys,res}}$	W	Power system residual imbalance
Δt	second	Time difference
Δt_{sim}	s	Simulation time step
ΔT	N m	Resulting torque
$\Delta\omega$	rad/s	Change in rotor speed per simulation step
α	–	Shear exponent
β	°	Pitch angle
δ	–	Relative difference between simulation and power balance verification normalized with the kinetic energy change
ϵ	J	Absolute difference between simulation and power balance verification
λ	–	Tip-speed ratio
λ_{opt}	–	Optimal tip-speed ratio
ρ_{air}	kg/m^3	Air density
ω	rad/s	Angular velocity, rotor speed
ω_{base}	rad/s	Base rotor speed
$\omega_{\max}$	rad/s	Maximum rotor speed

ω_{min}	rad/s	Minimum rotor speed

Frequently used indices

Index	**Desciption**
bal	Inertial response energy balance
i	i-th machine
k	k-th simulation sample
max	Maximum
n	Rated
pu	p.u. representation
rec	Inertial response recovery phase
ref	Reference
sup	Inertial response support phase

Bases for normalised values

Value	**Base**
E	$E_{\mathrm{rot,n}} = HP_{\mathrm{n}}$
P	P_{n}
ω	ω_{n}, ω_{base} (for wind turbines)

Abbreviations

AEP	annual energy production
DFIG	Double Fed Induction Generator
MERRA	Modern Era Retrospective-analysis for Research and Analysis
PMU	Phasor Measurement Units
RMS	root mean square
RoCoF	rate of change of frequency
TSO	transmission system operators
WEC	wind energy converter

Contents

1

Introduction

Electric energy systems world wide and especially in Europe experience a transition towards more sustainable generation. One of the main energy sources in this process is wind energy, which already has a remarkable share in energy production in many countries. The lead in this aspect is taken by Denmark, where wind power was responsible for 42.1 % of domestic consumption and a maximum of 138.7 % of instant power share in 2015 [1]. While wind power plays a less important role in Sweden, growth in installed power and annual production remain impressive, e.g. the share of wind power in the annual generation has risen from 2 % in 2010 to 10 % in 2015 [2]. The higher share of wind power results in the displacement of central power plants. Since central power plants are responsible for the majority of ancillary services, their decreasing availability and commitment demands new strategies and technology for the provision of those services by renewable generation units. These new approaches and solutions require a step-by-step redesign of the power system at higher penetration levels of wind power (higher than 30 %), and they have been found to be more likely an economic than a technical issue [3]. However, this should not hide the fact that the technology needed for the redesign is not yet readily available. In this report one aspect of this complex shall be considered, i.e. the provision of system inertia by wind energy converters (WEC's) .

1.1 Background

Many transmission system operators (TSOs) notice a decline of kinetic energy in their power systems. While the reasons for this trend are manifold, they are mainly linked to the growing share of converter connected generation and consumption units. These replace electrical machines originally coupled to the system frequency, i.e. synchronous machines connected without converter, which used to contribute to the so called system inertia. This effect is even worse in zero-emission scenarios because of the relatively slow response time and the negative initial reaction of hydro power plants. [4]

Since the electrical grid has no noteworthy implicit energy storages, production and consumption of electrical energy have to be balanced at every moment. Every deviation from this equilibrium is initially intercepted by the reaction of the rotating masses coupled to the system: If there is more consumption than generation, the rotational speed and electric frequency will decrease, thereby releasing stored kinetic energy to the grid and balancing the mismatch. If there is more generation than consumption, the effects will be reverse, accelerating rotation and increasing frequency. Less inertia means bigger frequency deviations in reaction to the same power imbalance [4]. This effect will be further discussed and quantified in Chapter 2.1.

Rotating masses which are connected to the grid by a converter do not show this inertial response since their rotational speed is decoupled from the system frequency. Nevertheless there is kinetic energy stored in their rotation, which can be changed through acceleration or deceleration, imitating a flywheel energy storage. This can be controlled to mimic the reaction of a classical synchronous generator [4]. Examples for converter connected units are industrial motor drives, wind turbines of type C or D (variable speed wind turbines, classification see [3]) and photovoltaic generation. Of those examples, the first two contain significant inertia. However, for most drive applications, a strict control regime on rotational speed is crucial, not allowing for grid-caused variations. This leaves wind turbines as a technology with a rising presence in power systems where rotational speed can be influenced within limits and where grid operators can dictate a inertial response mechanism through the grid code or a new ancillary services market. The possibilities, technical requirements as well as the benefits of inertia support by wind turbines are subject of on-going research and the matter of this report. It has to be noted that in context of this report WEC inertia support refers to the inertia support by variable speed wind turbines only, since fixed speed wind turbines show a fundamentally different behaviour and are of declining interest due to their small share in newly installed wind turbines.

1.2 Discussion of literature research results

In the present literature on power system inertia, inertia support from wind turbines receives a lot of attention. Still, most of the research articles focus on control strategies and single wind turbine characteristics without taking the complete power system into account. Furthermore, many of the papers that estimate the the influence of wind turbine inertia on characteristic reactions to frequency disturbances by power systems with high wind power penetration will use improper simplifications. The most frequent simplification is to assume all wind turbines in the system are operating at their rated wind speed and power output, e.g. in [5] and [6]. As shown in [7], [8] and [9], the amount of inertia available to the grid is strongly dependend on the operating point of the wind turbines, which would imply that this simplification is unacceptable for reliable results. Other sources give different results: In [10] the number of active wind turbines is mapped by a simple function to the instantaneous wind power penetration level, in [11] the same is done for the kinetic energy in reference to the hourly energy production from wind power and [12] states that at wind speeds above 15 % to 20 % a substantial contribution to system inertia from wind turbines could be expected, which furthermore would be relatively independent from the actual wind speed. Part of this report is therefore also to investigate the relation between wind power penetration level and the inertia support capability.

The authors considering different operating points take three different main types of approaches:

1. *Curve fitting approaches*: The first type of approaches relies on historical, measured and calculated values of wind turbine energy output or power and their kinetic energy. These values are then used to calculate a fitting curve. The curve gives an analytical expression relating a known dimension, i.e. the wind power energy output, to the kinetic energy in question. After the generation of this curve no wind speed values are necessary for the estimation of kinetic energy from wind turbines. Furthermore the spatial distribution of wind farms is irrelevant. An example for an approach of this type can be found in [11].
   Criticism of this method includes that it is overly simplified and due to the averaging nature of the approach all information about extreme values and the deviation from mean are lost, which is crucial information for system security.

2. *Statistical wind distribution approaches*: The second type of approaches utilizes historical wind speed data and determines one or more typical geographical wind speed distributions depending on the system wind generation level

for the power system in question with stochastical methods. The kinetic energy of wind turbines operating at different wind speed levels is calculated. Matching the spatial wind speed and turbine distribution these different energy levels are then weighted and aggregated, resulting in an estimation of the system wide kinetic energy. In [13] the application of an approach of this type can be found for the island of Ireland.
This type is also subject to a number of inaccuracies introduced by the undertaken simplification. The usage of one or a small amount of geographical wind speed distributions necessarily focuses on the most frequent distributions. This however neglects rare extreme events, which are of special interest for system stability analysis. Also, the method is relying on a constant geographical distribution of wind turbines, which is not necessarily the case for future scenarios, especially considering offshore wind farms.

3. *Synthetic wind speed approaches*: In [12] synthetic wind speed data is used for the evaluation of wind turbine kinetic energy. The synthetic time series are designed to reproduce diurnal and seasonal effects as well as geographical correlations and are based on random number seeds. They are calculated for 17 regions in the power system in question, aggregating all the wind turbines per region. For the case study 30 representative summer and winter days are chosen from the synthetic generated time series. The inertial response of the aggregated wind turbines is then estimated using the hourly mean wind speeds given by the synthetic time series. During this process the possibility of wind speed changes during the underfrequency event is also accounted for by a probabilistic approach assuming a particular control strategy for the inertia support.
While the results of approaches of this type are strongly dependent on the quality of the synthetic wind speed time series, they do not share the inherent problem of the two former types concerning the levelling effect. Still, approaches of this type strongly depend on detailed wind speed measurements and have a very limited spatial resolution. In the contemplated work the consideration of offshore wind parks has proven difficult. As a result of the chosen probablistic approach the insight into underlying correlations between wind speed and kinetic energy becomes impossible, limiting later case studies to the chosen control strategy.

To overcome the problems and limitations of these strategies and to use readily available data a different approach shall be taken in this work. Utilizing wind speed data from metereological reanalysis datasets of a medium spatial resolution (namely the MERRA-2 dataset) and a detailed wind park database, hourly wind energy production and kinetic energy of all wind turbines will be estimated. The data sources for this are described in detail in Chapter 3. Finally a certain inertia support control strategy will be assumed and the effects will be compared for different penetration levels.

1.3 Purpose and limitations

The purpose of this work is to

- analyse and quantify the amount of kinetic energy in wind turbines available for inertia support under different operational states of the power system.
- investigate the correlation between wind penetration level and inertia contribution.
- examine sources and margins of errors.
- identify important indicators for TSO's to determine the inertia support capability of wind energy under different operational conditions of the power system.
- if possible, compare frequency stability indicators like initial rate of change of frequency, frequency nadir and time to recovery after a disturbance for inertia control by wind turbines.

Because the focus of the report is on the first items, the last two items are only adressed in a preliminary manner and require further work to be thoroughly investigated. Further limitations due to the restricted extent of the project are the following:

- Wind speed and operational state of the power system, i.e. load and generation, are assumed to be constant during each sample (step length for the power system simulation is one hour).
- No detailed simulation of the power system will be employed, the electrical distance between all considered generation units is assumed to be 0.
- The effects of low inertia on rotor angle stability are not part of this investigation.
- The study and comparison of different control strategies for inertia support from wind turbines, in particular from a turbine perspective, is not in the focus of this report.

1.4 Report structure

This report is structured as follows:
Chapter 2 gives the necessary theoretical background of inertia in electrical power systems and the conversion of wind energy. It also portays different approaches to inertial response from variable speed wind turbines.

Chapter 3 treats with the data sources and the modelling of wind energy conversion. It also includes the description of the steady-state wind turbine model used in this work. The chapter also includes the results of the model and their discussion.

Chapter 4 presents the inertial response approaches investigated in this work and the dynamic wind turbine model used to simulate the inertial response of a single wind turbine. This is followed by a presentation of results and a discussion of the different investigated approaches.

In Chapter 5, the system-wide aggregation of inertial response from wind turbines is described. This is followed up by the description and discussion of the resulting figures.

Chapter 6 gives an estimation, which impact wind turbine inertial response could have on electric power systems and how the aforementioned figures relate to system inertia from synchronous generation.

Finally, in Chapter 7 the main conclusions and links for future work are presented.

2

Wind energy conversion and inertial energy

2.1 Inertia in electrical power systems

Like already layed out in Section 1.1, inertia damps frequency changes in power systems, which are caused by imbalances between generation and consumption. To illustrate this and the equations describing the phenomenon, a one-mass model representation of the power system similar to a flywheel will be used.

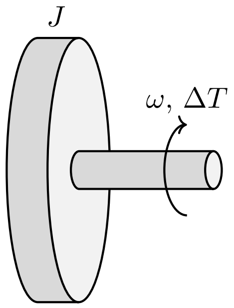

Figure 2.1: Demonstration of the one-mass model representation. J denotes the moment of inertia, ΔT the resulting torque and ω the angular velocity.

This model is illustrated in Fig. 2.1. It consists of a single rotating mass with a moment of inertia J containing the complete system's inertia. The angular velocity ω of the mass is fixed to the frequency of the electric system like it is in a synchronous machine. The resulting torque $\Delta T = T_\mathrm{m} - T_\mathrm{e}$ is the difference between mechanical and electrical torque and shows the effect of imbalances and disturbances.

The model can help to understand the relations in the power system by illustrating the process for a single mass. It will be described and quantified following the approach in [4]. For the balanced system, the resulting torque is zero because mechanical torque (e.g. from a turbine) and the generators electrical torque are equal. As a result, the systems kinetic energy and frequency remain constant. In the case of a power imbalance in the electric system, the needed (or excess) power ΔP evokes a resulting torque different from zero, the power will be taken from (or stored in) the rotational kinetic energy of the mass:

$$\frac{\mathrm{d}J\omega}{\mathrm{d}t} = \Delta T \tag{2.1}$$

When expressed using power instead of torque, this equation is called swing equation:

$$\frac{\mathrm{d}\frac{J\omega^2}{2}}{\mathrm{d}t} = \Delta P \tag{2.2}$$

Analogous to ΔT, the power imbalance is defined as $\Delta P = P_\mathrm{m} - P_\mathrm{e}$, the difference between mechanical and electrical power in the machine. Because of this, ΔP will be negative in the case of rising demand of electrical power ($P_\mathrm{e} > P_\mathrm{m}$). This results in a negative derivative of angular velocity, thus the mass decelerates in this case.

The expression on the left side of equation (2.2) is equivalent to the derivative of kinetic energy of the machine E_rot. Often it is rated to the machines power rating, S_n and represented at rated operation, marked by index n:

$$H = \frac{J\omega_\mathrm{n}^2}{2S_\mathrm{n}} = \frac{E_\mathrm{rot,n}}{S_\mathrm{n}} \tag{2.3}$$

H is the inertia constant of the machine in seconds. In equals to the timespan a generator could hypothetically provide its nominal power only from the kinetic energy stored in its mass. The values for H of typical synchronous generators range from 2 s to 9 s [4], another source stating 7 s as typical value for thermal generation units and 5 s for hydro generation units [6].
For wind turbines, the inertia constant can be calculated as follows:

$$H_\mathrm{WEC} = \frac{J\omega_\mathrm{n}}{2P_\mathrm{n}} \tag{2.4}$$

Note that the rating is done to the machines active, not apparent rated power. In this case, it is important that for geared turbines the moment of inertia J and the rated rotor speed ω_n are referring to the same drive-train component - this could be the fast spinning generator side as well as the slower turbine side. The moment of inertia has to include the complete drive train with generator and turbine. The typical range for inertia constants in WEC's has been found to be 2 s to 6 s [3]. Like stated before, in contrast to synchronous generation this inertia does not directly contribute to system inertia by itself.

Rearranging equation (2.2) with the help of equation (2.3) yields

$$\frac{\mathrm{d}H\frac{\omega^2}{\omega_\mathrm{n}^2}}{\mathrm{d}t} = \frac{\Delta P}{S_\mathrm{n}} \tag{2.5}$$

Substituting ω and ΔP to per-unit values and solving the outer derivative gives

$$2H\omega_\mathrm{pu}\frac{\mathrm{d}\omega_\mathrm{pu}}{\mathrm{d}t} = \Delta P_\mathrm{pu} \qquad \text{with} \qquad \omega_\mathrm{pu} = \frac{\omega}{\omega_\mathrm{n}},\ \Delta P_\mathrm{pu} = \frac{\Delta P}{S_\mathrm{n}} \tag{2.6}$$

The system frequency is considered a global parameter. This allows the actual power system, consisting of many different rotating masses, to be represented by the above mentioned single mass model. It has to be mentioned, that in this model only synchronous connected generation and load is included. This means, that variable speed wind turbines are excluded. The resulting equation is

$$2H_\mathrm{sys}\omega_\mathrm{pu}\frac{\mathrm{d}\omega_\mathrm{pu}}{\mathrm{d}t} = \Delta P_\mathrm{pu,sys} \qquad \text{with} \qquad \Delta P_\mathrm{pu,sys} = \frac{P_\mathrm{gen} - P_\mathrm{load}}{S_\mathrm{sys}} \tag{2.7}$$

In this equation $\Delta P_\mathrm{pu,sys}$ is the system-wide power imbalance referenced to the sum of rated power of all synchronous connected generation and load $S_\mathrm{sys} = \sum_i S_{\mathrm{n},i}$ and H_sys denotes the inertia constant of the complete power system (i.e. all synchronous connected rotating generation and load), which can be calculated by

$$H_\mathrm{sys} = \frac{\sum_i H_i S_{\mathrm{n},i}}{\sum_i S_{\mathrm{n},i}} = \frac{\sum_i E_{\mathrm{rot},i}}{S_\mathrm{sys}} \tag{2.8}$$

Assuming that the electrical frequency is close to its nominal value, which is equal to $\omega_\mathrm{pu} \approx 1$ p.u., equation (2.7) can be converted to

$$2H_\mathrm{sys}\frac{\mathrm{d}\omega_\mathrm{pu}}{\mathrm{d}t} = \Delta P_\mathrm{pu,sys} \tag{2.9}$$

This expression allows for, amongst other, two simple observations: Firstly, if the power imbalance is zero, i.e. when generation and load are perfectly in balance, the rate of change of frequency (RoCoF) is zero and the frequency is stable. Secondly, the initial RoCoF of a power imbalance event is proportional to the quotient of the power imbalance $\Delta P_{\mathrm{pu,sys}}$ and the system's inertia constant H_{sys}. This means that for a given power imbalance a higher system inertia results in a smaller RoCoF, giving primary frequency control more time to react and emphasising the importance of inertia to system stability.

In practice, measuring the RoCoF and estimating the system's inertia constant are difficult tasks involving a lot of inaccuracies. Some reasons for this include the dependency of the frequency and in particular the RoCoF on the position of the measurement in the power system, power system oscillations due to transients after a disturbance, different estimation methods and parameter sets for the estimation of the RoCoF from frequency measurements as well as missing data in respect of machine inertia constants and current generation in the moment of the disturbance [4], [14], [15]. The method chosen in this project is described in Section 6.1.

2.2 Wind energy conversion

The power of wind, which is nothing else than a stream of air, flowing through a certain profile can be described by the following equation:

$$P_{\mathrm{wind}} = \frac{1}{2}\rho_{\mathrm{air}} A v^3 \tag{2.10}$$

where ρ_{air} denominates the air density in kg/m^3, A the area of the profile in m^2 and v the wind speed orthogonal to the profile in m/s. A wind turbine will try to extract as much of this power contained in the wind stream as possible. Since this extractions slows the windstream and the moving air has to follow the continuity equation, extracting a higher share of the windstreams power will reduce the available amount of power. The optimum for power utilisation was discovered by Betz and can be determined with the following equation:

$$P_{\mathrm{Betz}} = \frac{1}{2}\rho_{\mathrm{air}} A v^3\ C_{\mathrm{P,Betz}} \tag{2.11}$$

with $C_{\mathrm{P,Betz}}$ being the dimensionless Betz-factor indicating the fraction of extracted power. Its maximum has been found to be 0.59 [3].

Real wind turbines can't reach this amount of power due to the number of deviations from Betz' idealising theory, examples being their limited amount of blades and wake effects. Also, their efficiency is dependent on the operating state. This fact is often modelled introducing a varying C_{P}, changing equation (2.11) to

$$P_{\mathrm{WEC}} = \frac{1}{2}\rho_{\mathrm{air}} A v^3 \; C_{\mathrm{P}}(\lambda,\beta) \tag{2.12}$$

with β being the pitch-angle (typically in degrees) and λ the dimensionless tip-speed ratio as given in

$$\lambda = \frac{R\omega}{v} \tag{2.13}$$

where ω denotes the angular velocity of the WEC's turbine in radians per second and R is the turbines rotor radius in metres. Depending on the electrical design of a wind turbine they either operate at one or two fixed angular velocities (*fixed speed WEC*) or will adjust their angular velocity within operating limits to work at their maximum possible C_{P} (*variable speed WEC*). Examples for these values and a description of the control regime of a typical variable speed WEC can be found in the Section 3.2, which deals with WEC modelling.

2.3 Inertia support from wind turbines

The topic of inertia support possibilities from variable speed wind turbines has been of increasing interest for science and industry in the last decade. A great number of contributions is available, where of the biggest share tackles the thematic of control strategies on turbine level. A good overview of current research contributions can be found in [16]. This section will outline the important basics of the topic.

At first, the difference between primary frequency control and inertial response shall be discussed. In thermal and hydro power plants, the two can be strictly and easily distinguished. Inertial response is not deliberately activated, but only depends on the system frequency deviation. It can not be given a certain shape or a fixed time frame, but only depends on the RoCoF and the machines inertia constant and power rating. The change in electrical power of the machine does not correspond to a change in mechanical power from the turbine but to a change in kinetic energy, i.e. rotor speed. Primary frequency control on the other hand needs to be activated, its shape and specifications are defined by the TSO and it goes along with a governor intervention to change the turbines mechanical power accordingly, e.g. by the opening of valves. Further the effect of the two differ fundamentally: While inertial response can only limit the RoCoF, primary frequency control adresses the underlying power imbalance and brings the change in frequency to an end. In the case of variable speed wind turbines, the two former criteria are not true anymore. Since the machine is mechanically decoupled from the grid, inertial response has, similarly to primary frequency control, to be imposed by the controller. This allows the operator or manufacturer to specify the form and speed of the response. However, the latter criteria remain true: inertial response is fuelled by change of kinetic energy while primary frequency control goes along with a change of the power input. In wind turbines a change in power input can be reached by derating the stationary operation from the maximum power point. While mainly connected to primary frequency control, derating can also be used in the context of inertia support to achieve operation at higher kinetic energy than at the maximum power point [7]. In this context, synergy has been observed between inertia support and primary frequency control [17]. However, this implementation is rarely discussed and therefore neither derating strategies nor primary frequency control are subject of this report. [7], [18], [19] and [20] contain further information on the interconnection between primary frequency control and inertia support in wind turbines. The inertial response from fixed speed wind turbines is similar to conventional power plants, which is why it is neglected in this report. Please refer to [17] for a detailed description of the peculiarities of fixed speed wind turbine inertial response. A detailed comparison between the inertial response from fixed and variable speed wind turbines can also be found in the abovementioned source and in [21].

Regarding the inertial response from variable speed WEC's, further difference apart from the decoupling from the system frequency and the tunability of the response can be made out in comparison to conventional power plants. WEC's need a recovery period after losing rotor speed to speed up again. While synchronous machines coupled to the system frequency are sped up again during frequency recovery (secondary frequency control phase), this seems to be to late for WEC since their efficiency decreases notably with a lower rotor speed. In result, the output power has to be reduced almost immediatly after the end of the inertial response to a setting considerably lower than initially to prevent further slowing down the turbine. This reduction in generation can cause a second frequency dip and is one of the urgent challenges concerning the design of WEC inertial response.
A second difference is the variability of the response due to the geographical distribution, different wind speeds and great variety of the turbines [13]. Also, inertial response from wind turbines triggers later than coupled rotating masses since it has to be activated [13]. It should be noted however, that the tunability of the response is a great advantage bearing the possibility of delivering a lot more stabilizing energy to the grid than conventional machines, albeit at the expense of a recovery phase [4], [18].

In terms of control strategies or "shapes" of the inertial response, three different approaches can be identified: the Δf response, the fixed trajectory response and the RoCoF response. The Δf response is, similar to the droop control in primary frequency control, depending on the deviation in system frequency from nominal. The fixed trajectory response starts a fixed response shape when triggered, e.g. by a deviation in frequency beyond a certain threshold. It is decoupled from the instantaneous system frequency. Lastly, the RoCoF response is depending on the RoCoF and thus emulating an inertial response of a system coupled synchronous machine. The different control strategies and their advantages and disadvantages are not subject of the report. In this report three specific fixed trajectory responses are chosen and compared, because this mechanism seems to be the only one already implemented by a TSO [22]. Furthermore, the fixed trajectory strategy can be simulated and analyzed independently from the disturbance, which is benefiting the objective of this work. The different trajectories are described in section 4.1.2.

Comparing type C and D wind turbines in respect of inertia support, a few differences can be noted. Double Fed Induction Generators (DFIG) are still coupled to some extent to the system frequency (a change in frequency at constant rotor speed will change the slip of the machine), however they do not deliver a substantial inertial response on their own [18]. This is similar to full scale converter turbines, which do not provide an inertial response at all if not explicitely designed to do so. The biggest difference between the inertial response of these two technologies are the restrictions and limits and the varying inertia constants. A number of limitations apply to the exertion of inertia support by variable speed wind turbines. WEC component ratings, i.e. for mechanical loading and converter and generator electrical ratings have to be respected. Also, other controls have to be taken into account like turbulence, drive-train and tower loads management [8]. Furthermore, the speed variation from normal operating speed has to be limited. In a DFIG, the converter voltage and power are depended on the slip [23]. Since there exist limits for those two values, the slip has to be restricted [24]. A full scale converter wind turbine (type D) is not subject to this restriction. But there is another limit for rotor speed deviation which applies to both types. Slowing the rotor reduces aerodynamic lift, which can cause the turbine to stall [8]. This must be avoided. The author could not find any tangible numbers for this limits, but in [12] it is stated that rotor speed deviation would be limited to $\pm 30\,\%$ for both type C and D wind turbines. This is roughly in accordance with the typical speed deviation limits from synchronous speed stated in [3]. The approach in this work focuses on maximum available kinetic energy, therefore wider limits are applied. They are described in Section 4.1.

Most research on this topic supposes stationary wind speeds and applies it to a single wind turbine. Thus, the effects of turbulence on the outcome of the inertial response simulation are neglected. They are highlighted in [25]. Also, the wake effects in a wind park have influence on the inertial response and can demand for a different control strategy. These are considered in [26]. Both effects are not considered in this work.

A quantification of the energy exchange during inertial response can be accomplished with the model and equations given in Section 2.1. Equation (2.5) describing the power balance and speed change can be formulated specifically for wind turbines using equation (2.12) (in the p.u.-representation as presented in equation (3.4)):

$$\frac{\mathrm{d}H\omega_{\mathrm{pu}}^2}{\mathrm{d}t} = P_{\mathrm{mech,pu}} - P_{\mathrm{el,pu}} \qquad \text{with} \qquad P_{\mathrm{mech,pu}} = \frac{1}{2}\rho_{\mathrm{air}} A_{\mathrm{r}} v^3 C_{\mathrm{P}}(\omega_{\mathrm{pu}}, \ldots) \tag{2.14}$$

Note that in contrast to the stationary cases described in equations (2.12) and (3.4) in this case electrical and mechanical power of the wind turbine are allowed to differ, thus causing a rotor speed change. Therefore the ambiguous variable $P_{\mathrm{WEC,pu}}$ is not used for the description of inertial response. Instead, the mechanical power of the wind turbine $P_{\mathrm{mech,pu}}$ and the electrical power the wind turbine feeds into the grid $P_{\mathrm{el,pu}}$ are used. It is also possible to calculate the energy exchanged in every given time period by integration:

$$\int\limits_{t_{\mathrm{start}}}^{t_{\mathrm{stop}}} \frac{\mathrm{d}H\omega_{\mathrm{pu}}^2}{\mathrm{d}t}\,\mathrm{d}t = \int\limits_{t_{\mathrm{start}}}^{t_{\mathrm{stop}}} P_{\mathrm{mech,pu}}\,\mathrm{d}t - \int\limits_{t_{\mathrm{start}}}^{t_{\mathrm{stop}}} P_{\mathrm{el,pu}}\,\mathrm{d}t \tag{2.15}$$

$$\Delta E_{\mathrm{rot,pu}} = E_{\mathrm{mech,pu}} - E_{\mathrm{el,pu}} \tag{2.16}$$

The change in kinetic energy stored in the rotating mass $\Delta E_{\mathrm{rot,pu}}$ is equal to the difference between the mechanical energy retrieved from the wind during the given time period $E_{\mathrm{mech,pu}}$ and the electrical energy delivered to the grid $E_{\mathrm{el,pu}}$.

The rate of change in rotor speed can be deduced by rearranging equation (2.14) and solving the derivative similar to equation (2.6):

$$\frac{\mathrm{d}\omega_{\mathrm{pu}}}{\mathrm{d}t} = \frac{P_{\mathrm{mech,pu}} - P_{\mathrm{el,pu}}}{2H_{\mathrm{WEC}}\omega_{\mathrm{pu}}} \tag{2.17}$$

If the mechanical power would stay constant, the rotor speed after an inertial response could be easily determined by use of the conservation of energy given in equation (2.16). However, as the rotor speed changes, the tip-speed ratio λ and the corresponding C_{P} change. This makes it necessary to integrate over the timespan of the inertial response taking into account the varying mechanical power. Section 4.1.3 describes how this process was implemented for this work using the equations given in this chapter.

3

Wind energy conversion data and model

This chapter describes the data used in this work, its sources and its structures. It is divided in three sections, the first describing the metereological data and the second the WEC data. The second section also contains the description of the steady-state WEC model. The third sections contains and discusses the results from the simulation of wind power generation.

3.1 Wind speed data

3.1.1 Data description

The data for wind speeds is composed of a set of hourly average wind speeds at the height of 10 m and 50 m calculated for a raster of gridpoints for the years 2010 to 2015. The choice of these years is arbitrary, however they are the most recent ones available and thus chosen for this work, while the amount of years is chosen as a compromise between representability and data size. The data is a subset of the Modern Era Retrospective-analysis for Research and Analysis (MERRA-2) data set produced by the Global Modeling and Assimilation Office. This data employs a geographical grid of $0.625° \times 0.5°$. The data can be obtained from a web portal [27] and a corresponding file specification is also available [28]. In this work, single level diagnostics have been used, namely the dataset tavg1_2d_slv_Nx. The used variables are listed in Table 3.1. To make sure the positions of all swedish WEC's are included and to allow for the addition of other countries in the nordic synchronous area, a broad geographic area has been selected. It ranges from 53.5° N to 73° N and from 3.125° E to 42.5° E. An example wind speed distribution as documented by MERRA-2 and an impression of the grid resolution are given in Fig. 3.1.

Table 3.1: Used variables from the MERRA-2 dataset tavg1_2d_slv_Nx.

Name	Description	Unit
lon	longitude	° E
lat	latitude	° N
time	minutes since first time in file	min
U10M	10-meter eastward wind	m/s
U50M	50-meter eastward wind	m/s
V10M	10-meter northward wind	m/s
V50M	50-meter northward wind	m/s

The data described in this section has to be processed to be used for the estimation of wind energy production and wind turbine inertia support capabilities. The significant parameter for this estimation working as an input to the WEC model is the hourly average wind speed at the turbines hub height. Since the spatial location of the WEC's diverts from MERRA-2's grid-points, a horizontal interpolation of the wind speed is necessary. A second interpolation step is then used to calculate the wind speed at hub height from the given altitude. The interpolation is applied to each hour in the considered time span of six years independently from the earlier and later values.

3.1.2 Horizontal interpolation

The estimation of the wind speed at the geographical position of the WEC's from the given grid points is achieved through a bicubic interpolation of north- and eastward wind speed components. This algorithm is chosen over the bilinear method suggested in [29], because it yields a smoother fit, the uniform grid point distance introduced in MERRA-2 makes the derivative calculation numerically stable and the increased computation time wasn't a problem in this work. It was implemented using MATLAB's interp2 function, which employs cubic convolution as described in [30]. The algorithm computes values at each query point (i.e. WEC spatial position) based on a cubic interpolation of the values at neighboring grid points. Fig. 3.2 illustrates the process. For a WEC positioned at the shown location, wind

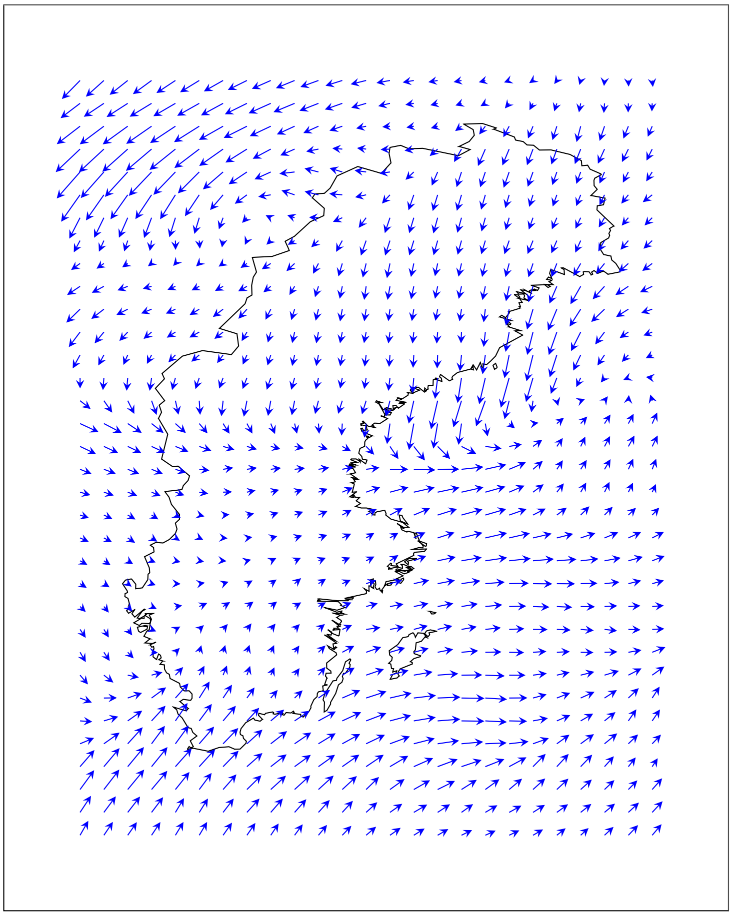

Figure 3.1: Wind speed and direction data at MERRA-2 grid points relevant for Sweden on 3rd of January 2010, 9 a.m.

speeds from all blue grid points are employed in the interpolation. With the use of this algorithm the long- and latitudinal wind speed components are interpolated for each WEC's location independently for both altitude levels present in the utilized MERRA-2 subset (10 m and 50 m). Finally, using the following equation the wind speed magnitude is calculated from the interpolated components:

$$v = \sqrt{v_{\mathrm{u}}^2 + v_{\mathrm{v}}^2} \tag{3.1}$$

in which v_{u} denotes eastward and v_{v} northward wind speed in m/s. The wind direction is not used in the further modelling and thus dropped in the process.

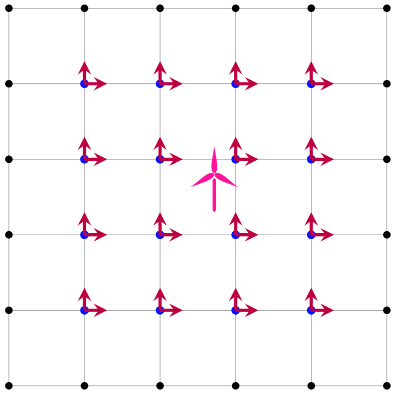

Figure 3.2: Illustration of grid points used during the horizontal wind speed interpolation for a single WEC location.

3.1.3 Vertical interpolation

For the estimation of the wind speed on hub height a logarithmic wind profile is assumed, following the power law given in [29] as

$$v(h) = v(h_{\text{ref}}) \left(\frac{h - d}{h_{\text{ref}} - d} \right)^{\alpha} \tag{3.2}$$

where h denotes height in metres, d displacement height in metres and α is the shear exponent. The displacement height is assumed to be 0 m, because to the author's understanding, any effect of canopy, buildings and geographic features is ignored in the wind modelling of MERRA-2 as well, so the height level of 10 m in MERRA-2 translates to 10 m above displacement height. The shear exponent α is backcalculated for each site from the average wind speeds for the given altitude levels over the complete timespan considered, described by the equation

$$\alpha = \ln \left(\frac{\bar{v}(50\,\text{m})}{\bar{v}(10\,\text{m})} \right) \left(\ln \left(\frac{50\,\text{m}}{10\,\text{m}} \right) \right)^{-1} \tag{3.3}$$

The average wind speeds over the complete timespan are denoted by $\bar{v}$. Finally, the wind speed at hub height is estimated employing equation (3.2), the site-specific shear exponent and the wind speed magnitude from the horizontal interpolation of the 50 m MERRA-2 layer. This wind speed is the input for the WEC model described in the next section.

Since the results of this simulation show considerable differences to the results documented in [31] (see also Section 3.3.1), their approach to determine α has been adapted. Starting with the results generated by the procedure described above, the shear exponent was varied for each site individually so that the simulated annual energy production (AEP) fits the AEP specified in the WEC database. In this process the average simulated AEP of the six years considered in the simulation (2010 to 2015) was used to allow for variation in annual production. The results from this variation of the wind speed show a better fit to the reference in [31], especially for the annual sum of production (see Section 3.3.1). This model using the shear exponent correction will be referred to as WEC system model and is the only one used for further analysis.

3.2 Wind energy conversion

3.2.1 WEC data description

The data about existing and planned WEC's located in Sweden is taken from [31]. It is described in detail in the mentioned report. From the different scenarios in the report ranging from an annual wind energy production of 14.3 TW h to 70 TW h, in this work the base scenario A1 corresponding to an installed WEC capacity of 7.48 GW with an annual energy production of 20 TW h is used, if not stated otherwise.
While the data is of acceptable quality for most existing WEC's, some of the needed values are missing or wrong. This is true for the hub heights of some existing and most planned turbines. Thus, missing or unrealistic hub heights have been estimated by a second order polynomial fit of rated power on the correct values. Fig. 3.3 illustrates the fitting. The pink marks denote all values for hub heights found realistic. The blue curve shows the fitting polynomial. The blue marks indicate all corrected hub height values. Future wind turbines in the database with a rated power above 3.8 MW are exclusively off-shore turbines. Their hub height has manually been set to 90 m reflecting the suggestions in [32].

The database does not contain any information about turbine manufacturers, models or technology. This significates that the distinction between fixed and variable speed turbines as well as between geared and direct drive can not directly be deduced from the available data. Instead, an estimation based on the data of the shares of different WEC types amongst newly installed wind turbines for the years 1995 - 2009 in [33] has been applied. The data shows that variable speed wind turbines (type III and IV) are responsible for the majority of sales from year 2001 on. As a first order appoximation, all turbines older than 2001 are treated as fixed speed in this work. These turbines account for 2.18 % of turbines and 1.26 %

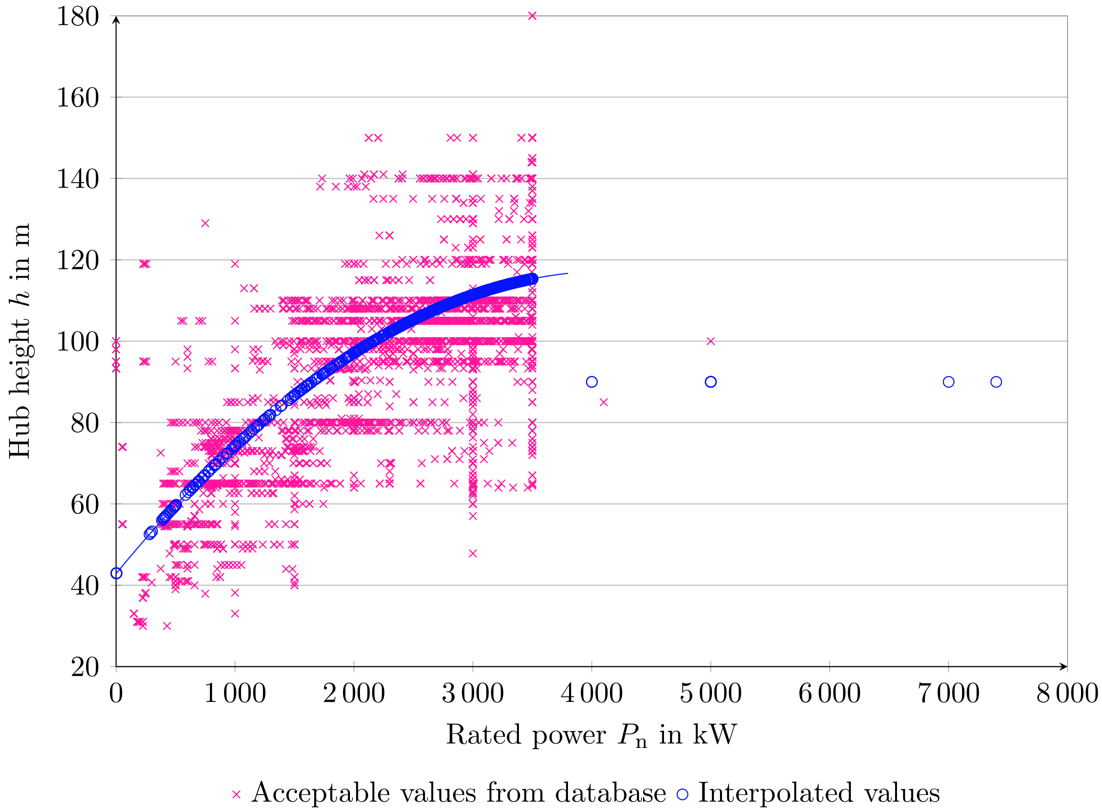

Figure 3.3: Interpolation of missing hub heights based on rated power.

of installed capacity in the base scenario. Since their inertial response is more similar to that of conventional machines, they are not included in the simulation of WEC inertial response. To ensure comparability, they are also excluded from the calculation of kinetic energy and the stationary energy production from wind turbines.

The database furthermore does not include data about the inertia constant of the WEC. Typical inertia constants for wind turbines are given in [3] as 2 s to 6 s, in the description of the rotor design and control principles employed in this project the inertia constant is stated as 5.74 s [34]. Therefore all calculations are made for the inertia constants 3 s, 4 s, 5 s and 6 s. The results presented in this report focus on the inertia constant 3 s, since this can be seen as a lower limit for the mean wind turbine inertia constant of the turbines currently in the system. The values for the other variants are presented as a parameter study in Section 4.3.
While it is obviously incorrect to assume that all wind turbines have the same inertia constant, the effect of this simplification will be negligible for the system-

wide aggregated results.

3.2.2 Steady-state WEC model

In the steady-state WEC model, a variable speed wind turbine is emulated following the principles of rotor design and turbine control depicted in the GE report [34]. The basic principle of this model contains a simple rotor aerodynamic model, a lumped drive train model and a turbine controller. The turbine is equipped with a DFIG and has a rated power of 3.6 MW. The choice between DFIG and full converter has been arbitrarily done. Since the turbine control model as well as the operating limits do not differ between the two types in the used report, the choice is not affecting the simulation results [34]. It is assumed that all mechanical and electrical losses of the turbine are accounted for in the power curve. The turbine specific relation between power coefficient C_P, tip speed ratio λ and pitch angle β is adopted from the source. The power curve is depicted in Fig. 3.4. It has to be noted that although the depicted curve is fitting well only for $3 < \lambda < 15$, it is still used for smaller tip speed ratios during the inertial response simulation. The influence of this error is discussed in Section 3.3.2.

Although in reality there is a big variety of different WEC brands and models in use, the same modeling is applied to all. This introduces imprecision and errors to the model, but is a necessary simplification, since it is not possible to model all brand-specific differences. The results of the modelling are adapted to different turbines by using appropriate rated power and varying the assumed inertia constants. To handle the big number of WEC's and operating states, the model is used to generate a lookup table containing electric power and rotor speed for wind speeds between 0 to 30 m/s at a resolution of 0.01 m/s.

The employed model and functions will be only described briefly with focus on the differences from the approach in the source, since the details are already stated there [34]. There are three different segments of operation - operation at low wind speeds, operation at maximum rotor speed and operation at maximum power, using different control regimes for each.

At a low wind speed, the rotor speed will be adjusted to yield the maximum efficieny, corresponding to the maximum power coefficient $C_\mathrm{P,max}$ and resulting in a fixed tip speed ratio λ_opt. The values for these can be found in Table 3.2. For the same reason the pitch angle will remain 0° in this state. It has to be noted that the resulting power curve slightly differs for very low wind speeds from the one generated by the reference speed approach in [34]. However, this approach has been selected since it is not necessary to resort to a reference speed for the

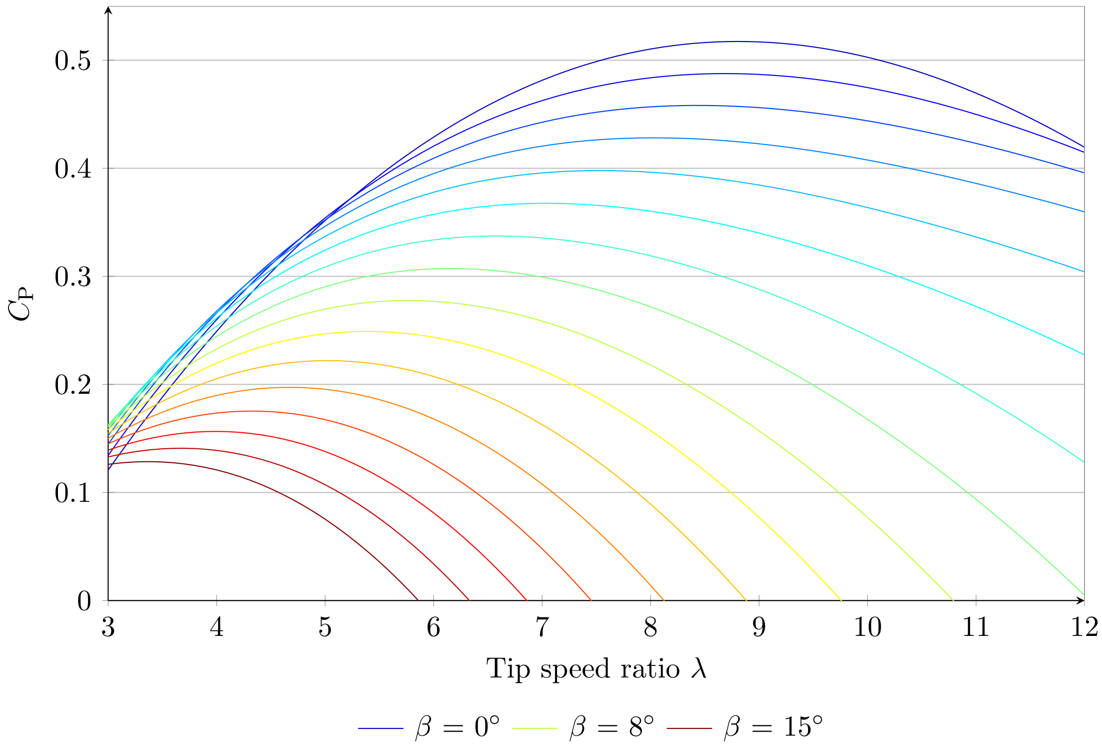

Figure 3.4: Power coefficient C_{P} as a function of tip speed ratio λ for a variety of pitch angles β.

Table 3.2: Constants used in the WEC model.

v_{in}	$3\,\mathrm{m/s}$
v_{out}	$25\,\mathrm{m/s}$
$v_{\omega_{\max}}$	$8.5\,\mathrm{m/s}$
$v_{P_{\max}}$	$11.45\,\mathrm{m/s}$
$\frac{1}{2}\rho_{\mathrm{air}}A_{\mathrm{r}}$	$1.45 \times 10^{-3}\,\mathrm{kg/(m\,W)}$
K_{b}	$62.337\,\mathrm{m\,rad/s}$
$\omega_{\mathrm{pu,max}}$	$1.2\,\mathrm{p.u.}$
$P_{\mathrm{WEC,pu},\omega_{\max}}$	$0.46\,\mathrm{p.u.}$
$C_{\mathrm{P,max}}$	0.5173
λ_{opt}	8.8046

use case at hand and it is more feasible to use a maximum power point tracking control. Basis for the approach is equation (2.12) along with (2.13). The equations are converted to the following per-unit representation:

$$P_{\mathrm{WEC,pu}} = \frac{1}{2}\rho_{\mathrm{air}} A_{\mathrm{r}} v^3 \; C_{\mathrm{P}}(\lambda,\beta) \quad \text{with} \quad A_{\mathrm{r}} = \frac{A}{P_{\mathrm{n}}} \tag{3.4}$$

$$\lambda = K_{\mathrm{b}} \frac{\omega_{\mathrm{pu}}}{v} \quad \text{with} \quad K_{\mathrm{b}} = R\omega_{\mathrm{base}} \tag{3.5}$$

where P_{n} is the WEC's rated electrical power in watts and ω_{base} is the base rotor speed in radians per second equaling to 1 p.u. Since the values for $\frac{1}{2}\rho_{\mathrm{air}} A_{\mathrm{r}}$ and K_{b} given in the source contradict other given values, K_{b} is backcalculated. To achieve this, equations (3.4) and (3.5) are formulated for the border between low wind speed and the maximum rotor speed state. For the relevant model this is the case at an power of $P_{\mathrm{WEC,pu},\omega_{\mathrm{max}}} = 0.46$ p.u. and a rotor speed of $\omega_{\mathrm{pu,max}} = 1.2$ p.u.. Thus, the wind speed at which maximum rotor speed is first reached can be calculated by

$$v_{\omega_{\mathrm{max}}} = \left(\frac{P_{\mathrm{WEC,pu},\omega_{\mathrm{max}}}}{\frac{1}{2}\rho_{\mathrm{air}} A_{\mathrm{r}} C_{\mathrm{P,max}}} \right)^{\frac{1}{3}} \tag{3.6}$$

By the application of equation (3.5) to this case, K_{b} can be calculated:

$$K_{\mathrm{b}} = \lambda_{\mathrm{opt}} \frac{v_{\omega_{\mathrm{max}}}}{\omega_{\mathrm{pu,max}}} \tag{3.7}$$

The calculated value for K_{b} can be found in Table 3.2. The calculated value for λ_{opt} is supported by the investigations in [35]. Under the assumption that the turbine operates at $C_{\mathrm{P,max}}$ and λ_{opt}, the WEC power and rotor speed are calculated for all wind speed steps between cut-in wind speed v_{in} and the wind speed at which the maximum rotor speed is reached $v_{\omega_{\mathrm{max}}}$ using equations (3.4) and (3.5).

The next segment of operation is at the maximum rotor speed but less than 1 p.u. power. In this segment the rotor speed is fixed to $\omega_{\mathrm{pu,max}} = 1.2$ p.u., therefore the turbine discontinues working at the optimal tip speed ratio and maximum power coefficient. The tip speed ratio is dictated by wind speed and the maximum rotor speed and can be calculated by equation (3.5). In the next step, the maximum power coefficient and the corresponding pitch angle are calculated for the given

λ, which are then used to calculate the WEC power with equation (3.4). This is done for all wind speed steps from $v_{\omega_{\max}}$ until the power reaches 1 p.u. Note that the pitch angle remains zero until maximum power is reached for the C_{P}-λ-curve used in this work.

The last segment is to operate at the maximum power. In this segment the rotor speed remains fixed to $\omega_{\mathrm{pu,max}} = 1.2$ p.u. and the power is set to $P_{\mathrm{WEC,pu,max}} = 1$ p.u. With the help of equations (3.4) and (3.5) the corresponding C_{P} and λ are calculated. By the means of these two values the pitch angle can be determined. This procedure is done for all wind speed steps from $v_{P_{\max}}$ to v_{out}.
For wind speeds outside this range, i.e. below v_{in} or above v_{out}, power and rotor speed are set to zero.

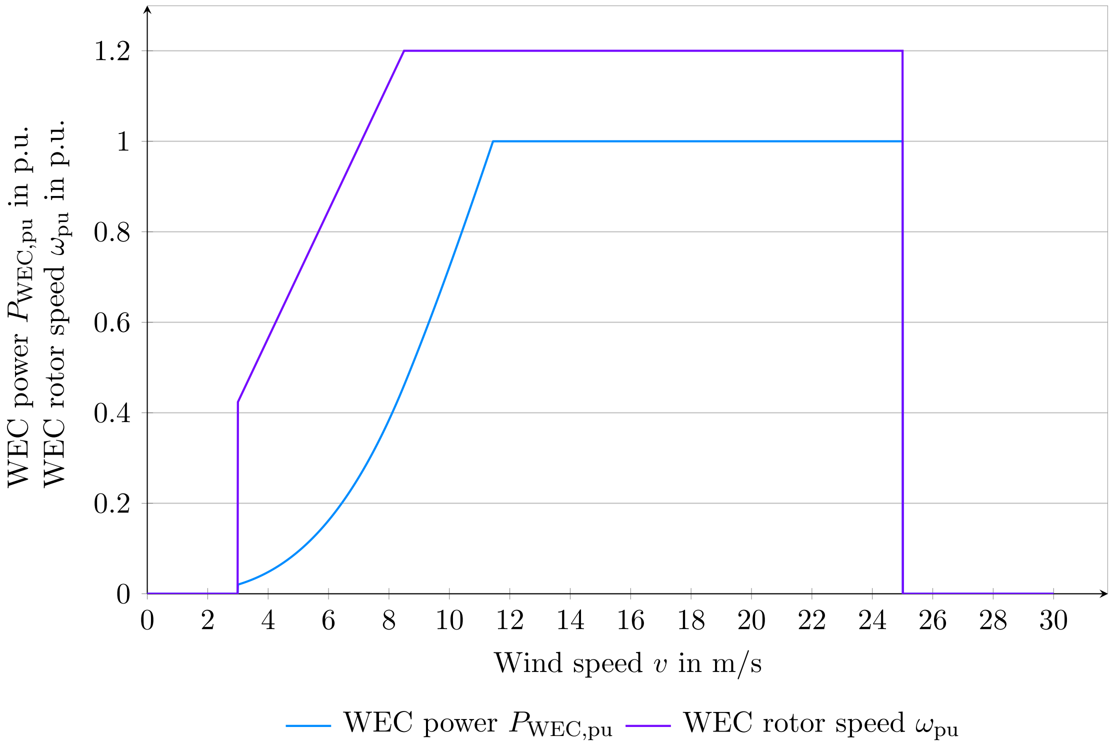

Figure 3.5: WEC power $P_{\mathrm{WEC,pu}}$ and rotor speed ω_{pu} over wind speed as simulated by the wind turbine model for stationary operation.

The resulting power curve and rotor speed curve are shown in Fig. 3.5. Fig. 3.6 illustrates the influence of the tip speed ratio on the power at different wind speeds. As soon as the maximum rotor speed of $\omega_{\mathrm{pu}} = 1.2$ p.u. is reached, the solid line, corresponding to the normal operation, leaves the maximum power point. During

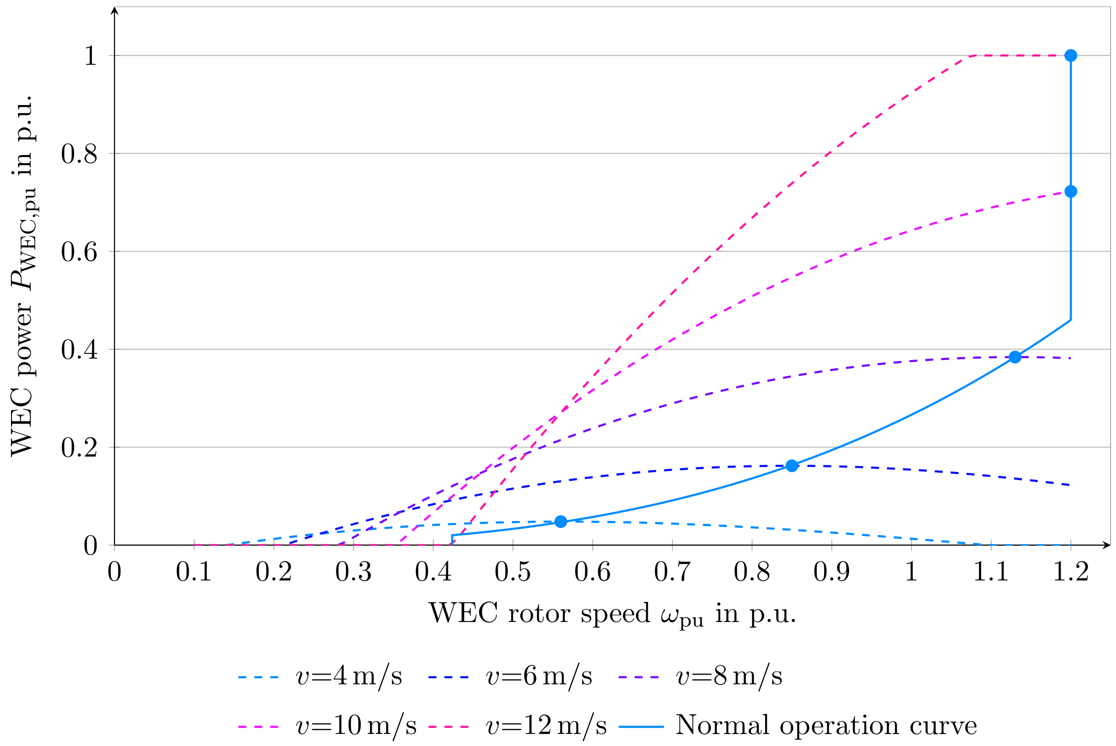

Figure 3.6: WEC power $P_{\mathrm{WEC,pu}}$ over rotor speed ω_{pu} with wind speed as a parameter.

inertial response, if a constant wind speed is assumed, wind turbines shift their operating point along the dashed lines to the left.

The final step of the WEC system model is to combine the corrected hourly mean wind speed gained by the variation of the shear exponent (Section 3.1) and the steady-statie WEC model described in this section. For each WEC in the database and each hour in the considered timespan, the optimal operating electrical power and the rotor speed are determined by using the wind speed and the power curve estimated by the stationary model. The electrical power output is transformed from the per-unit value to an SI-value by multiplication with the turbines rated power. These values are summed up for each hour to estimate the amount of energy produced during one hour by the WEC's included in the database for the investigated scenario (in this work scenario A1 from [31] is used, if not stated otherwise). Where suitable for better comparison, it is represented as the hourly average power from all included wind turbines:

$$P_{\mathrm{WEC,sys}} = \sum_{i=1}^{N_{\mathrm{WEC}}} P_{\mathrm{el,pu},i} P_{\mathrm{n},i} \tag{3.8}$$

where $P_{\mathrm{n},i}$ is the rated electrical power of the i-th WEC and N_{WEC} denotes the number of included WEC's. Please note that the energy production per hour and the hourly average power are used interchangeably in this work.

3.3 Simulation results and discussion

The results presented in this section and the subsequent chapters are based on the parameters shown in Table 3.3, if not indicated otherwise. First, the results of the wind energy production model are presented and compared to the results from [31], further on denoted as reference. This is followed by a discussion of the sources of errors.

Table 3.3: Standard parameters for the presentation of results.

WEC database	Scenario	A1 (20 TW h annual production)
Production simulation	Years	2010-2015
Inertial response simulation	WEC inertial constant H	3 s
	Length of inertia support t_{support}	10 s

3.3.1 Wind energy production

Since in the reference the newest data is available from 2014, the data from 2015 used for this work cannot be included in the comparison and only the years 2010 to 2014 are compared to the reference. Also, only the aggregated hourly energy production is compared, since this is the only data available. Wind and rotor speeds will not be presented. In this section fixed speed turbines are included to ensure comparability with the reference.[31]

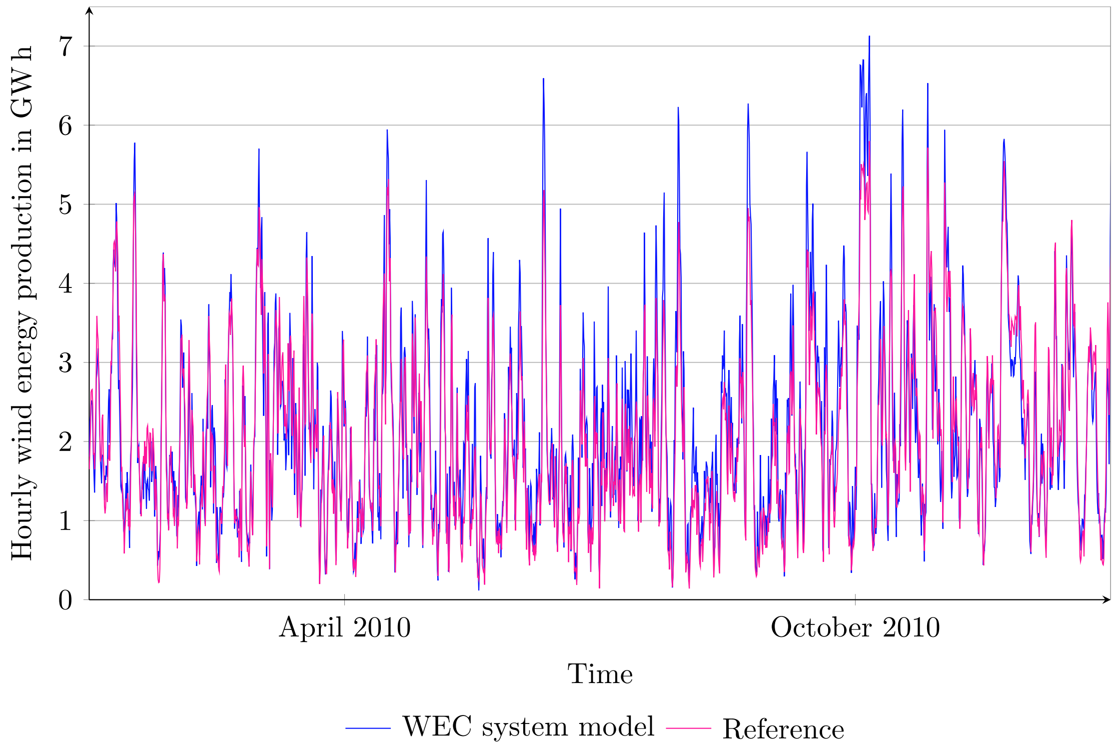

Figure 3.7: Hourly energy production from WEC's as simulated by the WEC system model and by the reference for the year 2010.

Fig. 3.7 presents the aggregated hourly energy production from WEC's as simulated by the WEC system model presented in this report and by the reference for the year 2010. The time series exhibit typical fluctuations and represent seasonal variations as well as short term weather conditions. The values from the WEC system model and the reference show a high correlation, but the WEC system model overshoots in particular during high production intervals.

The differences between the WEC system model and the reference can be depicted further. Fig. 3.8 demonstrates the difference between the hourly generation estimated by the WEC system model and the reference over the course of two years. It can be seen that there is a distinctive seasonal effect in the deviation with overshooting in late summer and autumn, while during winter and early spring the estimates are normally lower than the reference. Table 3.4 gives statistical parameters for the absolute model deviation such as the mean difference, the respective root mean square (RMS) as well as the difference in the annual energy production for the scenarios A1 and A8 (WEC fleet of 2014). In the relevant scenario A1 a deviation in overall energy production of 1.29 TW h, corresponding to 6.39 % (see

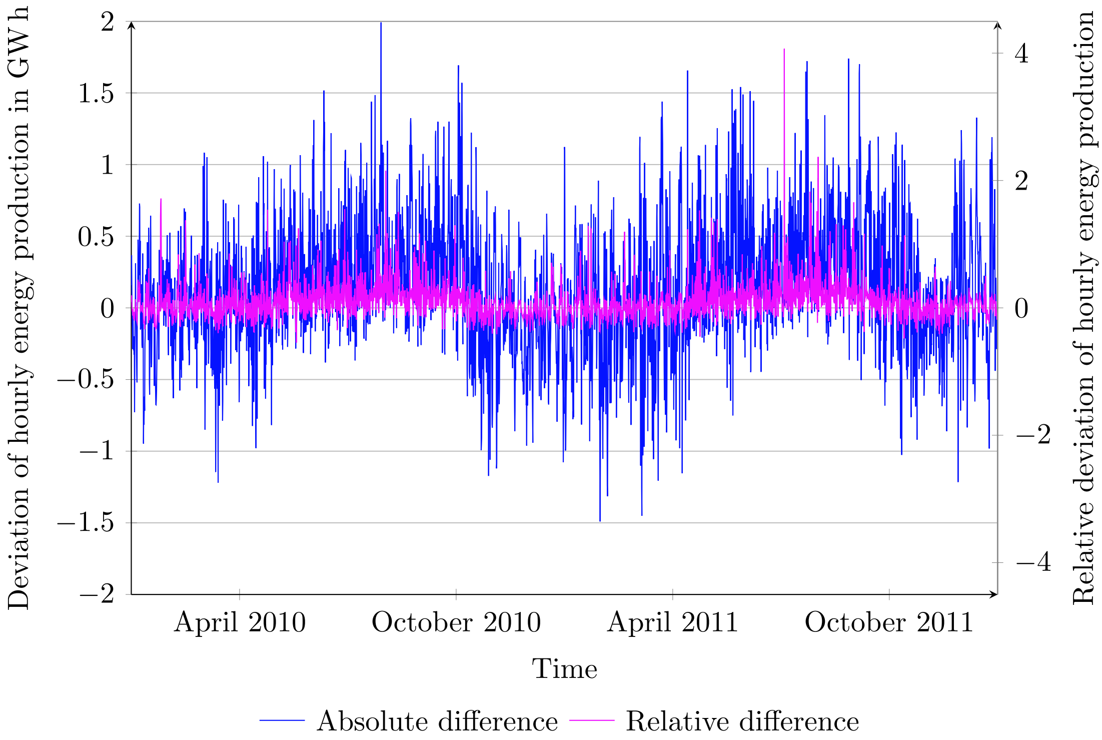

Figure 3.8: Absolute difference between WEC system model hourly generation and the reference.

Table 3.5) has been achieved by the improvements implemented in the model at the cost of an increased average difference. The same parameters are contained in Table 3.5 for relative differences.

The relative frequency of differences is illustrated by the histograms shown in Fig. 3.9 and 3.10. The first is a histogram of the absolute deviations as computed by equation (3.9) while the second contains the relative deviations as computed by equation (3.10):

$$\Delta P_{\text{mod}} = P_{\text{WEC,sys}} - P_{\text{WEC,comp}} \tag{3.9}$$

$$\Delta P_{\text{mod,rel}} = \frac{P_{\text{WEC,sys}} - P_{\text{WEC,comp}}}{P_{\text{WEC,comp}}} \tag{3.10}$$

The symbols ΔP_{mod} and $\Delta P_{\text{mod,rel}}$ denote the absolute respectively the relative difference between wind generation as computed by the improved model, $P_{\text{WEC,sys}}$, and the reference, $P_{\text{WEC,comp}}$. To improve readability outliers have been cut off. In Fig. 3.9 the values over 2 GW h amount to a share of 0.032 % with a maximum difference of 2.34 GW h. In Fig. 3.10 values with a higher relative difference than

Table 3.4: Absolute statistical parameters for the model deviation.

Scenario	Mean absolute difference	RMS absolute difference	Average absolute annual difference
A1 unimproved model	−242.8 MW h	357.8 MW h	−4.33 TW h
A1 WEC system model	143.4 MW h	496.5 MW h	1.26 TW h
A8 unimproved model	−115.8 MW h	215.1 MW h	−2.7 TW h
A8 WEC system model	99.9 MW h	356.9 MW h	0.88 TW h

Table 3.5: Relative statistical parameters for the model deviation

Scenario	Mean relative difference	RMS relative difference	Average relative annual difference
A1 unimproved model	-0.21	0.41	-0.22
A1 WEC system model	0.124	0.569	0.064
A8 unimproved model	-0.16	1.06	-0.19
A1 WEC system model	0.138	1.759	0.063

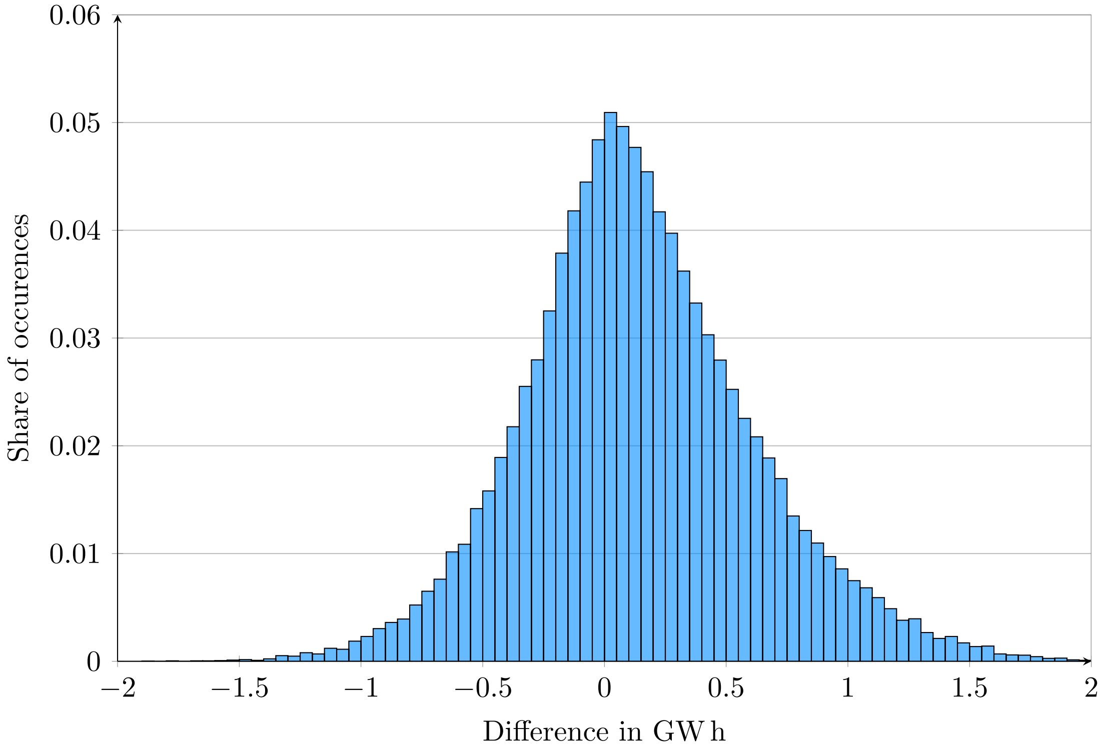

Figure 3.9: Histogram of absolute differences in GW h between the WEC system model system-wide hourly production and the reference. Positive values indicate a higher production in the WEC system model. Total share of values higher than the upper x-axis limit: 0.032 %.

200 % is not displayed. This corresponds to a share of 0.35 % of the values. The maximum relative difference is 8278 %, however this value corresponds to a very low production of 83.7 MW h. Both figures show, that the WEC system model employed in this work tends to surpass the reference slightly more often than to stay behind. There is also a tendency towards small differences, especially visible in the second figure.

A notable difference between the two simulation results are the different extrema of hourly energy production. While the WEC system model has a peak hourly energy production of 7.46 GW h, this value amounts to 6.42 GW h in the reference. Likewise, the minimal energy production differs from 10.2 MW h in the WEC system model to 0 MW h in the reference.

As an example for the operating behaviour simulated by the WEC system model, Fig. 3.11 demonstrates the production during October 2010 from a single wind turbine.

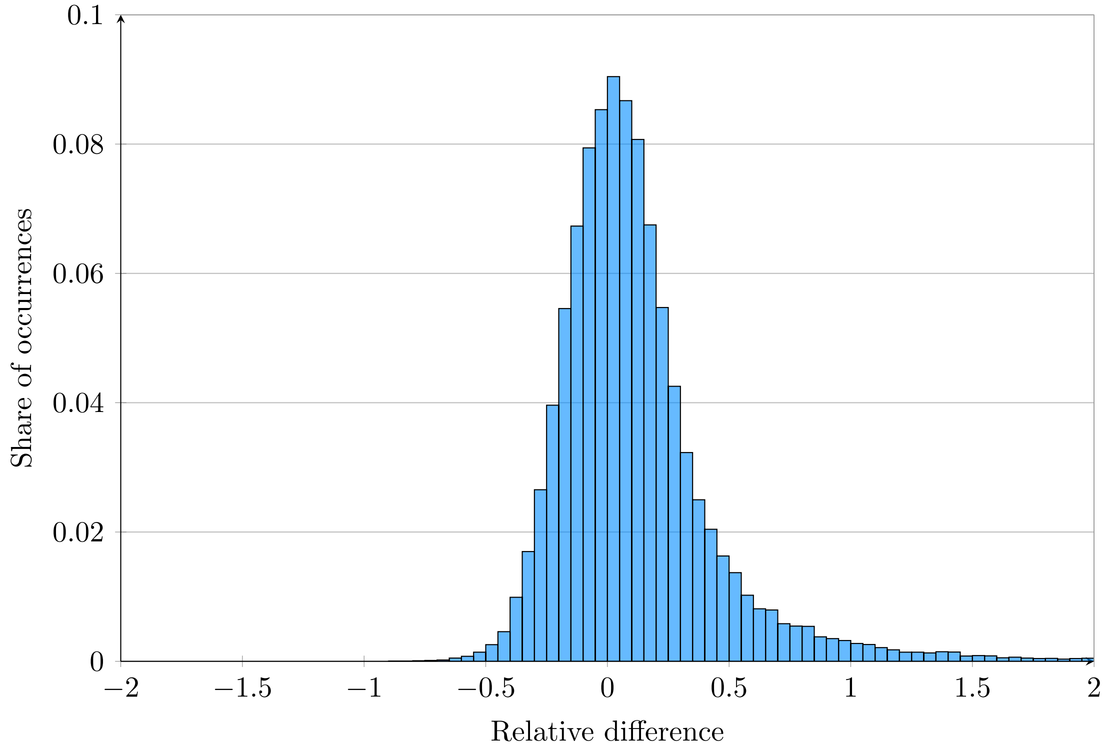

Figure 3.10: Histogram of relative differences between the WEC system model system-wide hourly production and the reference. Positive values indicate a higher production in the WEC system model. Total share of values higher than the upper x-axis limit: 0.35 %.

Fig. 3.12 displays the duration curve of the hourly energy production by wind turbines for the simulated years 2010 to 2015, excluding fixed speed wind turbines along the distribution of production values. Along other characteristics it can be seen that 50 % of the simulated time, the hourly production is above 2.09 GW h. This figure is useful as a reference for the figures shown in Chapter 5.

3.3.2 Discussion on results error

The wind speed data from the MERRA-2 model is re-analysis data, which could be described as the product of a prediction model taking real measurements as an input to generate rastered data. Therefore it has a limited accuracy. However, the most challenging part lies in the ignorance of the local conditions. No information was included about the site-specific canopy height and terrain roughness, which would affect the vertical wind speed interpolation considerably. But it was possible

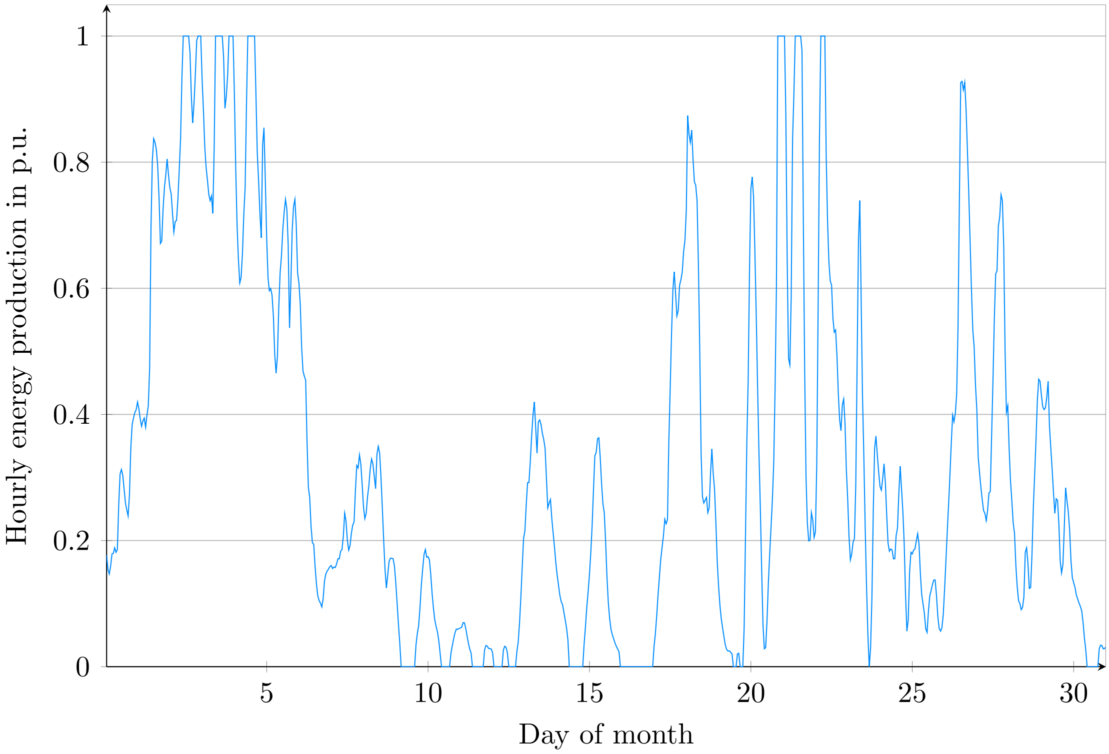

Figure 3.11: Exemplary hourly energy production from a single wind turbine in October 2010.

to restrict the error implicated by this through the correction of the site-specific shear exponent by the expected annual energy production.
As for the WEC data, it is difficult to find exhaustive and consistent data on the Swedish WEC's. It was attempted to combine the used data source with other available databases with the aim of correcting implausible or missing data, however it was not possible to match the individual turbines contained in the databases. Furthermore it would be desirable to have more information on the characteristics of the turbines, e.g. about wind turbine type, type- or model-specific power curves and inertia constants. Like stated in Section 3.2.1, for a notable amount of turbines data on hub heights is incorrect or missing. The error made due to the interpolation of the hub height is likely corrected by the variation of the shear exponent. However, this illustrates the importance of the AEP - if this value is off, the final result is affected heavily. The AEP should therefore collected and checked thoroughly.

As for the WEC system model, the match with the reference (which was matched quite well with real measurements) is acceptable in respect of the annual sum but

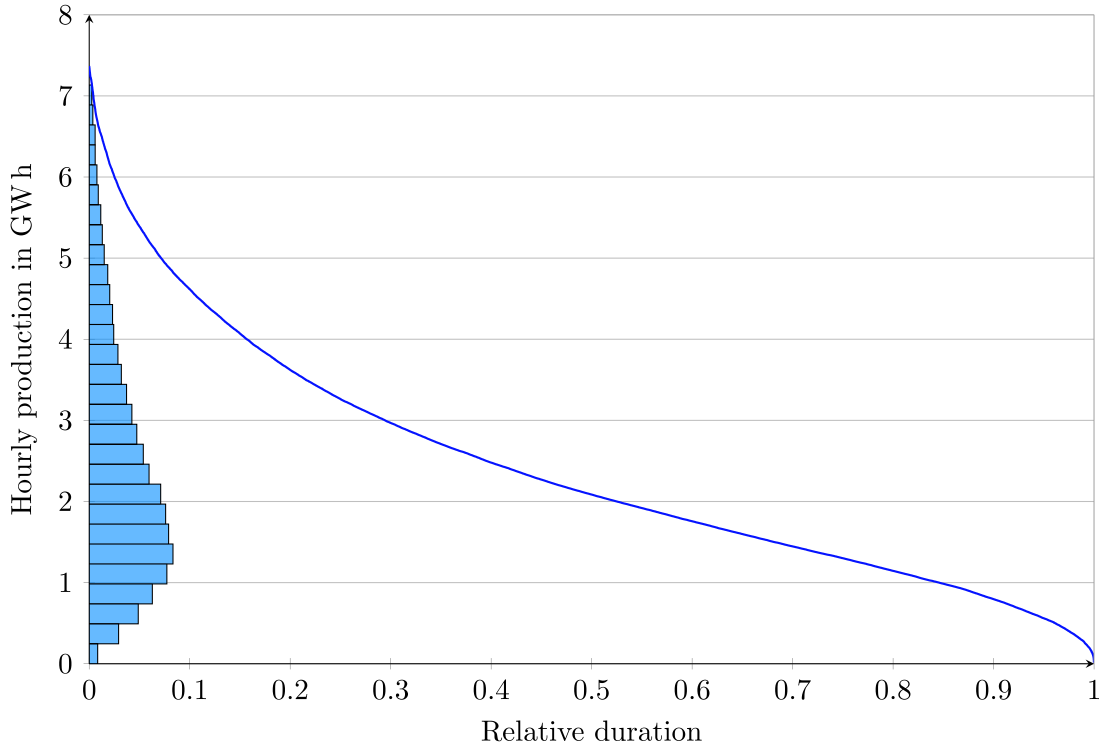

Figure 3.12: Duration curve (cumulative occurences) and distribution of the hourly energy production by wind turbines, excluding fixed speed wind turbines, for the simulated years 2010 to 2015.

far from satisfying in the hour-by-hour deviation, since the values for the mean and RMS difference are still high. This deviation can be caused by missing correction of seasonal bias, explaining the seasonal form of the error. Additionally, in contrast to the reference no correction for the energy contained in short-period frequency deviations has been made. Further effects that have been disregarded are wake effects in wind parks, wind direction, varying air density due to changes in temperature and humidity, inavailabilities and losses due to servicing, icing, turbulences as well as generation and conversion losses beyond the ones regarded in the stationary model power curve. Also, the usage of a single power curve for all installed WEC's obviously neglects the existence of differently optimised turbines for low and high wind speed locations as well as the historical development.
While the differences between the WEC system model and the reference (see also Section 3.3.1) are significant, they seem to be biased only slightly towards overproduction. From this it can be concluded that the data is acceptable for the kind of analysis applied later in this work. However, it would be worthwhile to regard some of the abovementioned effects, especially concerning localised capacity fac-

tors as well as different power curves and inertia constants to study the effects on the spread of data points for the aggregated inertial response.

4

Inertial response evaluation of a single wind turbine

4.1 Kinetic energy and inertial response

This section deals with the calculation of the WEC's kinetic energy and the dynamic model used to simulate the inertial response. In a first step, the kinetic energy of all wind turbines in the system is estimated. Secondly, certain inertia response patterns are assumed and the kinetic energies resulting from this are calculated, which correlates to the kinetic energy available to the system.

For the provision of inertia support by variable speed wind turbines it is crucial to take the operating limits of the supporting turbines into account. General limitations have already been introduced in Section 2.3. However, a quantification of these limits is necessary for the simulation of inertial responses. The limits applied to the different simulation cases employed in this study are given in Table 4.1. Their values are taken in a slightly adapted form from [34] and are further discussed in Section 4.4. A typical short-term overloading limit for generator and converter is given as 10 % in many publications, e.g. in [36]. The minimum rotor speed is set to 0.1 p.u. Like already stated above, many sources mention turbine stall caused by rotor speed deviation as a limit. However, since no reliable values could have been found for this limit, it is implemented by defining an arbitrary lower limit for the mechanical power. In this work, when the turbine generates less than 0.025 p.u. mechanical power, it is tripped as well. This also prevents numerical instability of the model, since the employed power factor parametrisation yields negative values for very low tip speed ratio, which are not allowed and anticipated this way. Turbines initially operating at less than this minimum mechanical power limit defined for the dynamical simulations, i.e. at very low wind speeds ($3\,\mathrm{m/s} < v < 3.23\,\mathrm{m/s}$), are excluded from the inertial response.

The inertia constant is another important parameter for the dynamic model of the wind turbine. In [34] for the 3.6 MW model this value is given as 5.74 s. To account for the big number of different wind turbine models and constructions present in the present Swedish power system, the calculations in this study are done for an inertia constant of 3, 4, 5 and 6 s. This sensitivity analysis allows further insights and gives a resilient estimation of upper and lower boundaries for the presented results.

Table 4.1: Operating limits used for the modelling of the inertial response.

$\omega_{\mathrm{pu,min}}$	0.1 p.u.
$\omega_{\mathrm{pu,max}}$	1.2 p.u.
$C_{\mathrm{P,min}}$	0
$P_{\mathrm{el,max}}$	1.1 p.u.
$P_{\mathrm{mech,max}}$	1.2 p.u.
$P_{\mathrm{mech,min}}$	0.025 p.u.

4.1.1 Kinetic energy calculation

At first the kinetic energy stored in the rotating masses of the wind turbines is calculated. This energy can not be made available to the grid in its entirety due to the operating limits but is still an important measure since it describes the upper limit for the available energy. It is calculated by the following equation, which is a rearranged form of equation (2.3):

$$E_{\mathrm{rot}}(\omega) = \frac{1}{2}J\omega^2 = HP_{\mathrm{n}}\omega_{\mathrm{pu}}^2 \tag{4.1}$$

Utilizing this equation, the kinetic energies for all individual wind turbines are calculated for every simulated sample and then aggregated to the system level.
In this work kinetic energies are normalised on the product of inertia constant and rated power. This means that a value of 1 p.u. corresponds to the kinetic energy of the machine during operation at rated rotor speed. The normalisation is given in the following equation:

$$E_{\mathrm{rot,pu}} = \frac{E_{\mathrm{rot}}}{P_{\mathrm{n}}H} \tag{4.2}$$

4.1.2 Inertial response control strategies

After the calculation of the total kinetic energy the inertial responses from three different control strategies are evaluated. The following control strategies are examined in this work:

- *Fixed power approach:*
  With this approach all wind turbines deliver a fixed electric power until they reach one of their operating limits. In this work this fixed power was set to the short term maximum power of 1.1 p.u. After the turbines operating limits are met, the power output is set to zero until the rotor speed has fully recovered to the same state as before the inertial response. This is necessary because at this point, the mechanical power of the turbine is so low that with any electrical output recovery would be impossible. This approach is illustrated in Fig. 4.1a. In this approach the main goal is to support the grid with the maximum available power and kinetic energy.

- *Fixed time approach:*
  With this approach the power output for each wind turbine is adapted so that the turbine will reach its operating limits just after the end of a specified support period. In this work support periods of 5 and 10 seconds are examined. The power output adaption is calculated through an iterative process with a sensitivity of 50 ms. This sensitivity denotes the length of the time period after the support period during which the limits would be hit. Instead of continuing the support until the limits are hit recovery is started at the end of the support period. For the same reasons as with the fixed power approach, during the recovery period the electrical power output of the turbine is set to zero. This approach is illustrated in Fig. 4.1b. In this approach the main goal is to deliver a maximum amount of support power fixed over a given time span while sacrificing some of the available energy.

- *Fixed power and time approach:*
  In this approach a fixed amount of extra power is delivered for a fixed amount of time. It is an approach similar to the regulation applied by Hydro-Québec TransÉnergie and the WindInertia mechanism implemented by GE [6], [22], [34]. If a wind turbine operates at a minimum power of 0.5 p.u., it will deliver an extra power of 0.1 p.u. for the specified support period of 5 or 10 seconds. Between a power of 0.5 and 0.2 p.u., the amount of additional power is linearly reduced to zero. Wind turbines operating at a power of 0.2 p.u. and less are not participating in the inertial response. The amount of additional support power is depicted in Fig. 4.2. In this figure the inertial response extra power seems non-linear because it is shown in relation to the

wind speed instead of the power.
After the end of the support period, a recovery period is started where the output power is reduced by 0.2 p.u. compared to the state before the inertial response, i.e. the steady-state operation. As soon as the rotor speed has been recovered, the power output is set to the initial value. For turbines with a low inertia constant which are operating in a very small wind speed segment just below rated wind speed, the reduced recovery power still exceeds the current mechanical power at the beginning of the recovery phase. To ensure rotor speed recovery, the electrical output for this turbines is further reduced during the recovery phase.
Turbines that meet their operating limits are tripped instantly. However, during the simulations of this response approach no wind turbine reached its operating limit. This approach is illustrated in Fig. 4.1c. It has the main goal of providing a moderate amount of support power without steering the turbines too far away from their normal operation point and therefore losing too much power during the recovery phase. It uses only a small share of the available kinetic energy.

Comparing the different approaches, it can be concluded that the fixed power and time approach is a conservative method, which is already implemented in a similar form in some wind turbines. On the other hand, the other two approaches put the turbines under unrealistic stress. Due to their aggressive utilization of the WEC's kinetic energy, they also involve a steep power dip during the recovery phase, which would cause a second frequency nadir, possibly deeper than the original one. This means these approaches are not suitable for the usage as a inertial response control strategy. Nevertheless they are studied in this work to determine the upper limits for the available inertia support from wind turbines and to correlate them with inertia from synchronous generation and the more realistic control strategy, i.e. the fixed power and time approach.

4.1.3 Dynamic WEC model

The dynamic model used to simulate the reaction of the wind turbines to these inertial responses is based on solving the differential equation given in (2.6) with the help of the explicit Euler method. The discretised form of the above-mentioned equation can be formulated as

$$\Delta\omega_{\mathrm{pu}} = \frac{P_{\mathrm{mech,pu}} - P_{\mathrm{el,pu}}}{2\omega H_{\mathrm{WEC}}} \Delta t_{\mathrm{sim}} \tag{4.3}$$

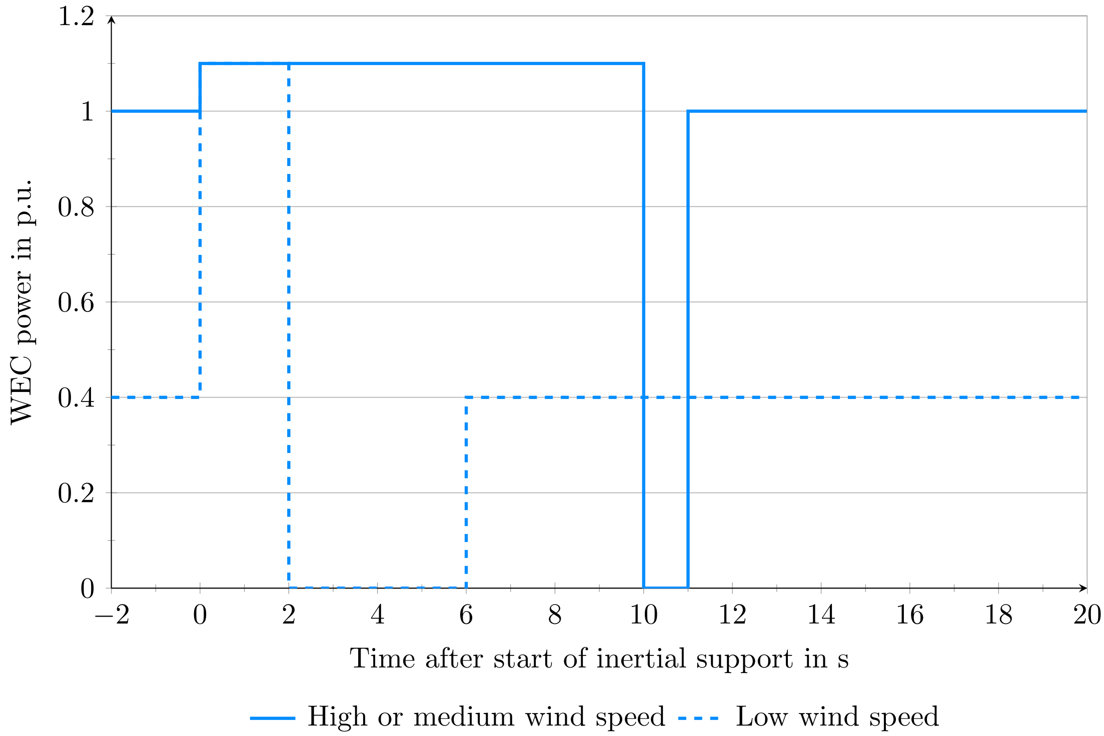

(a) Fixed power approach.

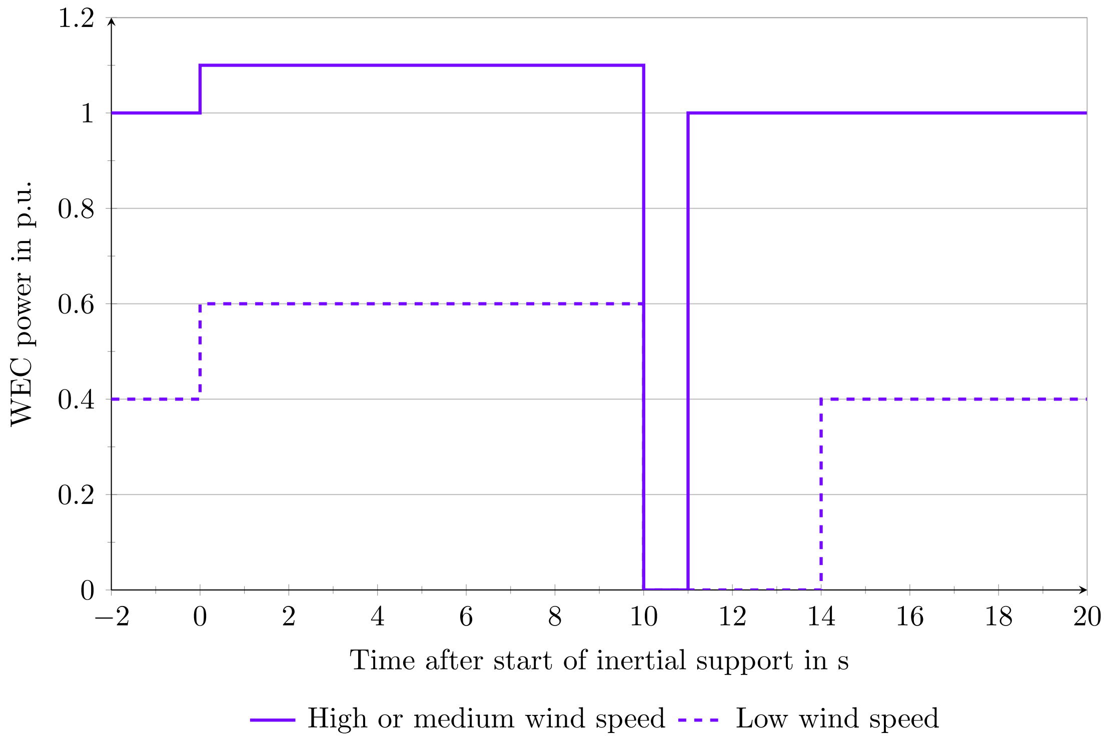

(b) Fixed time approach.

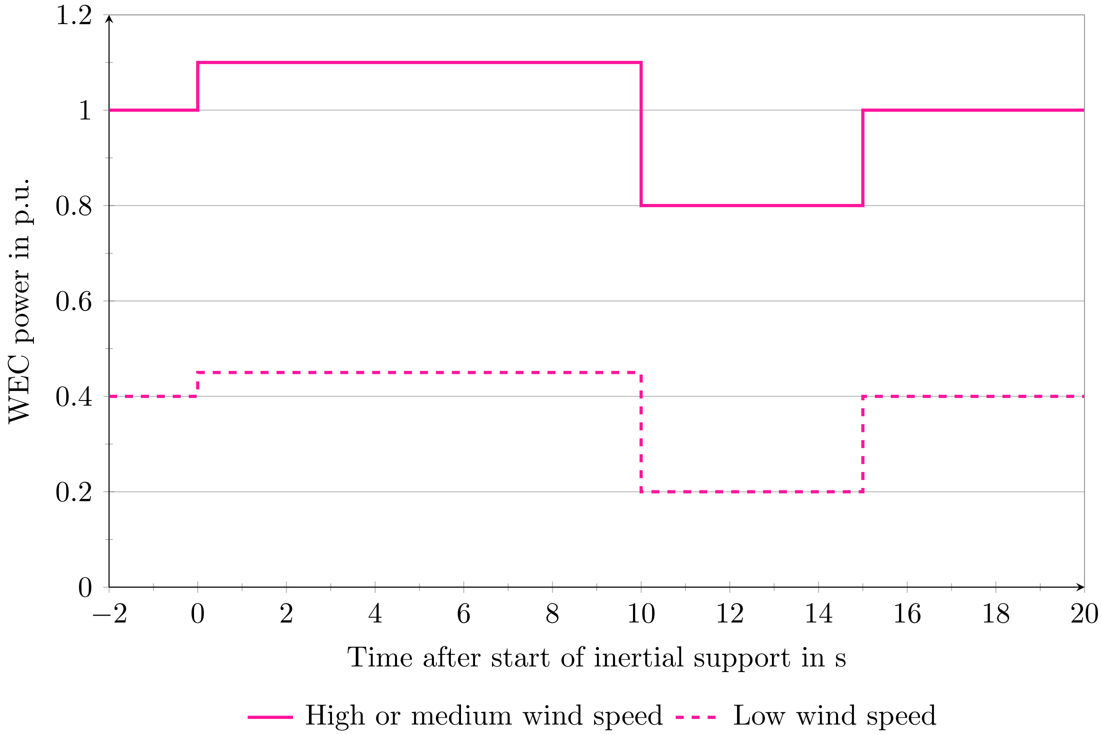

(c) Fixed power and time approach.

Figure 4.1: Examples of the three different inertial response approaches for two different wind speed domains.

where Δt_{sim} describes the length of the simulation step in time in seconds and $\Delta\omega_{\mathrm{pu}}$ the corresponding change in rotor speed in p.u. Instead of the infinitesimal time and rotor speed changes of the original differential equation, finite time steps and rotor speed changes are assumed. The time steps for the model are chosen to 5 ms in favor over the common half-cycle step length to ensure better accuracy and mitigate the missing precision of the chosen solving method. The chosen approach to solve the difference equation, the explicit forward Euler method, is a first-order procedure. The rule to determine the rotor speed at each simulation sample starting from the initial value is formulated as follows:

$$\omega_{\mathrm{pu},k+1} = \omega_{\mathrm{pu},k} + \Delta\omega_{\mathrm{pu},k} \tag{4.4}$$

In this rule $\omega_{\mathrm{pu},k}$ denotes the rotor speed at sample number k and $\Delta\omega_{\mathrm{pu},k}$ the rotor speed change at the same sample, determined by the corresponding form of equation (4.3):

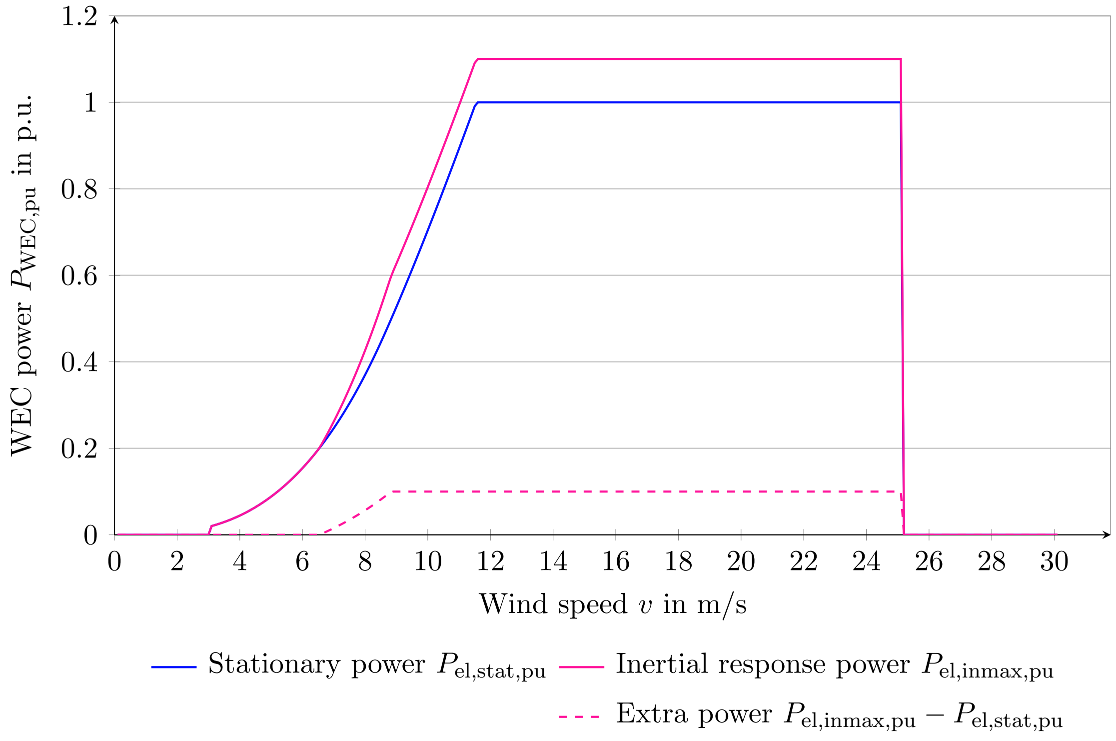

Figure 4.2: Linear increase of the inertial response extra power in relation to the WEC power for fixed power and time approach.

$$\Delta\omega_{\mathrm{pu},k} = \frac{P_{\mathrm{mech,pu},k} - P_{\mathrm{el,pu},k}}{2H_{\mathrm{WEC}}\omega_{\mathrm{pu},k}}\Delta t \tag{4.5}$$

This calculation is repeated for each simulation sample until the simulation time of 60 s is reached. During each step, the mechanical power $P_{\mathrm{mech,pu},k}$ has to be recalculated. While wind speed and pitch angle remain unchanged, rotor speed and thus C_{P} are subject to change. The pitch angle is left unchanged because it is unclear if it can react fast enough for inertial response to benefit. Furthermore, the chosen approach focuses mainly on the kinetic energy contribution from the wind turbine rotor inertia. However, the pitch angle is allowed to be adapted to limit the mechanical power to the current electrical power to prevent overspeeding. This is necessary because at high wind speeds, a reduced tip speed ratio results in a higher power coefficient if the pitch angle is held constant (see also Fig. 3.4). During the recovery period the pitch angle is also allowed to vary to increase the aerodynamic efficiency and thus to shorten the recovery time.

The equation to recalculate the mechanical power is given with help of equation (3.5) as follows:

$$P_{\mathrm{mech,pu},k} = \frac{1}{2}\rho_{\mathrm{air}} A_{\mathrm{r}} v^3 \; C_{\mathrm{P},k}(\lambda_k, \beta) \quad \text{with} \quad \lambda_k = K_{\mathrm{b}} \frac{\omega_{\mathrm{pu},k}}{v} \tag{4.6}$$

The simulations are carried out for each of the wind speeds used in the static model. After each completed simulation, a verification is conducted. The results are verified by the balance of energy. This is accomplished by employing equation (2.15) for each sample and wind speed:

$$\epsilon_k = H(\omega^2_{\mathrm{pu},k+1} - \omega^2_{\mathrm{pu},k}) - (P_{\mathrm{mech,pu},k} - P_{\mathrm{el,pu},k})\Delta t_{\mathrm{sim}} \tag{4.7}$$

In this equation, ϵ_k denotes the difference between the two methods to calculate the energy difference between two consecutive samples. Ideally, it should be zero. It can be set in relation to the energy difference calculated by the rotor speed change and is then named δ_k:

$$\delta_k = \frac{\epsilon_k}{H(\omega^2_{\mathrm{pu},k+1} - \omega^2_{\mathrm{pu},k})} = \frac{H(\omega^2_{\mathrm{pu},k+1} - \omega^2_{\mathrm{pu},k}) - (P_{\mathrm{mech,pu},k} - P_{\mathrm{el,pu},k})\Delta t_{\mathrm{sim}}}{H(\omega^2_{\mathrm{pu},k+1} - \omega^2_{\mathrm{pu},k})} \tag{4.8}$$

The results of this verification are shown and further discussed in Section 4.4.

4.1.4 Characteristics for further analysis

The results of the inertial response simulation are later aggregated to allow for a system-wide analysis. The following key characteristics are determined and estimated for each of the investigated wind speeds for the comparison and aggregation of the simulation results.

- *Maximum power:* This denotes the maximum electrical power output reached by a wind turbine at the given wind speed during the inertia support phase. It is given by:

$$P_{\mathrm{el,pu,inmax}} = \max(P_{\mathrm{el,pu},k}) \tag{4.9}$$

- *Minimum power:* This denotes the minimum electrical power output reached by a wind turbine at the given wind speed during the recovery phase. It is given by:

$$P_{\text{el,pu,inmin}} = \min(P_{\text{el,pu},k}) \tag{4.10}$$

- *Minimum rotor speed:* The minimum rotor speed during inertial response ω_{min}, normally reached at the end of the inertia support phase, is an important characteristic to calculate how much kinetic energy is left in the turbine rotor after the inertial support phase. It also illustrates how far it has been taken from its normal operation point and therefore allows to anticipate the losses and length of the recovery phase.

- *Support and recovery time:* The length of the support phase t_{sup} is variable for the fixed power approach while it is fixed for the two other approaches. In the former approach it is a good indicator of available energy and an important characteristic, though. The length of the recovery phase t_{rec} is measured from the start of the turbines recovery until it reaches its stationary operating point again and is a key characteristic for all approaches. It illustrates how far turbines have been taken from their stationary operating point and is furthermore an important characteristic because the recovery phase is critical for the frequency stability of the system.

- *Energy difference during support phase:* This characteristic describes the energy which is fed to the grid during the support phase additionally to the stationary operation. It can be computed by the following equation:

$$E_{\text{sup,pu}} = \sum_{k=k_{\text{sup,start}}}^{k_{\text{sup,end}}} (P_{\text{el,pu},k} - P_{\text{el,stat,pu}}) \frac{\Delta t_{\text{sim}}}{H} \tag{4.11}$$

  The symbol $P_{\text{el,stat,pu}}$ denotes the stationary electrical power output of the wind turbine, $k_{\text{sup,start}}$ and $k_{\text{sup,end}}$ stand for the sample number of the start respectively end of the support phase. Please note that for this and the following energies the same normalisation base has been chosen as for the kinetic energy (see equation (4.2)).

- *Energy difference during recovery phase:* This denotes the energy difference during the recovery phase, compared to the stationary operation. It is negative or zero and is computed by the following equation:

$$E_{\text{rec,pu}} = \sum_{k=k_{\text{rec,start}}}^{k_{\text{rec,end}}} (P_{\text{el,pu},k} - P_{\text{el,stat,pu}}) \frac{\Delta t_{\text{sim}}}{H} \tag{4.12}$$

The symbol $k_{\text{rec,start}}$ and $k_{\text{rec,end}}$ denote the sample number of the start respectively end of the recovery phase.

- *Energy loss during inertial response:* The energy balance during the complete inertial response compared to the stationary operation is computed by summing up the energy differences during support and recovery phase:

$$E_{\text{bal,pu}} = E_{\text{sup,pu}} + E_{\text{rec,pu}} \tag{4.13}$$

This number is negative when more energy is lost during recovery than gained during support. This is the case when the aerodynamical efficiency is lower than during the stationary operation, which is true for all wind speeds below rated wind speed.

4.2 Single turbine inertial response simulation results and discussions

4.2.1 Kinetic energy

In this section the results of the estimation of kinetic energy are presented. The default parameters used for these results are unchanged from the previous chapter and can be found in Table 3.3. The support time for all results presented in this and the following chapters is 10 s. The results for the simulation of 5 s support time are not presented in this work since they are very similar and do not contribute any additional insights.
The relation between rotor speed and kinetic energy is obvious, since the kinetic energy increases quadratically with the rotor speed as shown in equation (4.1). The relation between kinetic energy and wind speed is thus the square of the rotor speed curve shown in Fig. 3.5. An interesting observation can be made by studying the relation between the wind power and kinetic energy as shown in Fig. 4.3. This figure clarifies that at a power of $P_{\text{WEC},\omega_{\max}} = 0.46$ p.u., the maximum rotor speed is reached and consequently the kinetic energy does not increase further beyond this point. In the following sections it will be shown how the amount of energy for inertial response is comparing to this.

4.2.2 Inertial response

Exemplary time series of the three investigated WEC inertial response approaches considered in this work have already been presented in Fig. 4.1. Therefore in

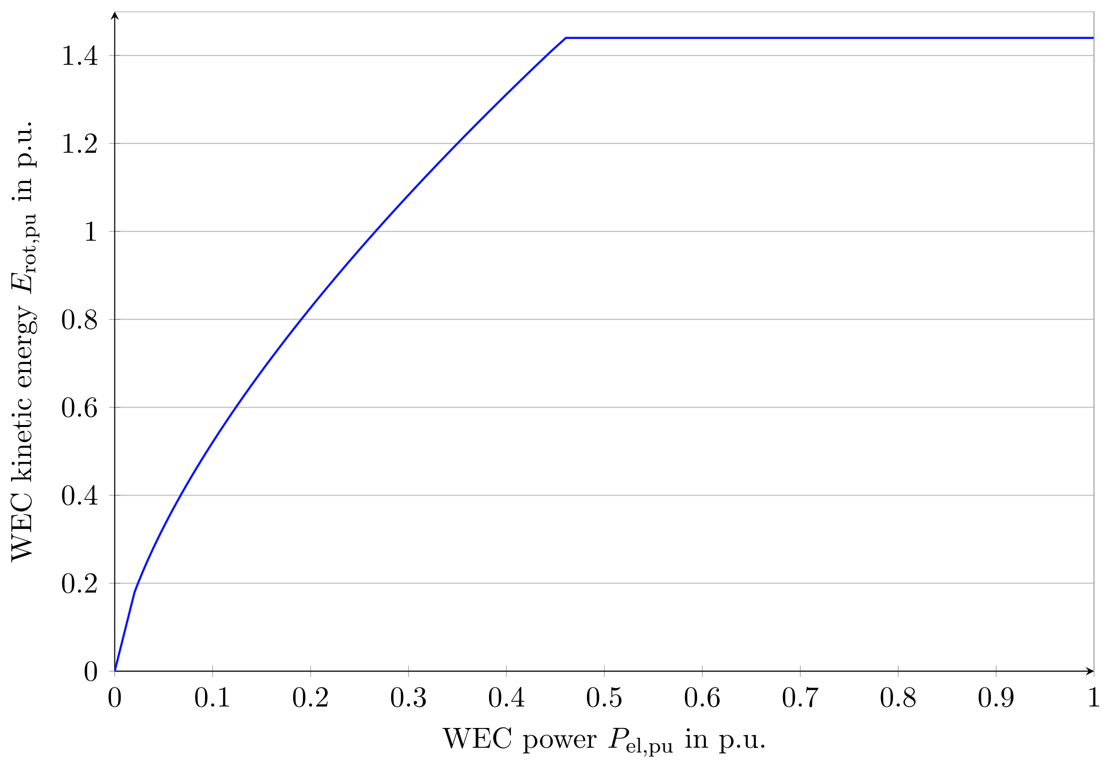

Figure 4.3: WEC kinetic energy $E_{\mathrm{rot,pu}}$ over WEC power $P_{\mathrm{el,pu}}$.

this section the relation between the wind speed and the different characteristics presented in Section 4.1.4 are in the focus.

The first characteristic to be considered is the maximum power during inertia support $P_{\mathrm{el,inmax}}$. Fig. 4.4 presents this characteristic in relation to the wind speed with the stationary power curve as a reference. For the fixed power approach, even for small wind speeds the maximum electrical power is delivered as per the approach specification. For the fixed power and time approach the curve also follows the curve given in the specification and shown in Fig. 4.2. The relation for the fixed time approach is the result of the iteration and the condition that the turbine should deliver as much power as possible without reaching its operation limit before the specified support time. In conclusion, the difference in support power between fixed time and fixed power and time approach is exceeding 0.1 p.u. for medium wind speeds in the range of 5 m/s to 11 m/s with its maximum reaching approx. 0.25 p.u. at $v_{\omega_{\max}}$. This difference is also depicted in the aforementioned figure. It has also to be noted that for wind speeds above $v_{P_{\max}}$ there exists no difference in support power from all three approaches due to the converters short term limit.

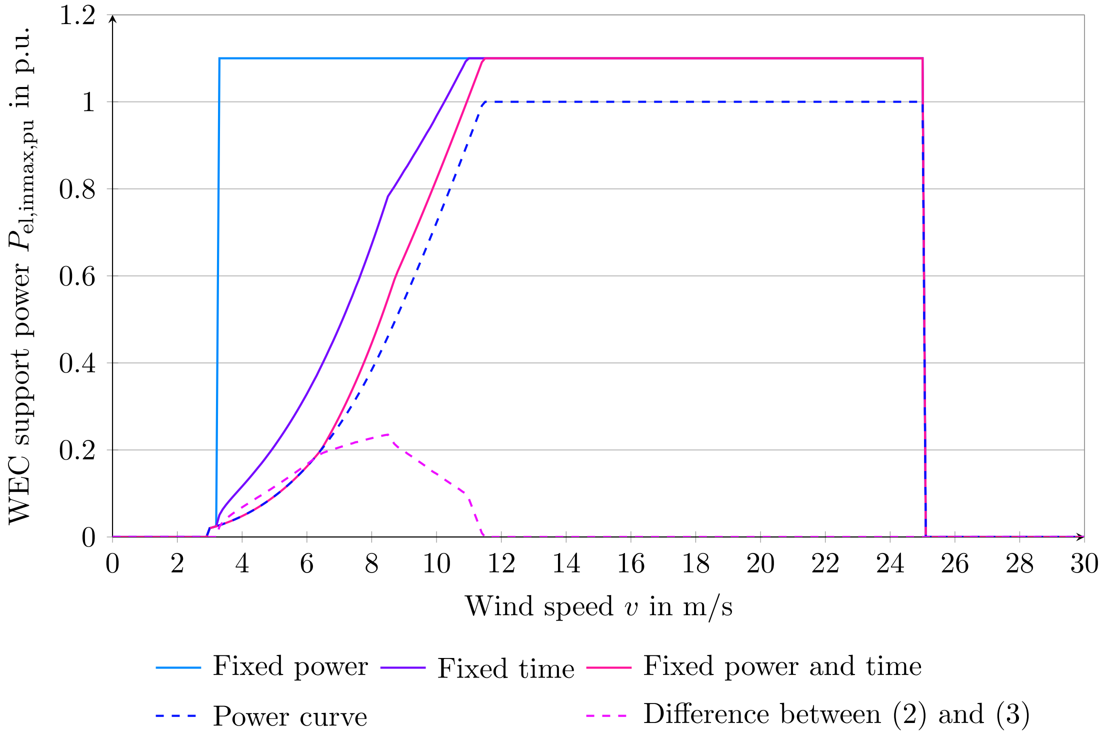

Figure 4.4: WEC inertia support power $P_{\mathrm{el,inmax,pu}}$ in relation to the wind speed v, including the stationary power curve and the difference between fixed time approach and fixed time and power approach as a reference.

The behaviour of the relevant energies during inertial response in relation to the wind speed is depicted in Fig. 4.5. The additional energy delivered during the support phase, $E_{\mathrm{sup,pu}}$, is depicted as dotted curves, the energy difference during the recovery phase, $E_{\mathrm{rec,pu}}$, is displayed as a dashed curve. The energy balance is presented as a solid line. All energies are shown normalised to rated power and inertia constant like described in equation (4.2). For both the fixed power and the fixed time approach the support energy reaches it maximum at $v_{\omega_{\mathrm{max}}}$. For the fixed power approach this is the case because the product of support time (see also Fig. 4.7) and the difference between support power and stationary power is the highest at this point. For the fixed time approach here only the latter is relevant, since the support time is fixed. Inspecting Fig. 4.4, it can be reassured that the extra power has its maximum at this point. After this maximum the support energies decrease again until they reach the same level as the third approach at $v_{P_{\mathrm{max}}}$. The cause for the difference between the two approaches can be found in the higher losses of the fixed time approach. Since the support period of the fixed time approach, during which the turbine generates less aerodynamic

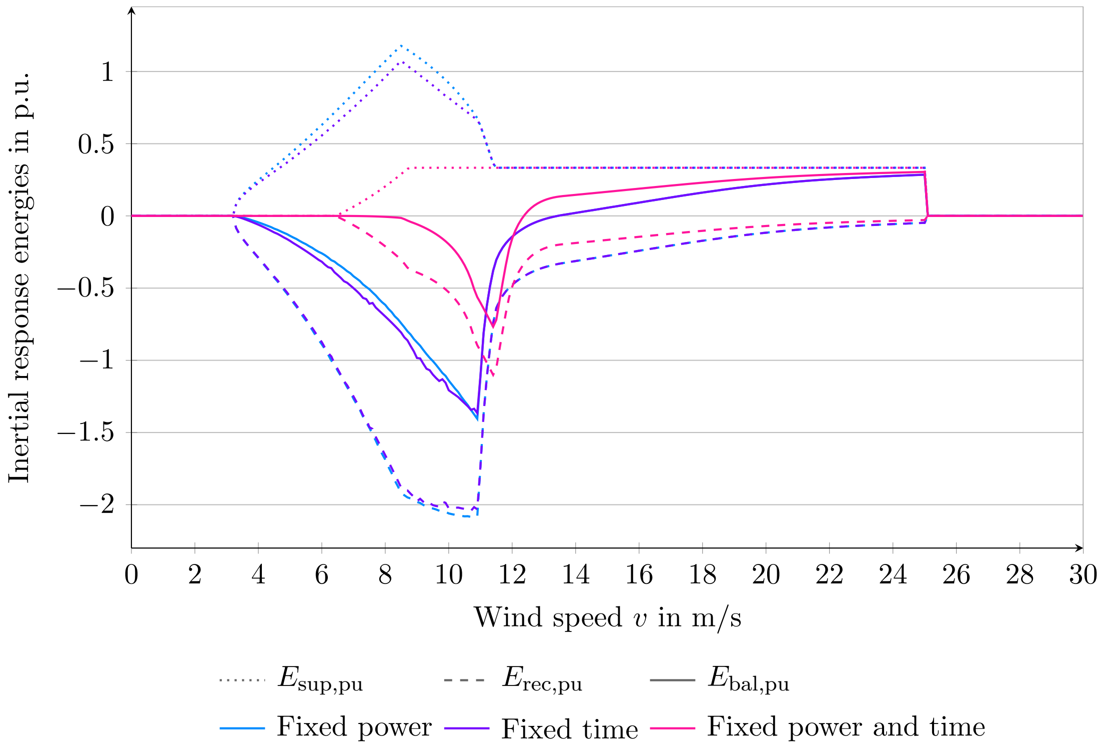

Figure 4.5: Normalised inertial response energies $E_{\text{sup,pu}}$, $E_{\text{rec,pu}}$ and $E_{\text{bal,pu}}$ for the three different approaches over wind speed v.

power than it feeds to the grid, is longer than in the fixed power approach, higher losses can be expected. As soon as the fixed power approach reaches a support time equalling the specification for the fixed time approach, the difference has vanished. For the fixed power and time approach the curve is initially, for wind speeds below approx. 6.5 m/s, zero because the turbines operating at this wind speed generate less than 0.2 p.u. power and deliver zero support power due to the specification of the approach. Further on the curve is increasing between $P_{\text{el,stat,pu}} = 0.2$ p.u. and $P_{\text{el,stat,pu}} = 0.5$ p.u. alongside the extra power. After the maximum extra power is reached, the amount of energy is held constant. The final value of the support energy is 0.33 p.u., with the maximum reached by the fixed power approach amounting to 1.18 p.u. This compares to a maximum of kinetic energy of 1.44 p.u. (compare Fig. 4.3). According to this, the fixed power approach would allow for the utilization of a maximum of nearly 82 % of the turbines kinetic energy, while the fixed power and time approach reaches it maximum at a share of 23 %.

The amount of energy lost during recovery, depicted with dashed lines, behaves very differently. It reaches its minimum for both the fixed power and the fixed

time approach at a wind speed slightly below $v_{P_{\max}}$ with a value of approximately -2.1 p.u. This position is caused by the complex connections between support time respectively power, minimum rotor speed (see Fig. 4.6) and the changing sensitivity of the power factor C_{P} to variations in tip speed ratio λ (see Fig. 3.6). The curve for the fixed power and time approach behaves more intuitively since the turbines are removed not as far from their stationary operating point as in the other two approaches. Corresponding to the rising gradient for higher wind speeds in Fig. 3.6, the necessary recovery energy is increasing until $v_{P_{\max}}$. Since at this point the turbine starts to adjust the pitch angle to limit the aerodynamic power to its rated power, a faster recovery is possible. The big difference between the first two and the last approach is caused by the bigger extraction of kinetic energy by the former. Hence a longer recovery phase, starting with a more unfavorable operating point, is necessary. It has also to be noted that for the first two approaches the electric output during the recovery phase is set to 0 p.u., while for the fixed power and time approach the turbine output is reduced only slightly during recovery. This explains the remaining difference at wind speeds beyond 12 m/s.
The energy balance of the inertial response, represented by the solid lines, is the sum of the two energies. It quantifies the net amount of energy lost during the inertial response. For a 3.6 MW turbine with an inertia constant of 3 s, this sums up in the worst case (fixed power at approx. 10.9 m/s corresponds to -1.4 p.u.) to 4.2 kW h, which can be calculated by (4.2). It can also be seen that for wind speeds above a certain threshold the net energy is positive. This is the case because during inertial response the turbines power rating is de-facto raised by 10 %, allowing for a higher energy gain during this period.

Another important characteristic is the minimum rotor speed reached during inertial response, shown in Fig. 4.6. For the majority of wind speeds, turbines during both fixed power and fixed time approach reach the operating limit of zero aerodynamic power before their rotor speed drops to zero. This is of course dependent on the turbine design and the parametrisation of the C_{P}-curve. However, it is a realistic effect resembling rotor stall due to dramatically decreased aerodynamic lift like mentioned in [8]. Since the turbines in both approaches are brought to their operating limits, the curves look very similar. The rising slope between wind speeds of 4.5 m/s and $v_{P_{\max}}$ can be explained by a look at Fig. 3.6, which illustrates that the roots of the power curve are at a higher rotor speed for higher wind speeds, resulting in a constant tip speed ratio. Since support time respectively power reach their maximum at $v_{P_{\max}}$, the minimum rotor speed rises steeply from this point until meeting with the curve of the last approach. The difference between stationary and minimum rotor speed approaches zero, because at higher pitch angles, which are caused by high wind speeds, the maximum of the power coefficient moves to a lower tip speed ratio than the steady-state λ. Therefore

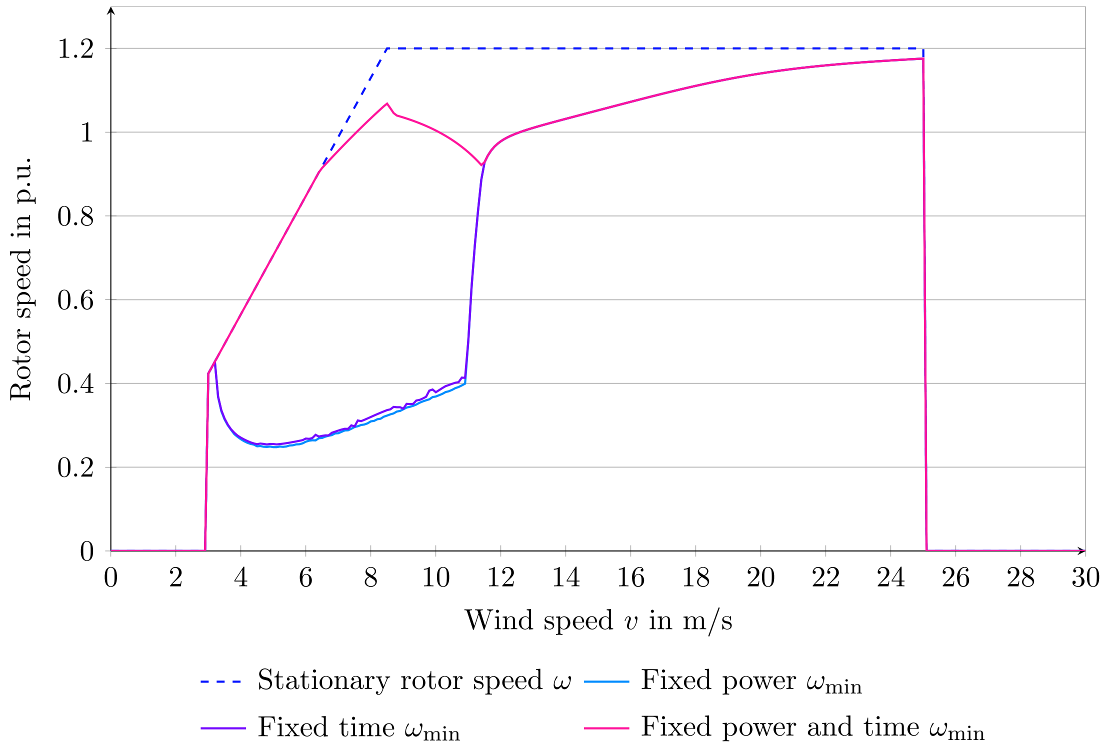

Figure 4.6: Minimum rotor speed during inertia support $\omega_{\text{min,pu}}$ over wind speed v, including the stationary rotor speed as a reference.

at high wind speeds a lower rotor speed is associated with a higher aerodynamic efficiency and power (see Fig. 3.4). The turbines in this wind speed range do not steadily lose rotor speed but are in a new stable operating point. There is a small difference between the fixed power and the fixed time approach. It is caused by the limited sensitivity of the iterative support power estimation of the fixed time approach: Not at all wind speeds the turbines reach their operating limits exactly at the end of the support time, so sometimes they can retain a small part of their kinetic energy. This is reflected by a slightly higher minimum rotor speed.
For the fixed power and time approach, due to the high power requisites of inertial response (0.2 p.u., reduced response until 0.5 p.u.) the rotor speed difference between minimum and normal operating rotor speed is small and increasing slowly at first. Shortly after $v_{\omega_{\max}}$, the maximum extra power of 0.1 p.u. is reached. Because of the increasing slopes of the curves in Fig. 3.6 associated with the further distance from the maximum power point at higher wind speeds, aerodynamic losses augment with the wind speed between $v_{\omega_{\max}}$ and $v_{P_{\max}}$. This results in a lower minimum rotor speed although the support energy remains constant.

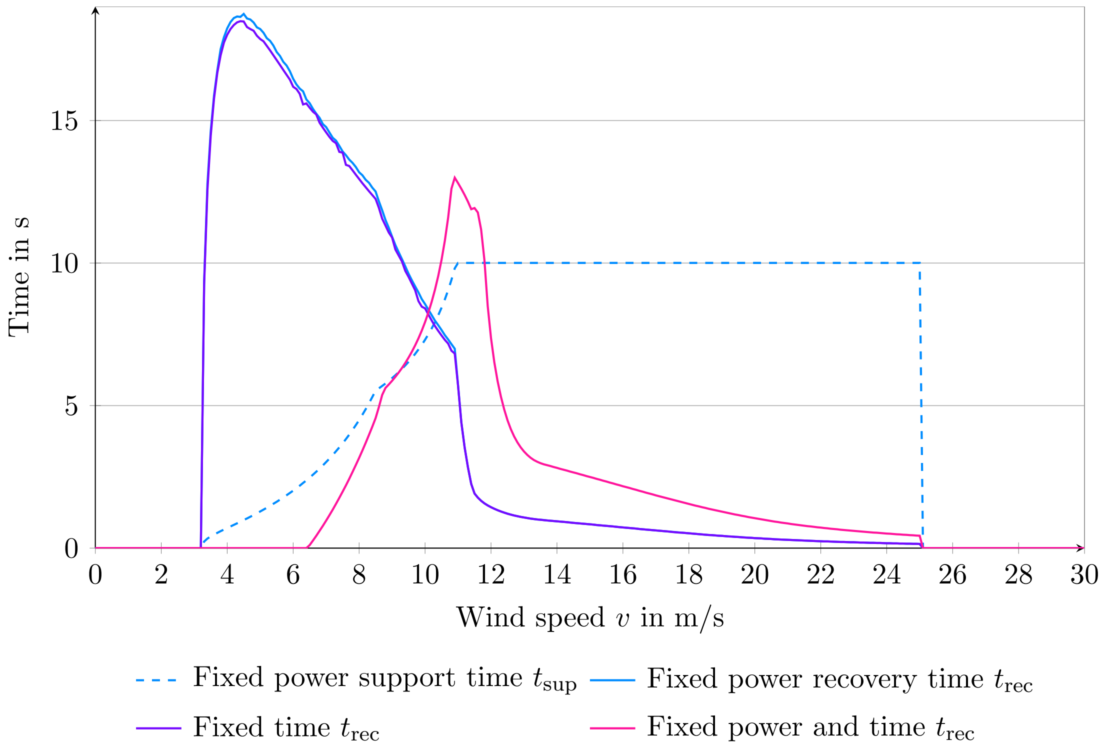

Figure 4.7: Recovery time t_{rec} in relation to the wind speed v for all three inertial response approaches, also including the support time t_{sup} of the fixed power approach.

The final characteristic considered in this section is the time needed for recovery. Fig. 4.7 presents recovery time t_{rec} and, in the case of the fixed power approach, the support time t_{sup}. For both fixed time and fixed power and time approach the support time is set to 10 s, hence these curves are omitted.
The fixed power support time, represented by the dashed line, increases with the wind speed until it is capped at 10 s to ensure comparability with the other approaches. The curves for the recovery time of both fixed power and fixed time approach have their maximum at the same position where the minimum rotor speed has been observed. It amounts to approx. 18.5 s at a wind speed of 4.5 m/s. The correlation between minimum rotor speed and recovery time is strong for the fixed power and time approach, which is why the explanation of the position of the extremum will not be repeated here.
As mentioned before, both fixed power and fixed time approach do not deliver any energy to the grid during recovery, whereas with the fixed power and time approach turbines are only allowed to reduce their output. In the wind speed range above 10 m/s this results in longer recovery times even when the minimum rotor

speed is higher, which is the case below $v_{P_{\max}}$.

4.3 Influence of inertia constant

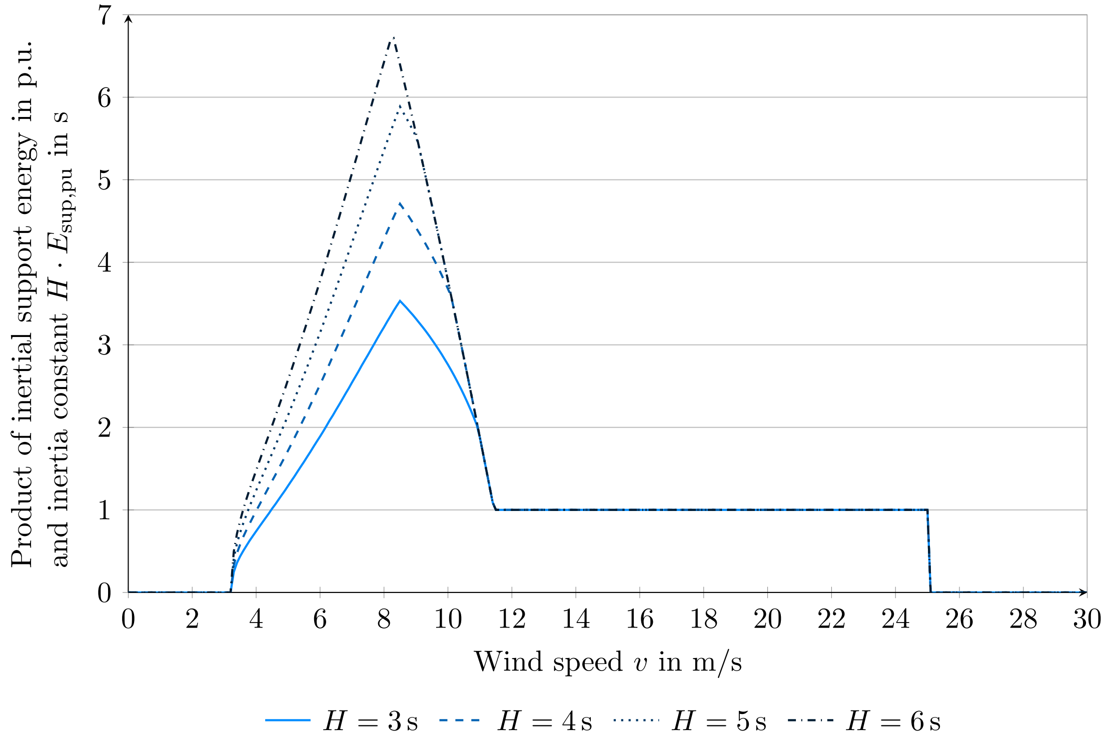

Figure 4.8: Product of inertial constant and normalised inertial support energy $H \cdot E_{\text{sup,pu}}$ in relation to the wind speed v for different values of H (fixed power approach).

As mentioned in 4.1, the simulations have been carried out with inertial constants of 3, 4, 5 and 6 s. For the results presented so far in this chapter, an inertia constant of 3 s has been assumed. Fig. 4.8 illustrates the effect of changing the inertia constant. It shows the product of normalised inertia support energy and the inertia constant $H \cdot E_{\text{sup,pu}}$ in relation to the wind speed v. The graph contains the product of support energy and inertial constant to express that the real amount of energy available during inertial response is increasing with the inertia constant. It is, however, not completely increasing at the same rate, which is why the normalised support energy would be decreasing with increasing inertia constant. The results of the parameter study are not surprising, increasing the inertia constant

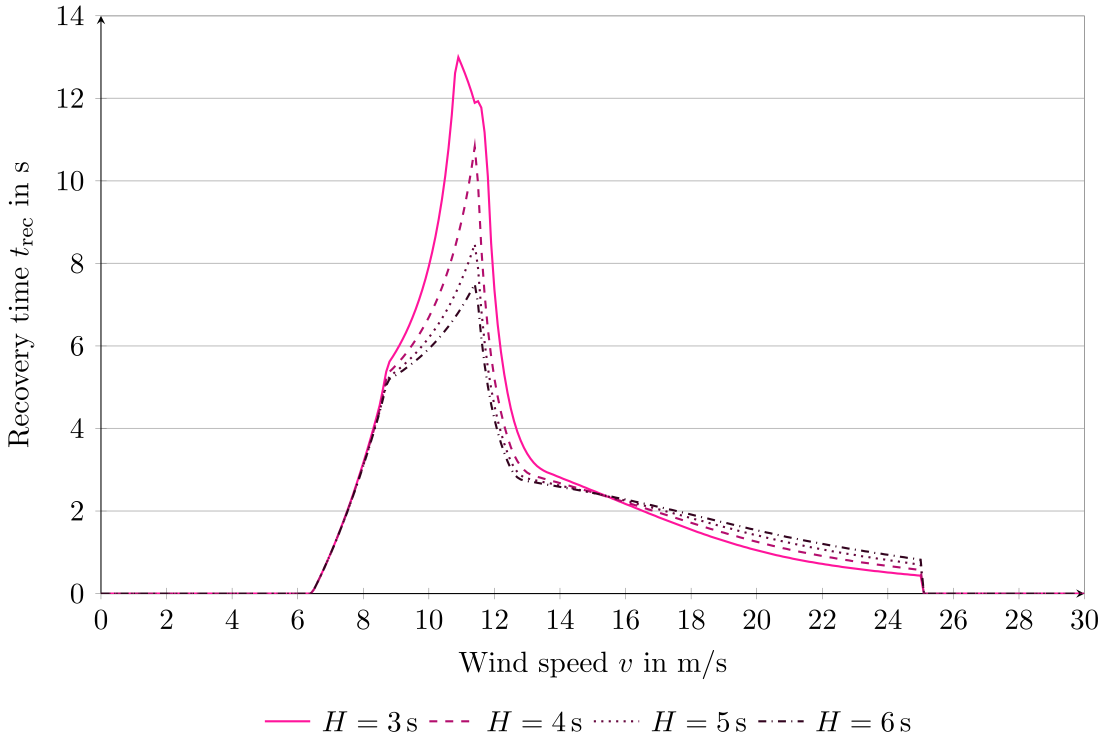

Figure 4.9: Inertial response recovery time t_{rec} in relation to the wind speed v for different values of H (fixed power and time approach).

increases the energy which can be made available during inertial response. However, it also increases the amount of energy necessary during recovery as well as the recovery time as long as the turbines are brought to their operating limits. These implications of increasing inertia constants remain largely the same for the fixed time approach.

The shown product does not change for the fixed power and time approach, though. This is rooted in the specification of the approach, which does not bring the turbines near their operating limits. However, the minimum rotor speed increases, which causes reduced aerodynamic losses during inertial response. Fig. 4.9 depicts the recovery time of the fixed power and time approach in relation to wind speed for changing inertia constants. It can be seen that especially in the medium wind speed range the recovery time (and equally rotor speed deviation and losses during recovery) is reduced greatly by an increasing inertia constant. But for high wind speeds, a contrary effect can be observed. The recovery time increases with the inertia constant, because in this wind speed range a decreasing rotor speed is associated with an increasing aerodynamical power. This means that although the minimum rotor speed is lower for lower inertia constants, the aerodynamic power during recovery does not differ very much. Because of this, the slowing effect of a higher inertia constant during re-acceleration becomes predominant, resulting in longer recovery times.

Overall, a higher inertia constant allows for higher gains or lower costs of inertial response, especially for the critical medium to low wind range.

4.4 Errors and inaccurracies of the inertial response simulation

The inertial response simulation introduced further simplificactions. The most significant effect, in particular for the first two approaches (fixed power and fixed time), probably is the estimation of the operation limits. While the values used in this work have been founded on different sources of investigation, other authors come to varying results. Although many authors agree that the turbine rotor will stall if it is slowed down too much, very few actually quantify a limit for this effect. Also, the curve fitting of the C_P curve is only ensured for tip speed ratios over 3, a value that is undercut in many cases during the investigated inertial responses, which questions the validity of this mean of expressing the stall effect. As for the minimum rotor speed, [3] recommends to limit the speed range of a DFIG between $-40\,\%$ and $30\,\%$ of synchronous speed. In [37], [38] a value of $\omega_{\mathrm{min,pu}} = 0.7$ p.u. is suggested, in contrast to $\omega_{\mathrm{min,pu}} = 0.1$ p.u. used in this work. However, as shown in Fig. 4.6, this value is not reached in any of the inertial response approaches investigated, emphasising the importance of the stall triggered operation limit. Effects that also have influence on the inertial response but are disregarded in this work are e.g. varying wind speeds and turbulence during the inertial response period (see [25]) and the wake effect of turbines in a wind park (see [26]). Obviously, the inertial response simulation is also dependent on the inertia constant of the machine, which is an additional source of error. The numerical error introduced during solving of the differential equations can be further reduced by choosing a more favorable algorithm or further reducing the step-size, however it is expected to be insignificant.

5

Inertial response evaluation of system-wide aggregated wind turbines

To allow for the analysis of the system-wide contribution to inertial response from wind turbines it is necessary to aggregate the individual inertial response of all wind turbines in the system according to their operational state, which means the combination of the different model components as illustrated in Fig. 5.1. This is done for each hour in the investigated time span from 2010 to 2015. While the kinetic energy can be aggregated similarly to the hourly energy production as described in the end of Section 3.2.2, the aggregation of the detailed inertial response time series with a resolution of 5 ms would result in excessive data sizes. Therefore in a first step key indices for the system wide aggregation are identified, which are described in the following section, and calculated in dependency of the wind speed. These values for power and energy are subsequently allocated according to the wind speed at each wind turbines position, scaled by the turbines rated power and aggregated for the complete power system, individually for each simulated time step.
The second section in this chapter describes the results of this aggregation. The default parameters for the generation of this results are the same like in the previous chapters and can be found in Table 3.3.

Please note that fixed speed wind turbines are excluded from all following figures, since their share in total installed wind capacity is small and their inertial response is fundamentally different.

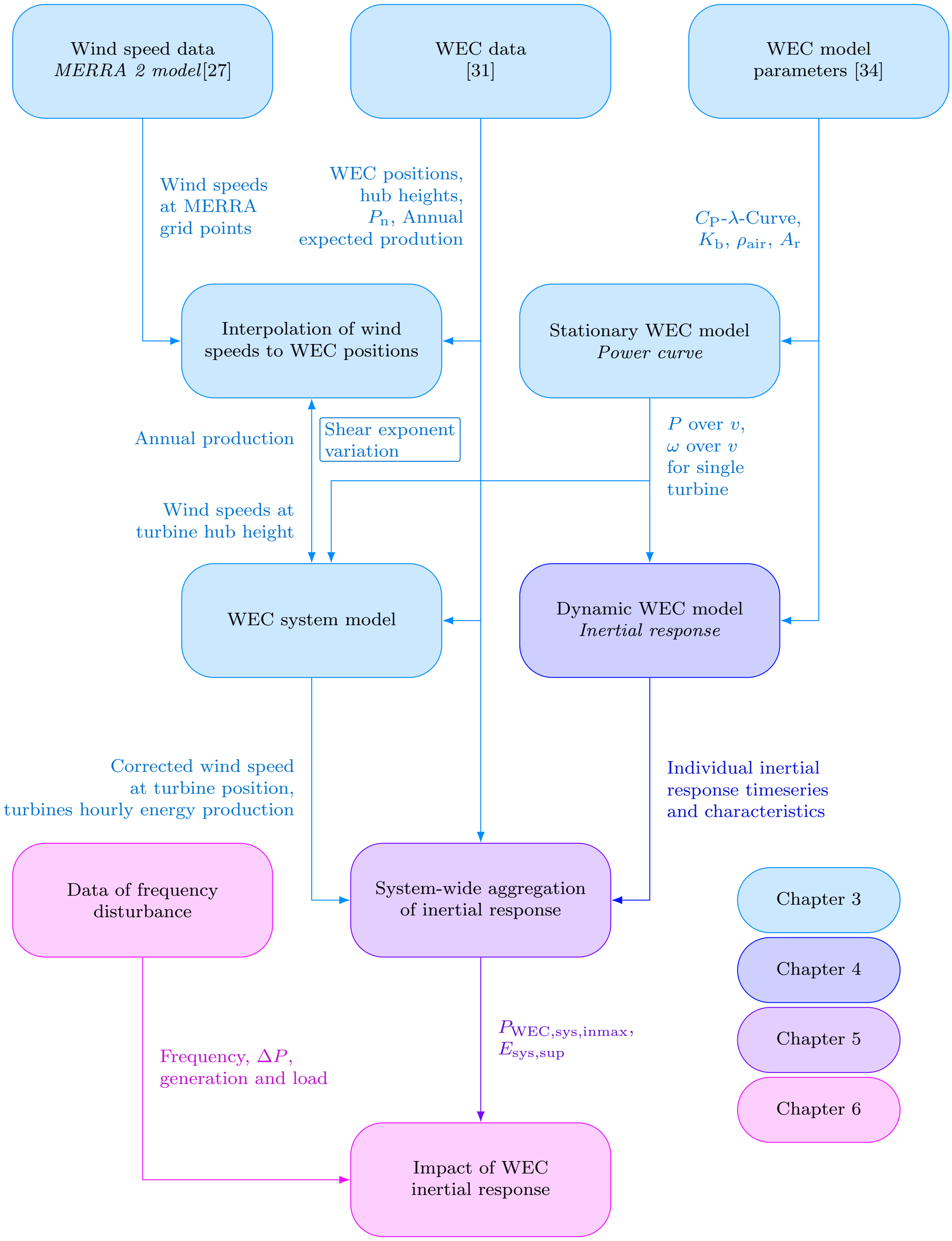

Figure 5.1: Schematic of the different model components and their relations.

5.1 Key indices for system-wide aggregation analysis

The following aggregated, system-level figures are calculated:

- *Hourly energy production from wind turbines:* This measure has already been introduced in Section 3.2.2 and is described by equation (3.8).

- *Total kinetic energy stored in WEC rotating mass:* The calculation of the amount of kinetic energy stored in the wind turbines rotating mass is given in Subsection 4.1.1. These values are assigned and aggregated similarly to the hourly energy production. They can then be aggregated:

$$E_{\mathrm{sys,rot}} = \sum_{i=1}^{N_{\mathrm{WEC}}} E_{\mathrm{rot,pu},i} P_{\mathrm{n},i} H_i \tag{5.1}$$

- *System-wide maximum power from wind turbines during inertial response:* This characteristic is the system-wide sum of the maximum power of all relevant wind turbines during inertial response. It is calculated by the following equation:

$$P_{\mathrm{WEC,sys,inmax}} = \sum_{i=1}^{N_{\mathrm{WEC}}} P_{\mathrm{el,pu,inmax},i} P_{\mathrm{n},i} \tag{5.2}$$

  For the fixed time and the fixed power and time approach, this value is equivalent to the system-wide sum of power of all relevant wind turbines during the complete inertial response, since all turbines contribute for the same timespan with a constant extra power. For the fixed power approach this value is only reached in the initial moment where all turbines are still participating in inertial support (this is illustrated also in Fig. 5.3a).

- *System-wide minimum power from wind turbines during inertial response:* This characteristic is the system-wide sum of the minimum power of all relevant wind turbines during inertial response. It is calculated by the following equation:

$$P_{\mathrm{WEC,sys,inmin}} = \sum_{i=1}^{N_{\mathrm{WEC}}} P_{\mathrm{el,pu,inmin},i} P_{\mathrm{n},i} \tag{5.3}$$

- *Energy gained system-wide during inertial response support phase:* This characteristic is the system-wide sum of extra energy gained during the inertial response support phase. It is estimated by the following instruction:

$$E_{\text{sys,sup}} = \sum_{i=1}^{N_{\text{WEC}}} E_{\text{sup,pu},i} P_{\text{n},i} H_i \tag{5.4}$$

- *Energy lost system-wide during inertial response recovery phase:* This characteristic is the system-wide sum of extra energy gained during the inertial response recovery phase. It is estimated by the following instruction:

$$E_{\text{sys,rec}} = \sum_{i=1}^{N_{\text{WEC}}} E_{\text{rec,pu},i} P_{\text{n},i} H_i \tag{5.5}$$

  Like $E_{\text{rec,pu}}$, it is a negative value describing the losses during the recovery phase compared to the stationary operation.

- *System-wide net energy loss during inertial response:* This measurement denotes the system-wide balance of energy gained and lost during the inertial response. It can be calculated by any of the following equations:

$$E_{\text{sys,bal}} = \sum_{i=1}^{N_{\text{WEC}}} E_{\text{bal,pu},i} P_{\text{n},i} H_i \tag{5.6}$$

$$= E_{\text{sys,sup}} + E_{\text{sys,rec}} \tag{5.7}$$

  This value is negative if more energy is lost than gained. It denotes the total energy difference due to the inertial response.

5.2 Aggregated inertial response simulation results and discussions

In this section, the results of the combination of the WEC system model for wind speed distribution and the inertial response simulation are presented by the means of the aggregated characteristics described in the previous section. Since many of the following figures would contain a lot of individual values, one for each hour in the simulated years 2010 to 2015, a statistical analysis has been applied. The dimension on the x-axis has been separated in 100 equally sized bins. For each bin, the mean as well as the 5th and 95th percentile have been calculated. In the figures the mean is represented by a solid line, the percentiles by dashed lines. This means that the filled area between the percentiles contains 90 % of all simulated values. It should be noted that for low numbers of online turbines respectively a low hourly production the number of samples per bin is low, which makes the statistical methods employed unreliable for this segment. However, they are a suitable tool of analysis for the majority of hours. The number of samples for each bin can be found in Table A.1 and Table A.2 in Appendix A. Please note that the results in this section are not only dependent on the inertial response simulation but also on the results from the WEC system model and the chosen scenario. As mentioned above all results are presented for the scenario A1, corresponding to 20 TW h annual production from wind turbines.

Table 5.1: Minimum and maximum values of online turbines and hourly energy production from wind for the simulated years 2010 - 2015, including fixed speed turbines.

	Minimum	Maximum
Online turbines	121	3252
Hourly energy production	10.18 MW h	7.46 GW h

Fig. 5.2 displays the hourly generation from wind turbines in relation to the number of online turbines. Online turbines in this context are defined as turbines experiencing wind speeds between cut-in and cut-out wind speed, i.e. producing any energy. In this figure, fixed speed turbines are included as well. The figure shows that, especially for a higher number of online turbines, the aggregated energy production is scattered widely for constant numbers of online turbines. This contradicts the assumptions described in Section 1.2 from [5], [6], [10], [11], where a specific energy production has been mapped to a specific number of online turbines and illustrates the inaccuracy introduced due to this assumption. The minimum and maximum values for online turbines and hourly energy production, which have been encountered in the simulated years, are shown in Table 5.1.

Taking the inertial response into focus, Fig. 5.3 presents time series for the system-wide total WEC power during inertial response. For this, four different production scenarios have been chosen, each corresponding to one hour in the simulation time. The scenarios consist of an hourly production from WEC's of 0.56 GW h, 2.09 GW h, 5.39 GW h and 7.37 GW h. These values are chosen because they are the 5th, 50th and 95th percentile and the maximum hourly production, therefore working well as examples for the different states of the system. Please note that the presented time series have mere exemplary character, because as shown by

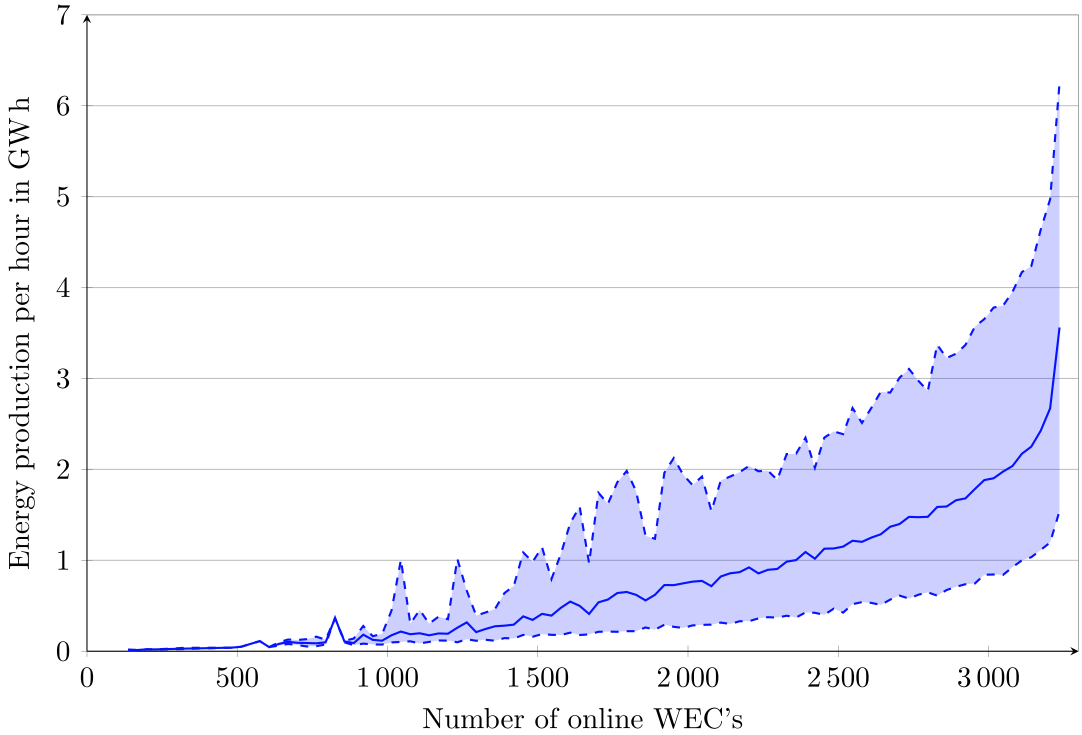

Figure 5.2: Mean, 5th and 95th percentile of hourly energy production from WEC in relation to the number of online turbines for the simulated years 2010 to 2015.

Fig. 5.2 a specific hourly production does not allow to deduce the amount of online turbines, their operational state or the amount of support power or energy they can contribute.

Fig. 5.3a depicts the aggregated time series for the fixed power approach. It can be seen that initially the power jumps a lot, for lower production to the multiple of the stationary power. However, apart from the highest production scenario, this power quickly drops even below the stationary level before the support time of ten seconds is over. Adjacent to the support phase, the recovery follows up. The lower the power, the longer the recovery takes. However, it can be supposed that the short recovery phase will cause more problems in the high production cases, where the power drop during recovery can be more than six times the dimensioning fault. For the scenarios corresponding to 5th percentile and median the inertial response would consist of a short, high power peak and a pronounced recovery phase. It is obvious that an inertial response in this form is unfeasible and more destabilising than supporting, similar to ocurrences described in [39]. However, it is still of interest to explore this approach as a quantification of the maximum available energy.

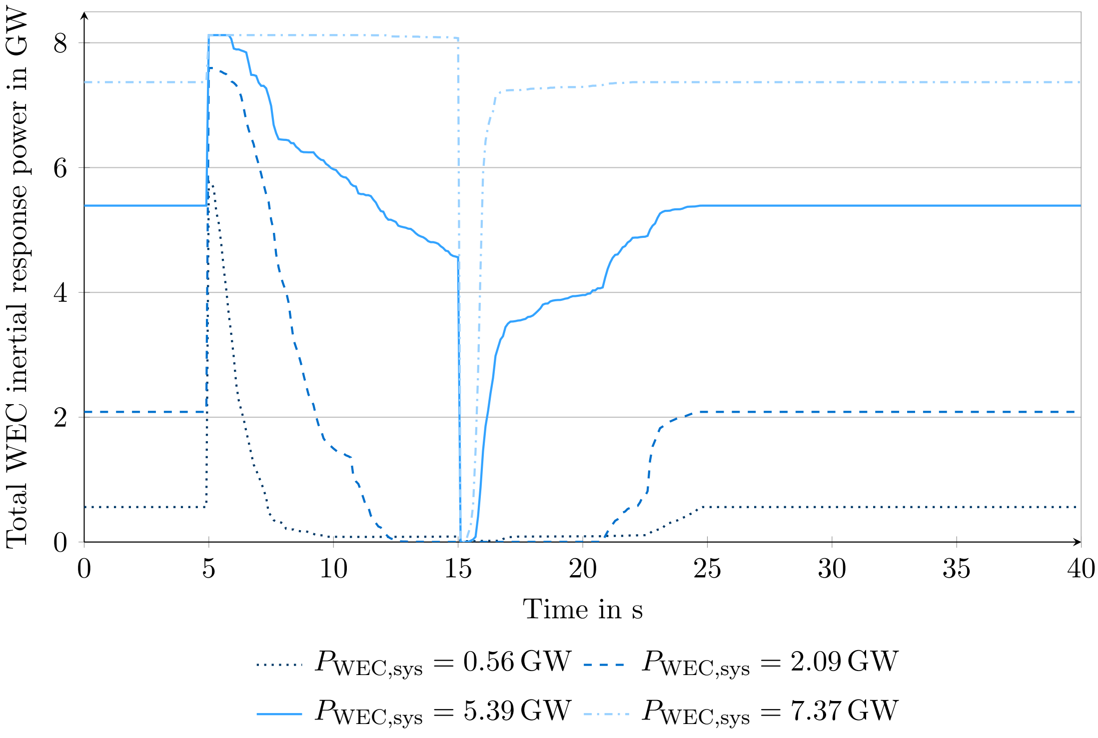

(a) Fixed power approach.

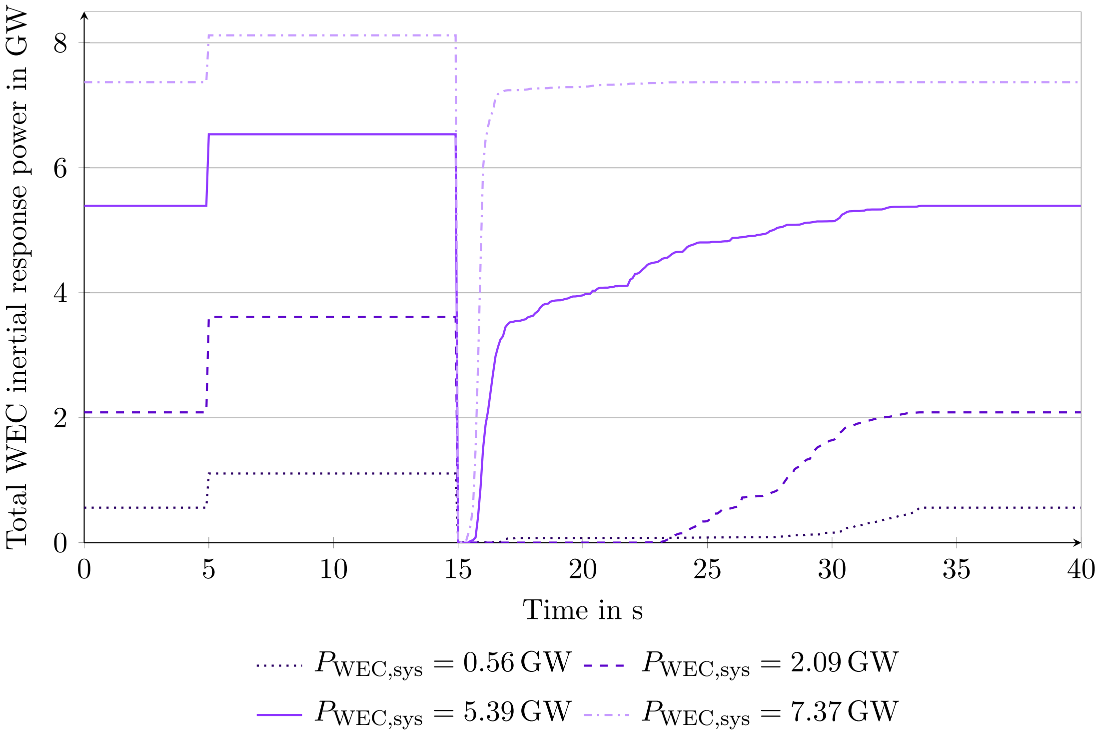

(b) Fixed time approach.

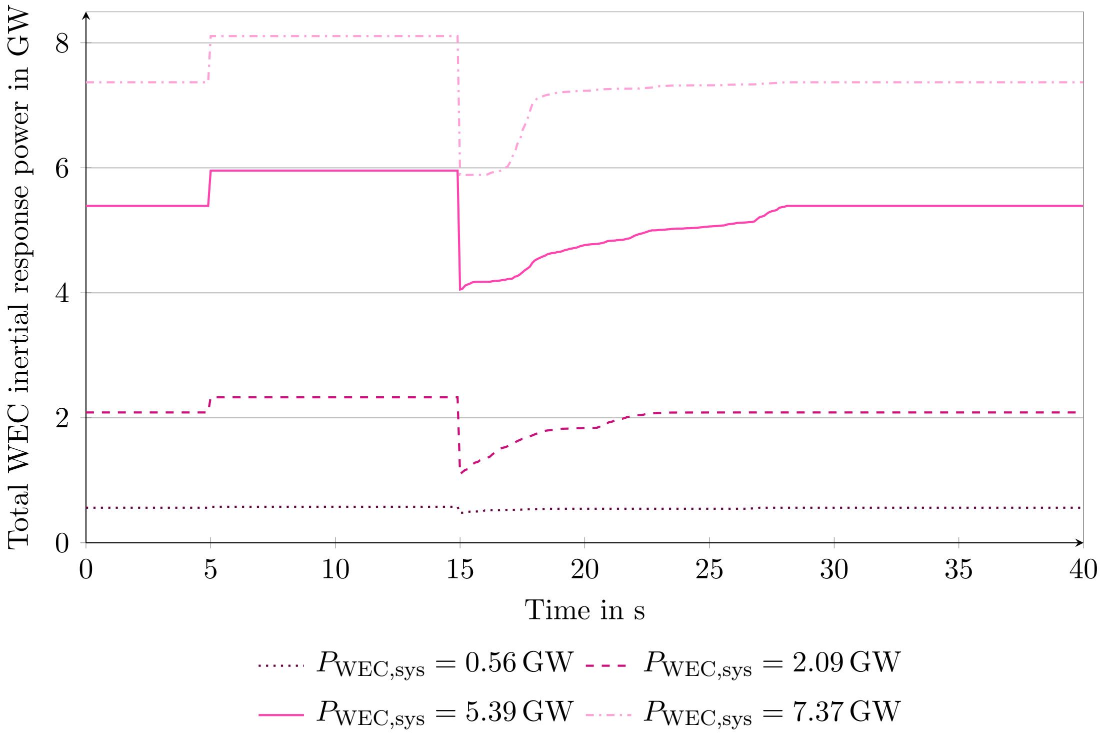

(c) Fixed power and time approach.

Figure 5.3: Timeseries for system-wide sum of WEC power during inertial response for four different production scenarios.

In Fig. 5.3b the aggregated time series for the fixed time approach are presented. In comparison to the fixed power approach, the difference between the inertial support power and stationary WEC power is a lot smaller. Also, the power remains constant during the support phase. Both characteristics would make this approach a lot easier to control for the system operator. The recovery phase differs from the fixed power approach because all turbines start their recovery at the same time due to the defined support time. This means that turbines operating at different wind speeds reach the end of the inertial response cycle, representend by the sum of support and recovery time, at very different points, while the ends of inertial response at different wind speeds are notably closer together in the fixed power approach (compare also Fig. 4.7). The transition between support and recovery phase also exhibits the pronounced drop caused by the simultaneous reduction of turbine output power to zero. This effect could be mitigated, especially for high production situations, by introducing a fuzzy support time, i.e. varying it for different turbines by up to two seconds, therefore creating a smoother transition.
The inertial response time series of the fixed power and time approach are shown

in Fig. 5.3c. It can be observed that, in contrast to the approaches investigated before, in this case the amount of extra power is increased with the stationary power. This is likely beneficial behaviour, since WEC inertial response is most important at high penetration scenarios. This nearly linear relation furthermore makes it easier for system operators to anticipate and estimate WEC inertia support capabilities depending on the current generation situation. The recovery phase is unsurprisingly a lot less pronounced than in the two approaches studied before. Nevertheless it would probably be necessary to introduce a fuzzy support time for this approach as well to prevent the formation of a secondary frequency nadir during the recovery.

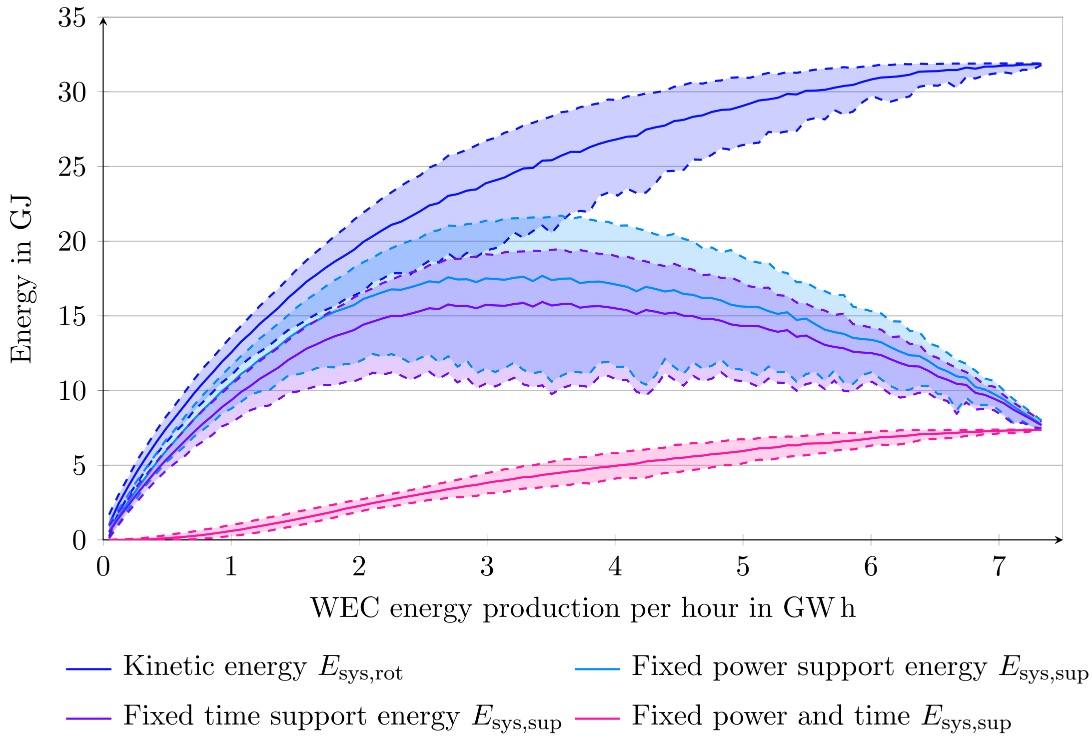

Figure 5.4: Mean, 5th and 95th percentile of inertial response energies in relation to hourly WEC energy production for the simulated years 2010 to 2015. Contains total kinetic energy as a reference.

To assess the amount of additional energy available to the system, it is necessary to consider the inertia support energy. Fig. 5.4 contains the 5th and 95th percentile as well as the mean of $E_{\mathrm{sys,sup}}$ in relation to the hourly WEC energy production. It also contains the total kinetic energy stored in the wind turbine rotors. The behaviour of the kinetic energy is as expected: For lower production scenarios, it has a steep slope since many wind turbines are operating below their rated rotor

speed. With increasing hourly production, more WEC's already operate at their maximum rotor speed, which makes changes in kinetic energy smaller and the curve less steep (see also Fig. 4.3).
The curves for both fixed power and fixed time approach are very similar. Their most remarkable feature is that they exhibit their maximum at an hourly production of approx. 3.5 GW h and are decreasing noticeably for higher production values. This can be easily explained by the position of the support energy maximum in Fig. 4.5, which lies at $v_{\omega_{\max}}$, well below rated wind speed. Due to the limited rotor speed and converter power, less additional energy can be fed into the grid when increasing the total energy production beyond this point. At maximum production, the curves for these approaches meet with the fixed power and time approach.
The fixed power and time approach exhibits a nearly linear correlation with a Pearson correlation coefficient of 0.975. On that account the figure confirms the problems of the former two approaches and the advantage of the better controllability of the fixed power and time approach already observed in Fig. 5.3. The correlation coefficients for the other approaches and different relations are displayed in Table 5.2. This also means that for this approach in contrary to what has been indicated before inertial response characteristics could be estimated from the hourly energy production by a linear function. A linear interpolation using the method of least squares yields a ratio of 1.13 between aggregated support power and stationary power, while the ratio between aggregated support energy and stationary power amounts to 1.3 J/W.

Table 5.2: Pearson correlation coefficients r for hourly average WEC power resp. number of online WEC's versus the inertia support energy resp. support power.

Correlation between	Approach		
	Fixed power	Fixed time	Fixed power and time
$r(P_{\text{WEC,sys}}, E_{\text{sys,sup}})$	0.472	0.509	0.975
$r(P_{\text{WEC,sys}}, P_{\text{WEC,sys,inmax}})$	0.57	0.98	0.999
r(No. of online WECs, $E_{\text{sys,sup}}$)	0.77	0.78	0.54

In Fig. 5.5 the spread of the curves in Fig. 5.4 is illustrated by the probility mass plot of kinetic energy and inertial response energies for an hourly production between 2 GW h and 2.17 GW h. This production segment accounts for the 5 % around the median of production (compare also Fig. 3.12). The width of the displayed bins has been chosen to 0.25 GW h. It can be observed that for the

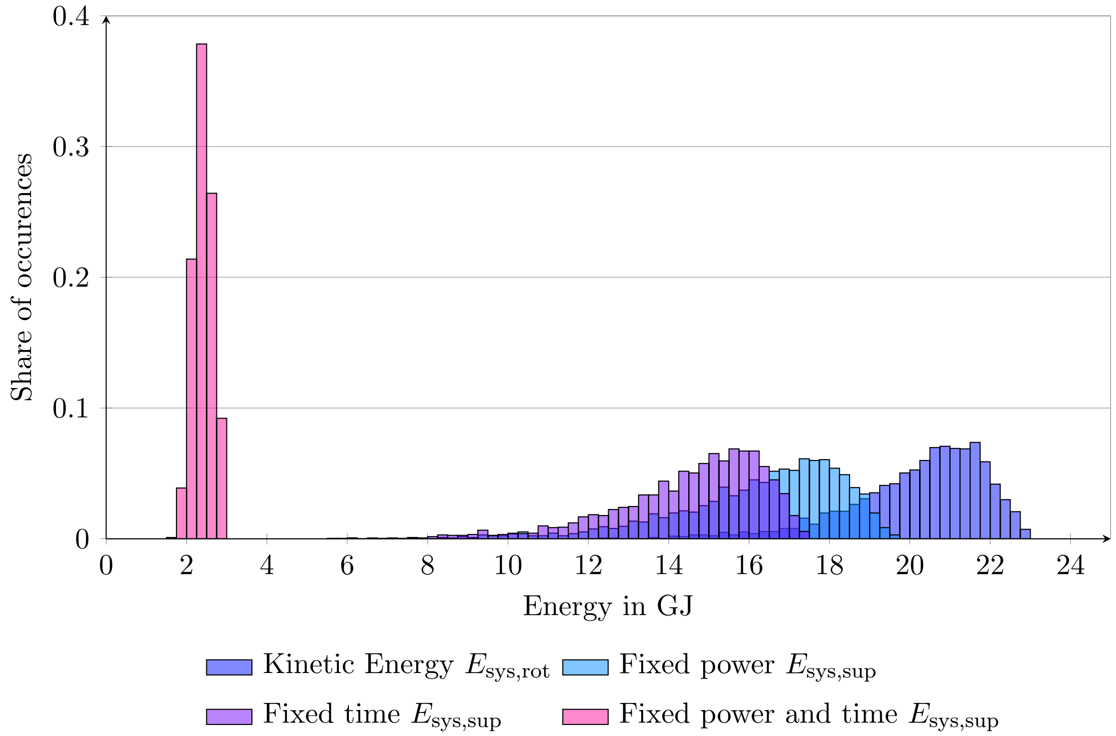

Figure 5.5: Probability mass plot of inertial response energies for an hourly production between 2 GW h and 2.17 GW h for the simulated years 2010 to 2015. Contains total kinetic energy as a reference.

kinetic energy as well as for both the fixed power and the fixed time there is a more pronounced decline on the upper side of the distribution, while the lower decline is very sustained. This corresponds to the bigger difference between median and 5th percentile compared to the difference between 95th percentile and median in Fig. 5.4. For the fixed power and time approach, a heavy concentration of the values can be observed, which corresponds to the small spread in Fig. 5.4.

In the following, the inertial response energies will be examined in detail. For each of the different approaches, the mean as well as the 5th and 95th percentile of the inertia support, recovery and balance energy can be found in Fig. 5.6.
Fig. 5.6a depicts the fixed power approach. Due to their similarity it will be discussed together with the curves for the fixed time approach shown in Fig. 5.6b. The curved form of the support energy has the same causes as the ones responsible for the decline of support power discussed above. The recovery energy shows a similar behaviour. It also exhibits an even wider spread. This makes these approaches even more difficult to contol, because with the current amount of live

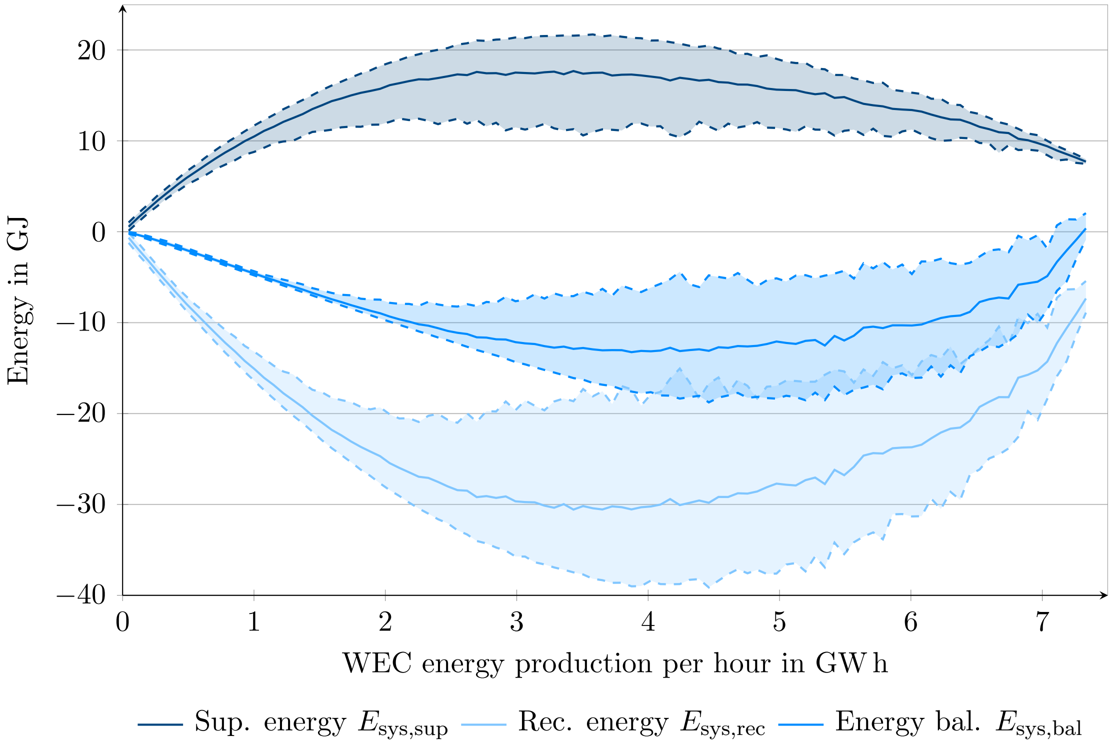

(a) Fixed power approach.

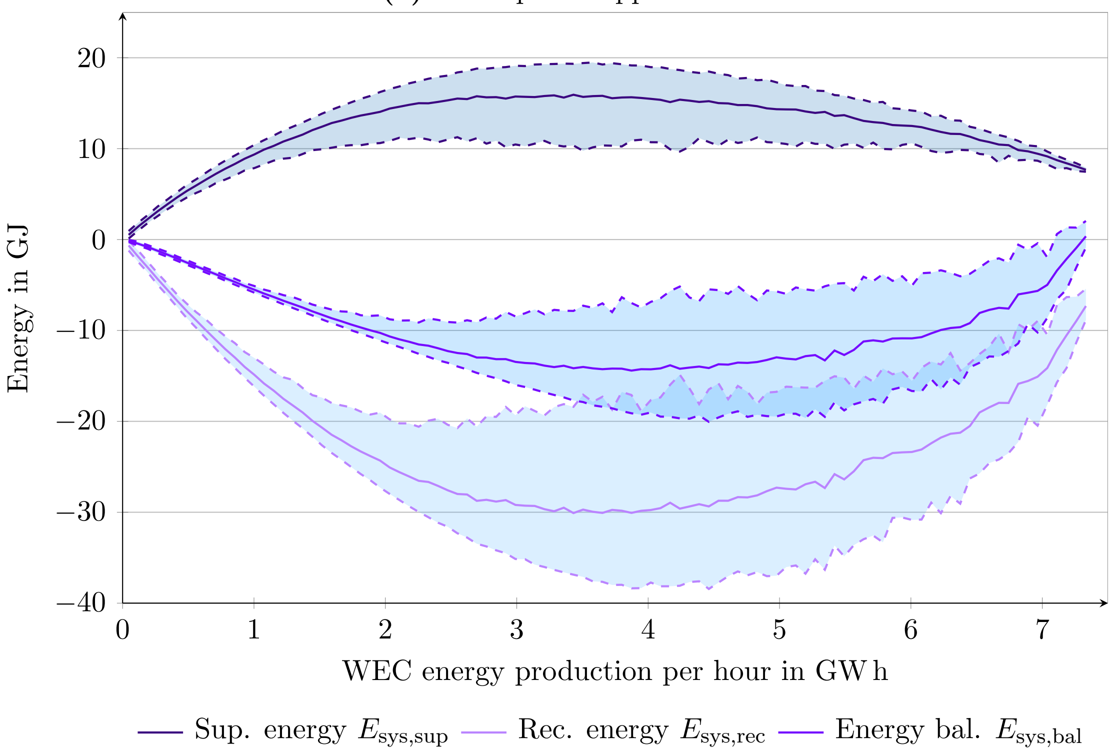

(b) Fixed time approach.

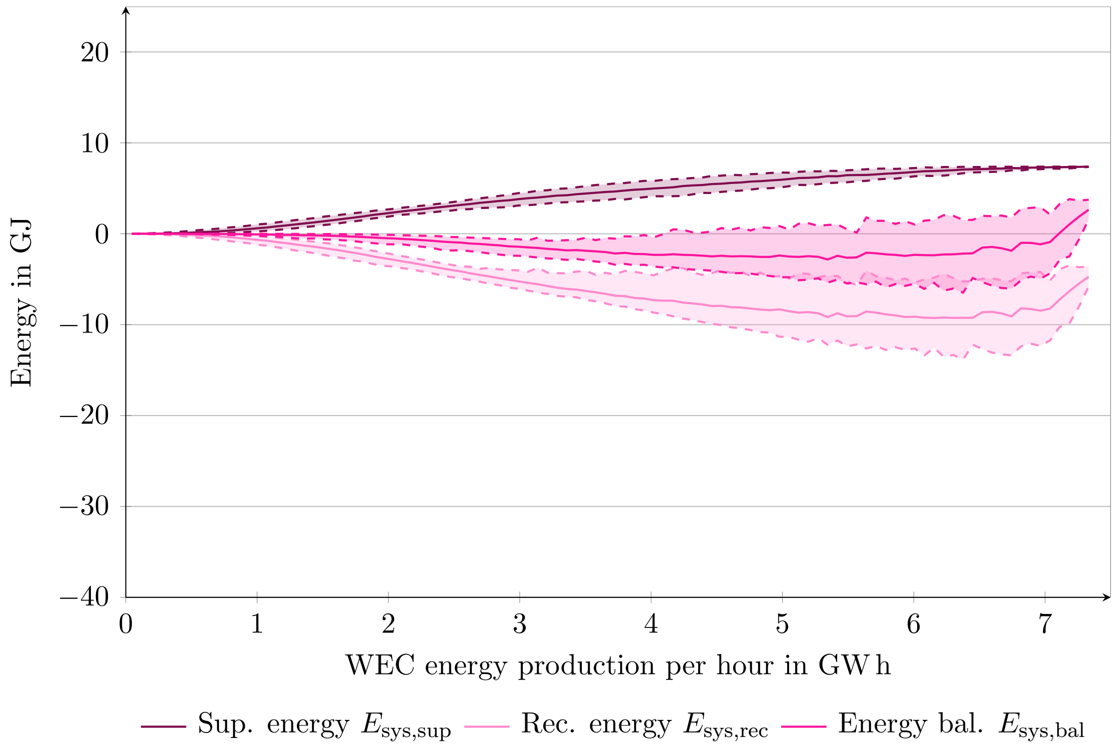

(c) Fixed power and time approach.

Figure 5.6: Mean, 5th and 95th percentile of the aggregated inertial response energies $E_{\mathrm{sys,sup}}$, $E_{\mathrm{sys,rec}}$ and $E_{\mathrm{sys,bal}}$ for all three inertial response approaches in relation to hourly WEC energy production for the simulated years 2010 to 2015.

information available to the system operator, it is not possible to anticipate how much energy is needed during the recovery phase. It should be noted that while the energy balance is presented in various contexts in this work, in reality support and recovery energy cannot compensate each other. On the contrary, if a second frequency dip shall be prevented, the complete recovery energy has to be supplied by the primary frequency control, in addition to compensating the disturbance that occured in the grid. This is another contraindication of inertia support approaches which remove the turbines too far from their operating point.

Looking at Fig. 5.6c, which contains the data for the fixed power and time approach, the differences are obvious. Not only the support energy, but also the recovery energy follows a nearly linear curve. However, the recovery energy still exhibits a substantial spread, although smaller (even in relation) than for the other approaches. This acknowledges that the design of the recovery phase is crucial for the contribution from WEC inertial response to frequency stability. Additionally the energy balance for this approach is positive more often than for the other two approaches due to the more beneficial characteristics, which means that during inertial response more energy is fed into the grid than during stationary operation of the same duration.

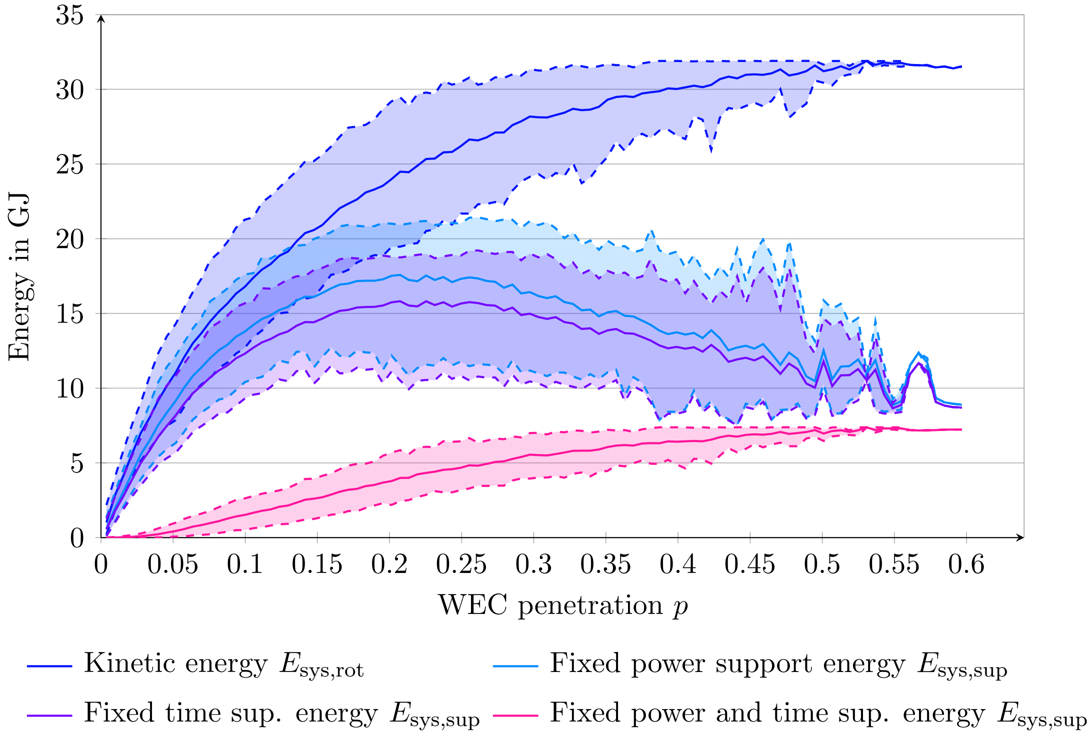

Figure 5.7: Mean, 5th and 95th percentile of inertial response energies in relation to instantaneous WEC penetration p for the simulated years 2010 to 2015. Contains total kinetic energy as a reference.

For the effects of WEC inertial response it is important not only to consider their total production, but also to be aware of their share among energy production in the complete system. This measure, the so-called penetration, has been computed for the years 2013 to 2015 by the following formula:

$$p(k) = \frac{P_{\mathrm{WEC,sys}}(k)}{P_{\mathrm{load}}(k)} \tag{5.8}$$

where $p(k)$ denotes the wind power penetration at the k-th simulation sample, i.e. hour. Please note that in this work, the base for the penetration is the load of the power system. The data is taken from [40]. Fig. 5.7 depicts the kinetic energy and the support energies from the three considered approaches in relation to the WEC penetration. Since the figure does not exhibit any major differences compared to Fig. 5.4, the deductions made above are supported.

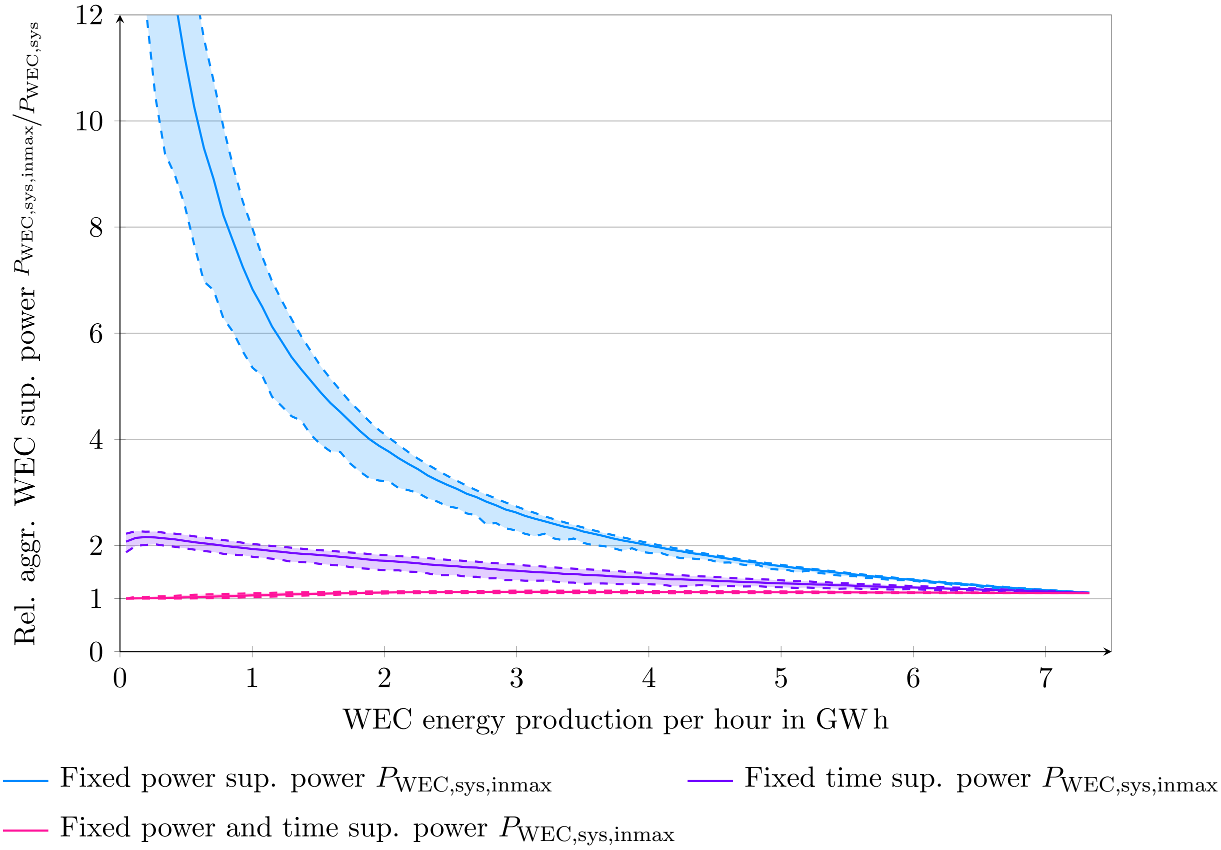

Figure 5.8: Mean, 5th and 95th percentile of maximum power during inertia support in relation to hourly WEC energy production for the simulated years 2010 to 2015.

As shown by the swing equation (equation (2.9)), the RoCoF is not dependent on the energy exchanged during a frequency disturbance (the frequency nadir is), but on the power imbalance. In Fig. 5.8 the relation between the system-wide aggregated maximum power during inertia support (i.e. the initial support power) and the aggregated stationary power is plotted over the hourly energy production. That means if the shown relation amounts to two, that the WEC power during inertia support is (at least initially) twice as much as the WEC power during stationary operation. The fixed power approach shows the highest numbers in this figure, especially for low production cases, since it orders all turbines to switch to their maximum power. This means that initially the aggregated support power is only dependent on the number of online turbines, not on the wind speed they are operating at. The mean of this curve starts at approx. 21, meaning that at an

hourly production of 50 MW h the turbines would deliver a support power during inertial response of more than 1 GW, at least for a short time. It goes without saying that this behaviour does not stabilise the power system.
The fixed time approach exhibits a more feasible behaviour. While it also has a high initial relation, its maximum is just above 2, which could still be controllable. Its further decline is close to linear and meets the other approaches for very high production cases.
In contrast to the others, which are declining, the curve of the fixed power and time approach increases with increasing WEC energy production. It reaches it maximum at 1.1, which is defined in the specification of the approach. At first sight, this lower support power might look problematic. However, in the case studied in Chapter 6, the tripping of a 1.1 GW nuclear power plant amounts to 2.5 % of the total generation. As presented in Section 6.3, even this most conservative approach is able to stop the frequency decline. It therefore can be concluded that the extra power during inertial support is of minor importance and can, if overdimensioned, even cause further instabilities.

6

Impact of system-wide aggregated wind inertial response on grid frequency

To illustrate the generated data and set the contribution from wind farms in relation to synchronous generation, a real disturbance has been analysed. The goal of the demonstration is to compare the initial RoCoF after the disturbance with respect to different methods of the wind inertial response. This demonstration is not the focus of this work and has been carried out with a number of simplifications, e.g. the ignorance of primary frequency control and the sole consideration of Swedish WEC's. Further careful analysis of the interdependency of the aggregated WEC inertial response and frequency stability is necessary to get a better understanding of the impacts of WEC inertial response.
The chosen disturbance was a planned trip of nuclear power plant Forsmark 2 at 14th May 2013. The data used in the following calculations was originally published in [41] and contains 50 Hz frequency measurements from Phasor Measurement Units located at Forsmark, Tempere (Finland) and Lund. The measurements around the time of the disturbance are depicted in Fig. 6.1.

The frequency measurement data is first used to calculate the RoCoF. Then this initial RoCoF is used to derive the system inertia constant according to equation (2.9) and to compare it with the RoCoF calculated with the contribution from wind turbine inertia support.

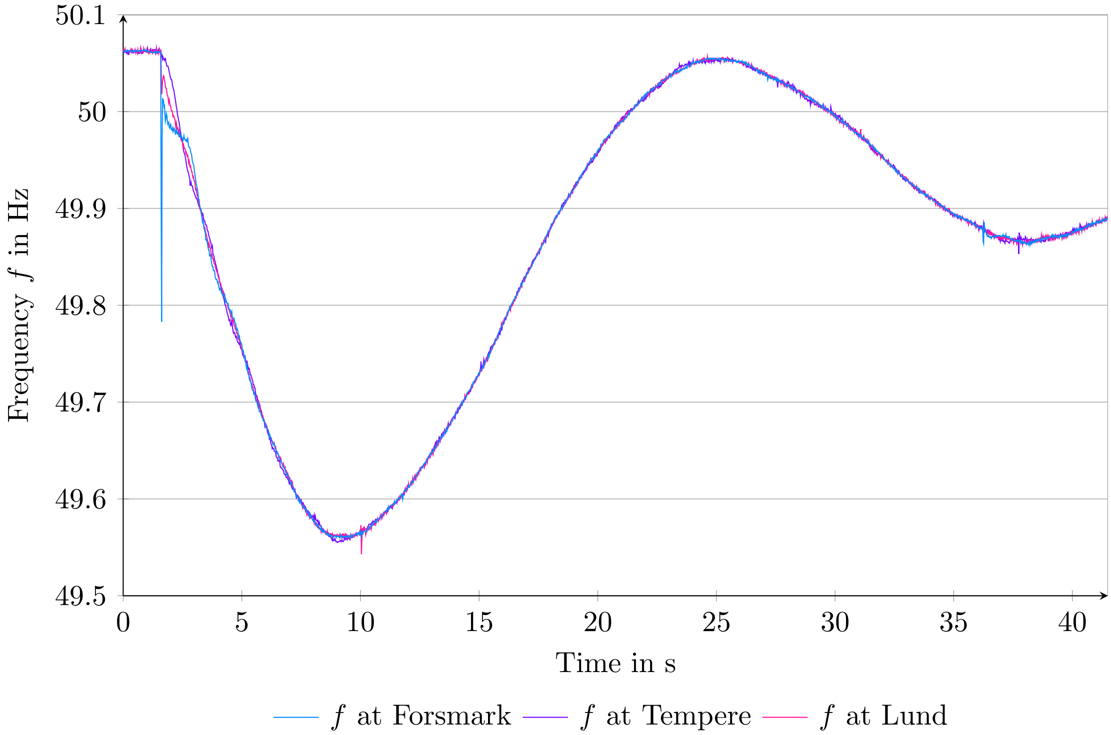

Figure 6.1: Frequency measurements from three different PMU locations.

6.1 Estimation of the initial RoCoF and the system inertial constant

As stated before, the estimation of the initial RoCoF during a disturbance is far from trivial. In this project, the following approach has been taken.

First of all, the signals from the three different PMUs are filtered. The filtering consists of an averaging downsampling with a moving average window and follows this equation:

$$f_{\mathrm{lr}}(n) = \sum_{i=5n}^{5n+4} \frac{f_{\mathrm{hr}}(i)}{5} \tag{6.1}$$

f_{hr} denotes the high resolution frequency measurement and f_{lr} the low resolution result. In this case, the window length for the averaging is chosen to five samples, resulting in a sampling frequency of 10 Hz. This is consistent with the cutoff frequency for the lowpass filter suggested in [14].

To calculate the RoCoF, a sliding window is used from the start of the disturbance until 5 s later. The window has a width of 500 ms, which corresponds to 5 samples of the downsampled frequency, and the RoCoF is calculated by substracting the measurement at the end of the window by the starting one:

$$\frac{\Delta f}{\Delta t}(n) = \frac{f_{\mathrm{lr}}(n+5) - f_{\mathrm{lr}}(n)}{0.5\,\mathrm{s}} \tag{6.2}$$

The RoCoF is denoted by $\Delta f/\Delta t$. The initial RoCoF of the disturbance used for further calculations is the minimum of the results of the sliding window. For the use in the swing equation it is normalised to the frequency just before the start of the disturbance f_0.
In the case of the measurement used in this work, the frequency signals from the three different locations are averaged to minimise the influence of the measurement location. The resulting frequency signal is then used to compute the RoCoF by the means of the sliding window. This method results in a RoCoF of $-0.106\,\mathrm{Hz/s}$.

According to equation (2.9), to calculate the system inertia additionally to the RoCoF, the quotient between power imbalance and total generation is necessary. In the case of this disturbance, the power imbalance is assumed to be the rated power of the tripping power plant: $\Delta P_{\mathrm{sys}} = 1100\,\mathrm{MW}$. The total generation in the Nordic power system is taken from historical production data published by Nord Pool, namely the dataset "production per country 2013 hourly" [42]. The average production in the Nordic region at 14th of May 2013 between 9 and 10 a.m. is assumed as the value for the total generation: $S_{\mathrm{sys}} = 43.572\,\mathrm{GV\,A}$. This neglects load inertia as well as reactive power, but does not affect the results of the following calculations. The system inertia constant is then calculated as follows:

$$H_{\mathrm{sys}} = \frac{\Delta P_{\mathrm{sys}}}{2 S_{\mathrm{sys}} \frac{\Delta f_{\mathrm{pu}}}{\Delta t}} \tag{6.3}$$

The resulting system inertia constant is $H_{\mathrm{sys}} = 5.95\,\mathrm{s}$.

6.2 Estimation of the impact of wind turbine inertial support

To simulate the frequency after the disturbance it is necessary to include the primary frequency control. If it is neglected, the frequency will just continue to fall with increasing RoCoF, since the causal power imbalance is never compensated.

A simulation considering these information is beyond the scope of this work, thus the estimation of effects is limited to a comparison of the initial RoCoF with and without the inertia support from WEC's. The latter is given by the original data and the calculations in the previous section, while the estimation of the former will be described subsequently.

In contrast to the inertia from synchronously connected generation the amount of power and energy delivered by wind turbine inertial response is (for the control regimes investigated in this work) independent of frequency and RoCoF. This means that the additional power from wind turbine inertial response can simply be deducted from the power imbalance causing the disturbance:

$$\Delta P_{\text{sys,res}} = \Delta P_{\text{sys}} - (P_{\text{WEC,sys,inmax}} - P_{\text{WEC,sys}}) \tag{6.4}$$

The RoCoF with inertia support from wind turbines ${}^{\Delta f_{\text{WEC}}}/_{\Delta t}$ is then calculated by the following modification of the swing equation (2.9), considering the resulting residual power imbalance $\Delta P_{\text{sys,res}}$ and the total generation prior to the disturbance without WEC production, $S_{\text{sys}} - P_{\text{WEC,sys}}$:

$$\frac{\Delta f_{\text{WEC}}}{\Delta t} = \frac{\Delta P_{\text{sys,res}}}{2H_{\text{sys}}(S_{\text{sys}} - P_{\text{WEC,sys}})} f_0 \tag{6.5}$$

This approach effectively computes the reaction of a smaller power system with the same inertial constant to a reduced power imbalance. It has to be noted that only Swedish WEC's are included in the calculation.

The estimation of the effects is conducted for all three inertial response strategies investigated in this work for a low, medium and high wind energy production scenario. The most conservative guess for the WEC inertial constant, $H = 3\,\text{s}$, is used for this case. The results can be found in Section 6.3. Please note that this estimation contains various extensive simplifications, for example it assumes instantaneous inertial response from WEC's and includes only Swedish WEC's. It therefore has a very limited accuracy and can only capture the overall trend of effects.

It is also possible to compare the amounts of energy exchanged during the disturbance. This is achieved by integration of equation (2.5) over a given time period, e.g. the length of the disturbance. It has to be noted that this equation does not consider the contribution from primary frequency control, which will appear as the difference between the right and left side of the equation. In the same manner the WEC inertia support power can be included. The resulting equation can be written as:

$$\Delta P_{\text{sys}}\Delta t = \Delta E_{\text{sys,rot,syn}} + E_{\text{pfc}} + E_{\text{sys,sup}} \tag{6.6}$$

$$\Delta E_{\text{sys,rot,syn}} = \frac{H_{\text{sys}}}{f_0}(f_{\text{nadir}}^2 - f_0^2)S_{\text{sys}} \tag{6.7}$$

$\Delta E_{\text{sys,rot,syn}}$ denotes the difference in kinetic energy stored in the power systems rotating masses, i.e. the extra energy fed to the power system, and f_{nadir} is the minimum frequency of the disturbance. For a frequency decline like in the investigated case, it is negative, illustrating that the kinetic energy of the power system's rotating masses has declined. E_{pfc} denotes the total energy supplied by primary frequency control (supply corresponds to negative values). In this case, the integration has been conducted until the frequency nadir is reached, corresponding to a length of $\Delta t = 7.6\,\text{s}$. This point is chosen because afterwards the synchronous generation speeds up again and starts to restore its original kinetic energy.
With the help of this equation it may be possible to guess the frequency nadir with WEC inertia support. However, the amount of energy from primary frequency control has to be changed as well, since the droop control governing primary frequency control is proportional to the frequency deviation. The resulting frequency nadirs can therefore not be estimated with the given methods.

6.3 Effects of inertia support on disturbances

The results from the estimation, carried out for the four different WEC generation scenarios already employed in Chapter 5 and the three different methods, can be found in Table 6.1. For nearly all production scenarios and inertial response approaches the resulting RoCoF is positive, meaning that the additional power from inertial response is greater than the original power loss. This would cause undesirable over-frequency and consequently activate primary frequency control for down-regulation. Apart from the obvious problem of the opposing control mechanisms this would be destabilizing, since during the inertial response recovery phase suddenly not only the original power loss but also the missing WEC power have to be compensated. This would happen even earlier for the fixed power approach due to its non-constant support power. It seems therefore essential to provide an adaptive control regimen and to tune the different power system components and their frequency control behaviour very well.

To be able to compare the support energies given in Section 5.2 with the energies normally delivered by synchronous generation during a frequency disturbance, these values have been calculated with the help of equation (6.6). The energy missing due to the power imbalance, $\Delta P_{\text{sys}}\Delta t$, amounts to $-8.36\,\text{GJ}$. The amount of

Table 6.1: Modified RoCoF after considering WEC inertial response.

$P_{\text{WEC,sys}}$ = / Approach	0.56 GW	2.09 GW	5.39 GW	7.37 GW
Fixed power	0.46 Hz/s	0.66 Hz/s	0.77 Hz/s	0.82 Hz/s
Fixed time	0.001 Hz/s	0.26 Hz/s	0.6 Hz/s	0.82 Hz/s
Fixed power and time	−0.05 Hz/s	0.12 Hz/s	0.54 Hz/s	0.81 Hz/s

kinetic energy fed into the grid can be calculated by the following part of equation (6.6):

$$\Delta E_{\text{sys,rot,syn}} = \frac{H_{\text{sys}}}{f_0}(f_{\text{nadir}}^2 - f_0^2)S_{\text{sys}} \tag{6.8}$$

Assuming the value for H_{sys} computed in Section 6.1, 5.95 s, $\Delta E_{\text{sys,rot,syn}}$ amounts to 5.16 GJ. This amount is reached even with the fixed power and time approach at an hourly average WEC power of 4.5 GW and more (see Fig. 5.4). This means that at this production level wind turbines would be capable of supplying the same amount of inertial energy like the assumed S_{sys} = 43.572 GV A of synchronous generation did in this case. It has to be noted though that the amount of inertial energy fed into the grid by synchronous generation is dependent on the frequency deviation and therefore case-specific. However, since the studied case is close to a dimensioning fault the comparison remains valid.

It has been showed that while other approaches allow for the usage of a greater fraction of kinetic energy, a conservative approach like implemented by the fixed power and time approach is sufficient and more beneficial system-wide. This is caused by the negative effects of veering the operating point too far from the maximum power point as well as the lack of necessity for this amount of inertia support. Generally, inertial response approaches exhibiting a fixed amount of support power for a fixed time seem favorable. If they should be preferred to strategies depending on frequency deviation or rate of change of frequency has to remain an open question. However, it should be noted that a non-constant inertia support power could be valuable for certain power systems. For example the hydro-dominated Nordic power system experiences a decline of power during the first seconds after the activation of primary frequency control [41], this effect could be cancelled out very well by a higher initial support power.

Essential for the overall effect of the inertial response is the precise design and control of inertial response, which includes both the inertial support and inertial recovery period. While the fixed trajectory (frequency independent) approaches studied in this work are comparably easy to analyse and implement, they bear a great risk of overcompensation, which may lead to over-frequency during the inertial support period. This is because the inertial response is, once triggered, independent from the causing disturbance. It seems therefore necessary to implement a control mechanism, e.g. by a correction of the support power by RoCoF feedback. However, this would introduce new challenges, i.e. measuring and filtering the RoCoF in a reliable manner (see also [41]). Apart from the control mechanism it also appears important to smooth out the transition between support and recovery phase, e.g. by varying the support time. It could also be necessary to review the parameters of the droop control, since inertial response from WEC's would likely limit the RoCoF more than before, but the demand for primary frequency control would likely be higher for a same sized disturbance due to the recovery phase.

The recovery phase is a critical part of the inertial response. It bears the risk of introducing a second, even deeper frequency nadir. Because of this an inertial response adapted to the particular disturbance seems favourable. It also constitutes the need for reliable primary control. It is likely that a higher amount of primary control is necessary, since the power missing during the recovery phase has to be added to the dimensioning fault. This is another reason why minimally invasive inertial response strategies should be preferred. The combination of WEC primary frequency control and inertial response seem to implicate synergies and should be further studied.

7

Conclusions and future work

7.1 Conclusions

In this work it could been shown that variable speed wind turbines are capable of a reliable and substantial contribution to frequency stability by inertia support. With increasing wind power production, this capability increases. In conclusion, at penetration levels where low inertia due to converter connected WEC becomes a problem, a careful designed WEC inertial response mechanism would be able to at least compensate the displaced synchronous inertia. Variable speed wind turbines are well capable of providing the same or higher amount of energy for inertial response like synchronous generation. However, this comes at the price of reduced production during the recovery period, which increases the demand for primary frequency control and includes the risk of causing a second frequency nadir.

The aerodynamic losses due to reduced rotor speed during inertial response cannot be neglected. They limit the maximum power during the recovery phase and are the highest at the medium wind speed range. For a sophisticated simulation of inertial response effects it is consequently not sufficient to consider the rotor speed at start and end of inertia support, but necessary to conduct a simulation of the turbine dynamics. Furthermore it could been shown that while for individual turbines the energy balance of inertial response might be positive, it is nearly always negative for the complete system.

In this work it has been demonstrated that a maximum of 82 % of a turbines kinetic energy can be extracted during inertial response. However, this is highly dependent on the operating conditions, the inertial response control and the assumed operating limits. For the more conservative fixed power and time approach, this maximum amounts to 23 % but can be reached at any wind speed above approx. 9 m/s.

To quantify the kinetic energy and inertial response from wind turbines it is necessary to consider the individual operating points. However, for certain inertial response strategies, e.g. the fixed power and time approach studied in this project, the aggregated inertia support power and energy appear as highly correlated linear functions of the WEC power. For this approach, by linear interpolation a ratio of 1.13 between aggregated support power and stationary power has been identified, while the ratio between aggregated support energy and stationary power amounts to 1.3 J/W. For the other investigated approaches a linear interpolation is not suitable due to the wide spread of values and the pronounced maximum at a medium production.

To improve the frequency stability in power systems with high wind power penetration, variable speed wind turbine inertial response is a viable and important strategy. Still, it depends on the careful tuning of the different elements of the particular power system to prevent dangerous frequency oscillations, deep frequency nadirs during the recovery phase or similar adverse effects. While the synchronous generation inertial response resembles more a passive resistance to changes in frequency, inertial response from converter connected generation should rather be regarded and designed as an active control mechanism which is allocated between inertial response and primary frequency control and has therefore to be specified carefully and consistent with the other means of frequency control.

7.2 Future work

This project leaves room for improved accuray and a number of open questions. For the investigation of the general topic of this work further research in the following areas would be beneficial:

The currently unsatisfactory accuracy of the estimations in this project could be increased by addressing the errors described in Section 3.3.2. The highest priority belong to the static and dynamic WEC model as well as the WEC database.

Most important for the successful implementation of WEC inertial response is the careful investigation of the interaction between the inertial response approach and the key indices of frequency stability. Questions that have to be answered in this respect are the amount of support power necessary, the length of inertial support and the design of the recovery phase. The results presented in Chapter 6 make clear that it is not necessary to maximise the amount of inertial response power or energy, but in contrary important to keep the turbines as close to their steady-state operational point as possible.

Furthermore it could be crucial to investigate the precise operation limits of wind turbines for inertial response. However, as suggested by the results of this work conservative response strategies appear more desireable, which would decrease the priority of this question.

To quantify the effects of WEC inertial response on frequency stability, it is necessary to do a power system stability analysis which incorporates primary frequency control. While simulations along these lines already have been carried out (e.g. in [6], [41]), they could be improved with the aggregated or distributed inertial response time series presented in this work. It would also be beneficial to compare the performance of fixed trajectory approaches like the ones investigated in this work to other control approaches, e.g. RoCoF proportional control.

Bibliography

[1] Energinet.dk. (Jan. 15, 2016). New record-breaking year for Danish wind power, [Online]. Available: `https://www.energinet.dk/EN/El/Nyheder/Sider/Dansk-vindstroem-slaar-igen-rekord-42-procent.aspx` (visited on 05/23/2016).

[2] Energimyndigheten. (May 23, 2016). Stor vindkraftsutbyggnad i Västernorrlands län under 2015, [Online]. Available: `http://www.energimyndigheten.se/nyhetsarkiv/2016/stor-vindkraftsutbyggnad-i-vasternorrlands-lan/` (visited on 05/23/2016).

[3] T. Ackermann, Ed., *Wind Power in Power Systems*, Chichester, West Sussex, England ; Hoboken, NJ: John Wiley, 2005, 691 pp.

[4] P. Tielens and D. Van Hertem, "The relevance of inertia in power systems", *Renewable and Sustainable Energy Reviews*, vol. 55, pp. 999–1009, Mar. 2016.

[5] M. Seyedi and M. Bollen, "The utilization of synthetic inertia from wind farms and its impact on existing speed governors and system performance", Energiforsk, 2013.

[6] R. Leelaruji and M. Bollen, "Synthetic inertia to improve frequency stability and how often it is needed", Energiforsk, 2015.

[7] B. Rawn and P. Lehn, "Wind rotor inertia and variable efficiency: fundamental limits on their exploitation for inertial response and power system damping", in *Proc. Eur. Wind Energy Conf*, 2008.

[8] N. Miller, K. Clark, and M. Shao, "Impact of Frequency Responsive Wind Plant Controls on Grid Performance", Dec. 2010.

[9] L. Ruttledge, N. W. Miller, J. O'Sullivan, and D. Flynn, "Frequency Response of Power Systems With Variable Speed Wind Turbines", *IEEE Transactions on Sustainable Energy*, vol. 3, no. 4, pp. 683–691, Oct. 2012.

[10] F. Teng and G. Strbac, "Evaluation of Synthetic Inertia Provision from Wind Plants", in *Power & Energy Society General Meeting, 2015 IEEE*, IEEE, 2015, pp. 1–5.

[11] R. Doherty, A. Mullane, G. Nolan, D. Burke, A. Bryson, and M. O'Malley, "An Assessment of the Impact of Wind Generation on System Frequency Control", *IEEE Transactions on Power Systems*, vol. 25, no. 1, pp. 452–460, Feb. 2010.

[12] L. Wu and D. Infield, "Power system frequency management challenges – a new approach to assessing the potential of wind capacity to aid system frequency stability", *IET Renewable Power Generation*, vol. 8, no. 7, pp. 733–739, Sep. 1, 2014.

[13] L. Ruttledge and D. Flynn, "Emulated Inertial Response From Wind Turbines: Gain Scheduling and Resource Coordination", *IEEE Transactions on Power Systems*, pp. 1–9, 2015.

[14] P. M. Ashton, C. S. Saunders, G. A. Taylor, A. M. Carter, and M. E. Bradley, "Inertia Estimation of the GB Power System Using Synchrophasor Measurements", *IEEE Transactions on Power Systems*, vol. 30, no. 2, pp. 701–709, Mar. 2015.

[15] E. Ørum, M. Kuivaniemi, M. Laasonen, A. I. Bruseth, E. A. Jansson, A. Danell, K. Elkington, and N. Modig, "Future system inertia", ENTSO-EE, Nordic Analysis Group, 2015.

[16] C. Seneviratne and C. Ozansoy, "Frequency response due to a large generator loss with the increasing penetration of wind/PV generation – A literature review", *Renewable and Sustainable Energy Reviews*, vol. 57, pp. 659–668, May 2016.

[17] E. Muljadi, V. Gevorgian, M. Singh, and S. Santoso, "Understanding inertial and frequency response of wind power plants", IEEE, 2012.

[18] G. Lalor, A. Mullane, and M. O'Malley, "Frequency Control and Wind Turbine Technologies", *IEEE Transactions on Power Systems*, vol. 20, no. 4, pp. 1905–1913, Nov. 2005.

[19] J. Morren, S. de Haan, W. Kling, and J. Ferreira, "Wind Turbines Emulating Inertia and Supporting Primary Frequency Control", *IEEE Transactions on Power Systems*, vol. 21, no. 1, pp. 433–434, Feb. 2006.

[20] K. Das, M. Altin, A. D. Hansen, P. E. Sorensen, and H. Abildgaard, "Primary reserve studies for high wind power penetrated systems", in *PowerTech, 2015 IEEE Eindhoven*, IEEE, 2015, pp. 1–6.

[21] J. Ekanayake and N. Jenkins, "Comparison of the Response of Doubly Fed and Fixed-Speed Induction Generator Wind Turbines to Changes in Network Frequency", *IEEE Transactions on Energy Conversion*, vol. 19, no. 4, pp. 800–802, Dec. 2004.

[22] J. Brisebois and N. Aubut, "Wind farm inertia emulation to fulfill Hydro-Québec's specific need", in *Power and Energy Society General Meeting, 2011 IEEE*, IEEE, 2011, pp. 1–7.

[23] T. Burton, Ed., *Wind Energy Handbook*, 2nd ed, Chichester, West Sussex: Wiley, 2011, 742 pp.

[24] B. G. Rawn, M. Gibescu, and W. L. Kling, "A static analysis method to determine the availability of kinetic energy from wind turbines", in *Power and Energy Society General Meeting, 2010 IEEE*, IEEE, 2010, pp. 1–8.

[25] L. Wu and D. G. Infield, "Towards an Assessment of Power System Frequency Support From Wind Plant - Modeling Aggregate Inertial Response", *IEEE Transactions on Power Systems*, vol. 28, no. 3, pp. 2283–2291, Aug. 2013.

[26] C. Kim, Y. Gui, and C. C. Chung, "Coordinated wind power plant control for frequency support under wake effects", in *Power & Energy Society General Meeting, 2015 IEEE*, IEEE, 2015, pp. 1–5.

[27] Goddard Earth Sciences Data and Information Services Center. (Jun. 11, 2016). MDISC Data Subset, [Online]. Available: `http://disc.sci.gsfc.nasa.gov/daac-bin/FTPSubset2.pl` (visited on 06/11/2016).

[28] M. G. Bosilovich, R. Lucchesi, and M. Suarez, "MERRA-2: File Specification", 2016.

[29] J. Olauson and M. Bergkvist, "Modelling the Swedish wind power production using MERRA reanalysis data", *Renewable Energy*, vol. 76, pp. 717–725, Apr. 2015.

[30] R. Keys, "Cubic convolution interpolation for digital image processing", *IEEE transactions on acoustics, speech, and signal processing*, vol. 29, no. 6, pp. 1153–1160, 1981.

[31] J. Olauson, H. Bergström, and M. Bergkvist, "Scenarios and time series of future wind power production in Sweden", Energiforsk, 2015.

[32] J. M. Jonkman, S. Butterfield, W. Musial, and G. Scott, *Definition of a 5-MW Reference Wind Turbine for Offshore System Development*. National Renewable Energy Laboratory Golden, CO, USA, 2009.

[33] T. Ackermann, Ed., *Wind Power in Power Systems*, 2nd ed, Chichester, West Sussex ; Hoboken, N.J: Wiley, 2012, 1049 pp.

[34] K. Clark, N. W. Miller, and J. J. Sanchez-Gasca, "Modeling of GE wind turbine-generators for grid studies", 2010.

[35] M. Ragheb and A. M. Ragheb, *Wind Turbines Theory-the Betz Equation and Optimal Rotor Tip Speed Ratio*. INTECH Open Access Publisher, 2011.

[36] F. Hafiz and A. Abdennour, "Optimal use of kinetic energy for the inertial support from variable speed wind turbines", *Renewable Energy*, vol. 80, pp. 629–643, Aug. 2015.

[37] B. Motamed, "The effect of high penetration of wind power on primary frequency control of power systems", *Chalmers University of Technology, Goteborg, Sweden*, 2013.

[38] N. Ullah, T. Thiringer, and D. Karlsson, "Temporary Primary Frequency Control Support by Variable Speed Wind Turbines - Potential and Applications", *IEEE Transactions on Power Systems*, vol. 23, no. 2, pp. 601–612, May 2008.

[39] ENTSO-E, "Assessment of the System security with respect to disconnection rules of PV Panels", Apr. 25, 2012.

[40] ——, (2015). Consumption Data, [Online]. Available: `https://www.entsoe.eu/data/data-portal/consumption/Pages/default.aspx` (visited on 11/21/2016).

[41] M. Persson, "Frequency response by wind farms in islanded power systems with high wind power penetration", Department of Energy and Environment, Electric Power Engineering, Chalmers University of Technology, 2015.

[42] Nord Pool, *Production per country 2013 Hourly*, Nov. 12, 2015.

A

Appendix A: Bin sample numbers for online turbines and hourly energy production

Table A.1: Bin sample counts for online wind turbines.

Lower bin edge	Bin samples	Lower bin edge	Bin samples	Lower bin edge	Bin samples
121	5	1 185.54	14	2 218.77	217
152.31	1	1 216.85	16	2 250.08	232
183.62	2	1 248.16	21	2 281.39	259
214.93	1	1 279.47	28	2 312.7	264
246.24	0	1 310.78	32	2 344.01	286
277.55	0	1 342.09	26	2 375.32	287
308.86	3	1 373.4	28	2 406.63	320
340.17	0	1 404.71	29	2 437.94	343
371.48	0	1 436.02	31	2 469.25	356
402.79	0	1 467.33	32	2 500.56	430
434.1	0	1 498.64	45	2 531.87	422
465.41	1	1 529.95	43	2 563.18	465
496.72	1	1 561.26	40	2 594.49	490
528.03	0	1 592.57	45	2 625.8	534
559.34	1	1 623.88	55	2 657.11	581
590.65	1	1 655.19	57	2 688.42	592
621.96	2	1 686.5	61	2 719.73	691
653.27	4	1 717.81	70	2 751.04	763
684.58	4	1 749.12	75	2 782.35	772
715.89	6	1 780.43	73	2 813.66	827
747.2	6	1 811.74	93	2 844.97	934
778.51	3	1 843.05	85	2 876.28	1 006
809.82	1	1 874.36	90	2 907.59	1 077
841.13	4	1 905.67	72	2 938.9	1 162
872.44	4	1 936.98	123	2 970.21	1 239
903.75	4	1 968.29	121	3 001.52	1 286
935.06	4	1 999.6	125	3 032.83	1 546
966.37	9	2 030.91	136	3 064.14	1 639
997.68	18	2 062.22	162	3 095.45	1 885
1 028.99	11	2 093.53	180	3 126.76	2 350
1 060.3	12	2 124.84	176	3 158.07	2 891
1 091.61	18	2 156.15	202	3 189.38	3 837
1 122.92	13	2 187.46	203	3 220.69	19 864
1 154.23	9				

Table A.2: Bin sample counts for hourly energy production.

Lower bin edge in GW h	Bin samples	Lower bin edge in GW h	Bin samples	Lower bin edge in GW h	Bin samples
$9.2781 \cdot 10^{-3}$	32	2.5115	802	4.9402	241
0.0829	113	2.5852	895	5.0138	225
0.1565	228	2.6587	817	5.0874	229
0.2301	336	2.7323	747	5.161	210
0.3037	439	2.8059	751	5.2346	187
0.3773	516	2.8795	714	5.3082	212
0.4509	594	2.9531	694	5.3818	198
0.5245	752	3.0267	668	5.4554	185
0.598	789	3.1003	670	5.529	188
0.6716	829	3.1739	644	5.6026	161
0.7452	933	3.2475	572	5.6762	143
0.8188	909	3.3211	544	5.7498	140
0.8924	1 091	3.3947	555	5.8234	143
0.966	1 251	3.4683	516	5.897	119
1.0396	1 174	3.5419	516	5.9706	121
1.1132	1 237	3.6155	469	6.0442	119
1.1868	1 246	3.6891	432	6.1178	105
1.2604	1 255	3.7627	453	6.1914	93
1.334	1 343	3.8363	452	6.265	91
1.4076	1 310	3.9099	395	6.3386	97
1.4812	1 272	3.9835	404	6.4122	82
1.5548	1 266	4.0571	386	6.4858	112
1.6284	1 194	4.1307	388	6.5594	86
1.702	1 234	4.2043	349	6.6329	63
1.7756	1 187	4.2779	379	6.7066	62
1.8492	1 196	4.3515	362	6.7801	47
1.9228	1 192	4.4251	330	6.8537	49
1.9964	1 154	4.4987	320	6.9273	36
2.07	1 106	4.5723	305	7.0009	40
2.1436	1 055	4.6458	321	7.0745	37
2.2172	980	4.7195	307	7.1481	54
2.2908	899	4.793	267	7.2217	53
2.3644	906	4.8666	277	7.2953	32
2.438	905				